Hydraulic Structures to Control Sedimentation

Optimising the design of a navigation lock facing high sediment transportation

Rosa Verhees

TU Delft

Witteveen + Bos

Hydraulic Structures to Control Sedimentation

Optimising the design of a navigation lock facing high sediment transportation

by

Rosa Verhees

Committee members:	Dr.ir.C. Mai Van
	Dr.D.S. van Maren
	Ir.R.A. de Heij
Project Duration:	September, 2024 - February, 2025
Faculty:	Faculty of Civil Engineering, Delft

Cover: Mongla-Ghasiakhali waterway in Bangladesh (Delta Context & Witteveen+Bos, 2024)

TU Delft Witteveen+Bos

Preface

This thesis is written to obtain the master's degree in Hydraulic and Offshore Structures at the Delft University of Technology. It was carried out in cooperation with Witteveen+Bos, a consultancy and engineering firm based in the Netherlands. I have enjoyed this combination of partially working at the university and having discussions with my fellow students and professors, and partially working at the office of Witteveen+Bos and getting new insights from my colleagues. It was a challenging but rewarding experience and I am grateful to those who supported me throughout this process.

I would like to thank my entire thesis committee for the supervision and support you provided me during the duration of my project. I want to thank my main supervisor, Cong Mai Van, for helping me get started on this project with enthusiasm and for your ongoing involvement in the next phases. Your feedback and advice were able to help me structure my work, keep me on track of it and tackle the stressful parts. I also want to thank my supervisor Bas van Maren, for your expertise and insights into the sedimentation and modelling aspects of the project. Your explanations helped me in addressing the complex topics and let me gain new knowledge that will keep benefitting me in the future. To Robert de Heij, my company supervisor, thank you for the discussions on how to approach certain challenges and present the results effectively. Your extensive feedback, practical tips and encouragement helped me to stay focused and keep moving forward.

In addition, my gratitude goes out to my direct colleagues at Witteveen+Bos who pushed me not to give up and provided me reassurance during difficult moments. I am also grateful to Leon de Jongste, whose guidance in the early stages of the project helped me refine the modelling approach.

Last of all, I want to thank Luka, for re-reading my report and providing helpful suggestions. Your practical and emotional support kept me motivated during the more challenging moments of writing the thesis.

I hope you enjoy reading this thesis.

Rosa Verhees
Delft, February 2025

Abstract

Asymmetrical tides cause an uneven sediment redistribution within a system. The faster water level rise during the flood tide, compared to the slower decline during ebb tide, activates a tidal pumping process that transports additional sediment into the waterway. When the duration of the ebb tide exceeds that of the flood tide, there is less resuspension during ebb. Sediment primarily settles during slack tide, gradually filling the riverbed. The highest sedimentation rates occur near the tidal meeting zone. One of the most significant consequences of this process is the decline in navigability of the waterway. An example of such an asymmetrically tide-dominated delta can be found in the southwest of Bangladesh, specifically in the Mongla-Ghasiakhali waterway. This area experiences high sediment concentrations and substantial sedimentation volumes. To address the sedimentation, a conceptual design has been developed, introducing locks at Mongla and Ghasiakhali.

The amount of sedimentation within the lock chamber and channel is strongly influenced by the frequency of lock gate operations. The primary water exchange processes during lock operation include the filling and emptying of the chamber, density currents, and boat movements. The schematized box method is employed to model the water and sediment movements resulting from these water exchange processes.

Two operational scenarios are considered for modelling a single operational cycle. Scenario 1 and 2 consist of ten and eight phases, respectively, each with a specific duration. Under critical conditions, the sedimentation layer thickness after one operational cycle for scenario 1 is $6.93 * 10^{-4}\ m$ inside the chamber and $3.65 * 10^{-7}\ m$ in the channel. For scenario 2 these values are comparable.

A tidal cycle consists of multiple operational cycles and, depending on the operational scheme that is used, possibly a resting period. Two operational schemes were simulated: a two way traffic scheme with 12 out of 24 operating hours and a fully operational scheme. The simulation of one tidal cycle is repeated in various sequences to model the sediment conditions after one month of operation. Sedimentation in the chamber and channel can be minimised by adopting the two way traffic scheme with a flushing cycle after every 12-hour operating period. Under these conditions, the sediment layer thickness is $2.65 * 10^{-1}\ m$ in the chamber and $2.19 * 10^{-3}\ m$ in the channel after one month. When the growth of the sediment layer thickness is extrapolated to represent one year of operation, the annual sediment layer thickness growth is $3.22\ m$ in the chamber and $2.67 * 10^{-2}\ m$ in the channel. The sedimentation values remain below the expected maximum thresholds.

After analysing the behaviour of sediment, the optimum choices for the structural and maintenance design of the lock system are evaluated. These choices are based on the functional requirements, with a focus on sediment characteristics. The most suitable lock gates, considering sediment dynamics, are mitre gates, vertical lift gates, and radial (or tainter) gates. These gates offer low to moderate opening/closing times and are effective at pushing sediment away from the lock system. For the Mongla-Ghasiakhali waterway, the mitre gate is the optimal choice. The preferred filling and emptying system for locks dealing with high sediment concentrations, is openings in lock gates. Additionally, it may be beneficial to lengthen, deepen, or widen the lock chamber to accommodate more sedimentation.

The annual dredging volume inside the chamber is $4.60 * 10^{3}\ m^3$. For the channel, this volume is $5.79 * 10^{4}\ m^3$ per year. The total required dredging volume is approximately 35 times smaller than what would be required in the absence of the lock construction. The minimum frequency of dredging the chamber is once per year, whereas the channel can be dredged once every 37 years. The dredging of the chamber must be carried out during the lock's non-operating hours, while the channel dredging can take place throughout the day. The introduction of two navigation locks will reduce the total maintenance costs for the Mongla-Ghasiakhali waterway.

Contents

List of symbols

Symbol	Description	Unit
v	Velocity	m/s
g	Gravitational acceleration	m/s^2
Δ	Difference	$-$
h	Height of water column	m
Q	Discharge	m^3/s
a	Area gate openings	m^2
C	Discharge coefficient	$-$
V	Water volume	m^3
f_3	Vertical exchange coefficient	$-$
b	Width of chamber	m
ρ_w	Water density	kg/m^3
dt	Time step	s
t	Time	s
L	Length of chamber	m
c	Suspended sediment concentration	kg/m^3
ρ_d	Sediment density	kg/m^3
b_d	Width of design vessel	m
d	Draught of design vessel	m
S	Sedimentation rate	$kg/m^2/s$
D	Deposition rate	$kg/m^2/s$
E	Erosion rate	$kg/m^2/s$
V_s	Sediment volume	kg/m^3
A	Area water body	m^2
$w_{s,eff}$	Effective settling velocity	m/s
Σ	Sum	$-$
δ_s	Sediment layer thickness	m
τ_b	Applied bottom shear stress	N/m^2
τ_{ce}	Critical shear stress for erosion	N/m^2
$\frac{dm}{dt}$	Erosion rate	$kg/m^2/s$
m_e	Erosion constant	$kg/N/s$

V_e	Erosion volume	kg/m^3
$\overline{u}$	Depth-averaged velocity	m/s
C_h	Chézy coefficient	$m^{1/2}/s$
n	Manning coefficient	$m^{1/3}/s$
V_{se}	Sediment volume minus erosion	kg/m^3

1

Introduction

Background

Sluices and their navigation locks are typically designed to maintain a specific water level or protect an area from high water levels. However, in some regions of the world, there is a need for a new approach. The rivers in these areas require a sedimentation-based solution rather than a water level-based one. Sedimentation can become a problem when the water velocity is low, causing sediment particles to settle at the bottom or sides of the waterway. As this process repeats itself, the navigability of the waterway can be compromised. The navigability can be partially or completely disrupted due to the accumulated sediment. This can result in environmental degradation as well as social and economic losses for local communities and organisations dependent on the waterway.

The case study area requiring a sedimentation-based solution is the Mongla-Ghasiakhali navigation route in Bangladesh. This waterway is affected by an asymmetrical tide, which causes inflowing sediment to settle. To maintain the navigability of the waterway, a hydraulic structural design is needed to mitigate sediment inflow.

Project scope

There is a plan to construct two sluices, each with one or two navigation locks, on either sides of the waterway between Mongla and Ghasiakhali. The aim of this thesis is to identify the sedimentation issues and conduct a study on how the hydraulic structures can be optimally designed to address the sedimentation within the waterway.

A hydraulic structural design involves various elements. This project will primarily focus on the design of a navigation lock to facilitate sluice passage while managing sedimentation. The study area for this project is the waterway route between Mongla and Ghasiakhali. While the potential effects on other parts of the area will be considered, the main focus will remain on the design of the hydraulic structures.

Methodology

The first step of the project is to analyse the problem and study area through a comprehensive literature review. To understand the issue, the case study focuses on the Mongla-Ghasiakhali route in Bangladesh, which serves as an example of how to design a sluice to manage large sedimentation. The study will examine how sedimentation occurs in the presence of sluices. To determine the size and location of the design challenges, calculations are performed to predict the water and sediment inflow into the sluice chambers. The results of these calculations will provide insights into the amount of sedimentation that occurs in the chamber and in the channel between Mongla and Ghasiakhali during both an operational and tidal cycle. Once the specific design problems are analysed, the optimal design option for each sub-question will be determined across multiple chapters.

Report structure

The report begins with a problem analysis in which the project's sub-questions are presented. Following this, the area analysis and methodology are described. Next, each sub-question is analysed along with their potential design options. Finally, the most suitable design option is selected and the design and methodology are critically evaluated in the discussion section of the report.

2

Problem analysis

Due to a lack of understanding of morphological processes in the past, human interventions were made that are now still negatively impacting tidal waterways. An example of such an intervention is creating a polder upstream of a delta. The reduction of fresh water supply from upstream the system, decreases the tidal volume and creates a tidal asymmetry in the system. In an asymmetric tidal system where the ebb tide lasts longer than the flood tide, sediment is distributed unevenly. Riverbed sedimentation will occur mostly during slack tide. In addition, an enhanced tidal pumping process due to the absence of fresh water flow will also contribute to the increased presence of sediment in the water channels (Center for Environmental and Geographic Information Services, 2014). The channel dimensions will decrease as a result of the sedimentation. As the channel dimensions decrease, the tidal volume will decrease as well. This means that the process keeps repeating itself when no other measures are taken, resulting in a declining navigability.

In the southwest part of Bangladesh, the waterway problems started around 1980 when smaller river channels were cut off for the purpose of shrimp cultivation (Rahman et al., 2013). This process was increased by the construction of polders upstream in the year of 1990. The shrimp cultivation as well as the polders reduced the tidal volume of water in large parts of the river system. The absence of the fresh water inflow together with an increased tidal pumping process, caused sedimentation to occur in multiple channels in the area. As mentioned earlier, the process repeats itself resulting in a large amount of sediment settling in the waterway. The waterway between Mongla and Ghasiakhali in Bangladesh is important for the navigation between the west and east part of the country. An image of the route is given in Figure 2.1.

Figure 2.1: Mongla-Ghasiakhali waterway in southwest Bangladesh.

In 2010, this route had to be dredged to maintain the navigability. The flow area was increased by $90\ m^2$ after the dredging was done. However, there was still a natural imbalance and the waterway

started refilling rapidly causing the route to be completely filled again just three months after dredging. The same problem occurred again after dredging was done in 2011. Figure 2.2 shows the filling of the cross section of the channel due to sediment accumulation after the dredging in 2010.

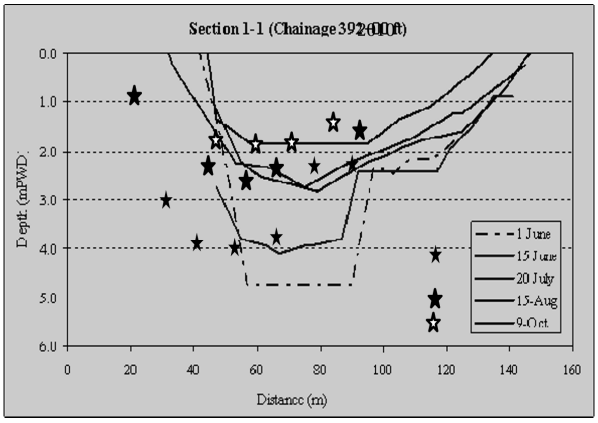

Figure 2.2: Monitoring results of cross section survey Mongla-Ghasiakhali route after dredging in 2010 (Rahman et al., 2013).

2.1. Problem formulation

The described problem can occur in a tide dominated delta. In such a system, the tide redistributes the sediment over the delta, following the tidal rivers. When the system is disturbed and an imbalance occurs, the tide can become asymmetrical. An asymmetrical tide also causes an asymmetric redistribution of the sediment in the system. When the ebb tide occurs over a longer period of time than the flood tide, the mean water level rises faster during flood than it decreases during ebb. This phenomena causes not only the resuspension during ebb tide to be less than during flood, but also causes the activation of a tidal pumping process that brings more sediment into the waterway (Center for Environmental and Geographic Information Services, 2014). It is during every slack tide that sediment will settle and slowly fill up the riverbed. The positive feedback process of riverbed sedimentation followed by a further decrease of tidal volume can continue for a long time period. One of the most important consequences of this process is that the navigability of the waterway will decline until there might eventually be no navigability possible at all in the specific waterway route.

The Mongla-Ghasiakhali waterway finds itself in a tide dominated delta with a weak tidal asymmetry. The period of ebb tide is 6.43 hours and the period of flood tide is 6 hours (Center for Environmental and Geographic Information Services, 2014). Next to this, the waterway transports a large amount of fine sediment concentrated in the water every tidal cycle. From Mongla to Rampal (a place between Mongla and Ghasiakhali, shown in Figure 2.1) there is about $12,100$ tonnes of sediment transported per cycle (Center for Environmental and Geographic Information Services, 2014). From the Ghasiakhali side to Rampal, $3,550$ tonnes of sediment is transported per cycle.

2.2. Desired solution direction

Several partial solutions exist to address specific aspects of the problem. The overall solution will likely involve a combination of these approaches. One straightforward solution, but with only temporary effects, is dredging the waterway channel. However, when the asymmetric tide is still present and no other solution is introduced, the riverbed sedimentation will soon start again after the dredging. Then, within a relatively short amount of time, the channel needs to be dredged again, resulting in high annual dredging costs. Another option is to increase the water volume upstream or to decrease the tidal fluctuation and sediment inflow in the navigation route. This thesis will focus on maintaining the latter option.

For the route between Mongla and Ghasiakhali in Bangladesh, there is already a plan to construct two sluices in the waterway; one at Mongla and one at Ghasiakhali. The purpose is to stop the tidal range and thereby decrease the sediment inflow. In 2014, a combined plan for the waterway between Mongla and Ghasiakhali was presented including multiple solution directions (Center for Environmental and

Geographic Information Services, 2014). The plan consists of constructing the sluices in combination with the dredging of the channel, a re-excavation of adjacent channels and the construction of an artificial loop-cut. This thesis will focus on only the sluices, and specifically on how the navigation locks of the sluices at Mongla and Ghasiakhali can best be designed to withstand the amount of sediment in the river system.

2.3. Problem statement and design objective

The problem statement of the thesis is that there is no experience in designing a sluice system, more specifically a lock design, for operating in a waterway with high sediment concentrations. The design objective is therefore to perform a study on how the navigation locks of sluices are best designed to face high sediment transportation in a waterway. The study can be divided into three parts: a sedimentation analysis, structural design considerations and maintenance design considerations. The research questions that are formulated, are stated below.

1) How much sedimentation will occur in a lock chamber and channel, during an operational and tidal cycle, and where will it concentrate?

2) How can sedimentation be reduced through improvement of lock design and operation?

3) How frequent is maintenance required in a lock dealing with high sediment concentrations and what steps can be taken to optimise the maintenance process?

In order to design a proper methodology to answer the research questions, first the study area and a conceptual lock design are analysed.

3

Study area

Information about the area that should be known includes the natural boundary conditions of the rivers and their flow regime, the hydraulic conditions, and the topographical and morphological characteristics. In a delta, it is essential to understand the tidal range and associated water velocities. Because this project focuses on the sedimentation in a waterway, the sediment concentration and characteristics of the sediment are very important. With the Mongla-Ghasiakhali waterway being an important navigation route, the nautical conditions and shipping frequency and size are important parameters to include in the analysis of the area.

This chapter provides an analysis of the area near Mongla and Ghasiakhali in Bangladesh. First, a general description of the location and existing climate is given. After this, a discussion of the tidal conditions and the current sedimentation is presented. In the final part of the chapter, the navigation needs of the area are analysed.

3.1. General

The area of the case study is in the southwest of Bangladesh, as could be seen in Figure 2.1. Bangladesh has several large rivers distributing water from the mountains into smaller rivers in the deltas. The deltas of Bangladesh are in the south part of the country.

Mongla is a town and a port located at the confluence of the Pashur (south), Rupsa (north) and Mongla river. Ghasiakhali is situated east of Mongla at the confluence of the Pangunchi (south), Dharatana (north) and Mongla river. The waterway between Mongla and Ghasiakhali is $31\ km$ long (Center for Environmental and Geographic Information Services, 2014). The waterway consists, from west to east, of the Mongla Nula, the Kumarkhali River and the Mongla-Ghasiakhali channel (further referred to as MG channel). The MG channel is manmade and was excavated in 1970 to enhance the navigation possibilities. From a bathymetry search, it is concluded that the water depths in the waterway vary from about 2 to $8\ m$. Overall, the MG channel has smaller water depths than the rest of the waterway.

Bangladesh has a sub-tropical humid climate (Rashid, 1991). The main characteristics of this climate are wide seasonal variations in rainfall, moderately warm temperatures and a high humidity. The climate can be divided into four seasons: dry winter (December to February), pre-monsoon hot summer (March to May), rainy monsoon (June to September) and post-monsoon autumn (October to November) (Shadid, 2010). The average temperature during winter is between 7.2 and $12.8\ ^{\circ}C$ and during summer between 23.9 and $31.3\ ^{\circ}C$.

3.2. Tidal conditions

The delta in which the Mongla-Ghasiakhali route finds itself, is dominated by an asymmetrical tide. During flood tide, water comes into the waterway both from the western side at Mongla, as well as the eastern side at Ghasiakhali. There is not one specific point where the tide meets, but it is often found to be in a range near Rampal. There are no measurements on a possible superimposed residual flow

due to the tidal flows from both sides, but it is expected that they are present in some form. After the lock is constructed, there are no tidal flow velocities in the channel anymore. Hence, the superimposed residual flow due to these tidal velocities are assumed to not play a role in this phase.

In 2014, the water levels at Mongla in the Mongla-Ghasiakhali navigation route have been measured for three months; from the end of January till the end of April (Center for Environmental and Geographic Information Services, 2014). The results of the water level analysis are given in Figure 3.1. In this figure it can be seen that the highest water level in the three months in 2014 was about $+2.0\ m\ PWD$ and the lowest was about $-2.0\ m\ PWD$. PWD in these measurements is the Public Works Datum established by the Department of Public Works, Bangladesh (Haque & Sakil, 2020). In Bangladesh, the PWD is $0.46\ m$ below Mean Sea Level (MSL). The maximum tidal range in spring tide is four to five meters. The tidal range during neap tide is around two and a half meters.

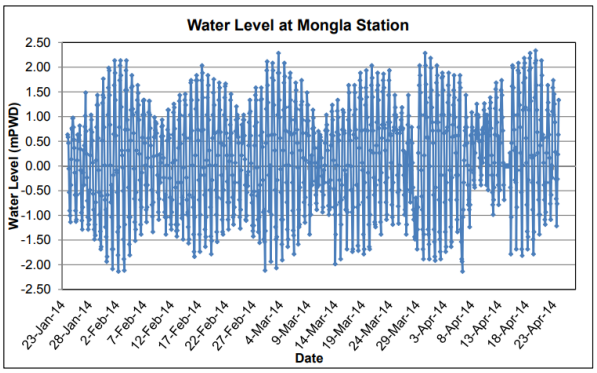

Figure 3.1: Water levels at Mongla in 2014 (Center for Environmental and Geographic Information Services, 2014).

Due to the tidal asymmetry in the system, the maximum velocity and discharge during flood tide, are higher than the maximum velocity and discharge during ebb tide on both sides of the channel. At Mongla, inside the channel, the maximum velocity during flood tide measured in 2014 is $1.01\ m/s$ and the maximum ebbing velocity is $0.53\ m/s$ (Center for Environmental and Geographic Information Services, 2014). The periods of flood and ebb tide have also been measured in March 2014. The period of flood tide then was $6\ hrs$ and the ebbing period was $6.43\ hrs$.

Another source has also reported to have measured the water levels at the entrances of the Mongla-Ghasiakhali waterway in March 2024 and calculated the discharges with this (Delta Context & Witteveen+Bos, 2024). The measurements were done at three locations: at the western side of the Mongla Nula, at the south end of the Doratana river and at the northern end of the Panguchi river. The ebbing period has been measured to occur between $06:00$ and $12:00$ in the morning. The flooding would then occur in between $12:00$ and $18:00$. The water level at Mongla varies with about 4 to $5\ m$ during spring tide. During flood, the water level is high and during ebb, the water level is low. The maximum flood discharge at spring tide at the Mongla station is about $2,000\ m^3/s$ and the maximum ebb discharge during spring tide at this location is around $1,500\ m^3/s$.

3.3. Sedimentation

Southern Bangladesh consists of a large delta which is characterized by its high concentration of fine sediment. During flooding, this sediment is transported land inwards, and during ebbing, the sediment is transported back to the Bay of Bengal. The suspended sediment concentration will peak just after the peak discharge of ebb tide is reached. The concentration decreases when the tide moves from ebb to flood. The peak concentration during the tide that was described earlier, is assumed to be around $6.0\ kg/m^3$ at Mongla in the Mongla Nula. The suspended sediment concentration is the highest near the bed of the channel and will be somewhat lower near the water surface. The mean concentration near Mongla is around $3.0\ kg/m^3$. The median sediment grain size of bed samples for the western end of the Mongla Nula and for the eastern end of the MG channel, near Ghasiakhali, are $46\ \mu m$ and $52\ \mu m$ respectively (Delta Context & Witteveen+Bos, 2024). The measured sediment sizes both correspond to the material silt, and more specifically, coarse silt (Brunner, 2020; The GeoTech: Geotechnical Engineer's Knowledge Base, n.d.).

The flow velocities during ebb tide are lower than the flow velocities during flood tide, which leads to less resuspension during ebb than during flood. Next to this, the asymmetry in the tide leads to a faster mean rise of the water level than the decrease of the water level. With these conditions, a tidal pumping process is activated (Center for Environmental and Geographic Information Services, 2014). During the tidal pumping process, sediment is brought to the Mongla-Ghasiakhali waterway and sedimentation is enhanced. Sedimentation will mainly occur during slack tide where there is little to no horizontal movement of tidal water. The sedimentation occurs every cycle, causing the waterway to silt up. In the Mongla-Ghasiakhali waterway, the largest sedimentation occurs near Rampal, because the lowest flow velocities occur here. This is due to the two tides coming from the west (Mongla) and east (Ghasiakhali) that meet each other around this point, this is called the tidal meeting zone (Center for Environmental and Geographic Information Services, 2014). The sedimentation rate of the route between Mongla and Ghasiakhali is given in Figure 3.2.

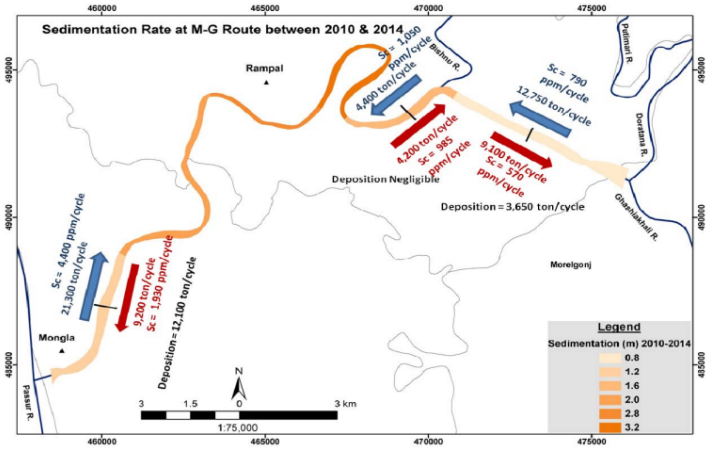

Figure 3.2: Sedimentation rate of the Mongla-Ghasiakhali route from 2010 to 2014 (Center for Environmental and Geographic Information Services, 2014).

The sedimentation in the waterway is causing severe bed level changes over the whole waterway length. To maintain a navigable depth in the waterway, an average volume of $2.2\ Mm^3$ is currently dredged per year (Delta Context & Witteveen+Bos, 2024). The highest annual bed level change occurs near Rampal at the tidal meeting zone, but there is also a large change near other bends as the velocity will have decreased here.

3.4. Navigation

3.4.1. Navigation route

The Mongla-Ghasiakhali canal is part of the Indo-Bangladesh protocol route that connects two parts of India through inland waterway navigation. Both India and Bangladesh can experience benefits from the inland navigation route as it enhances the travelling and trading possibilities that are also often less expensive than other transportation methods. The inland navigation route can be seen in Figure 3.3.

When the Mongla-Ghasiakhali waterway would not be functional, the other option of water navigation is to travel south from Mongla. However, in this area the Sundarbans start which is a protected mangrove forest in the river delta of the Ganges. Travelling through the Sundarbans poses an enormous risk on the ecosystem of the forest (Center for Environmental and Geographic Information Services, 2014). Next to this, it would lead to a length increase of the route of $60\ km$.

3.4.2. Water vessels

Based on the observed vessels of the inland waterway transport (IWT) fleet, the spread of the vessels passing through the system is determined. After consideration of the inland waterway classification system of the European Conference of Ministers of Transport, three design vessels are identified. The lengths and widths of the design vessels are shown in Table 3.1. The first design vessel has a length of $20\ m$ and a width of $5\ m$. The second design vessel has a length of $50\ m$ and a width of $11\ m$, and

Figure 3.3: Indo-Bangladesh protocol route (Menon, 2023).

the third has a length of $75\ m$ and a width of $12\ m$. On top of this, smaller vessels need to be taken into account when assessing the lock operations.

Table 3.1: Design vessels IWT fleet in Mongla-Ghasiakhali waterway.

Design vessel	Length [m]	Width [m]
Small	20	5
Medium	50	11
Large	75	12

3.4.3. Frequency

In the Mongla-Ghasiakhali route, there is only daylight navigation as there are no aids of navigation to make night navigation possible. The average speed of the vessels is $9\ km/h$, resulting in an average passage time through the canal of $3.5\ hrs$.

With the current conditions, the route is only navigable during high water as the water levels during low water do not result in a large enough navigation depth. The vessels have to wait each morning before entering the canal until the required water level is reached. Together with the information stated above and a Google Earth search, it can be concluded that 95 vessels passing the canal on a daily basis is a good estimate for the IWT frequency.

4

Conceptual lock design

To deal with the sedimentation, a conceptual lock design has been made, introducing a lock at Mongla and at Ghasiakhali (Delta Context & Witteveen+Bos, 2024). The goal of the lock design is to stop the sediment from entering the Mongla-Ghasiakhali waterway and to take away the tidal influences on the canal. Major benefits that would be extracted by the design is that a certain minimum water level can be sustained in the canal such that navigation is possible at any time and that the required dredging volume would be decreased significantly.

This chapter goes into the conceptual lock design. It provides a general analysis of the design and presents an overview of the new tidal conditions, sedimentation properties and navigation options when the design would be constructed.

4.1. General

The proposed design consists of a lock at the western end of the Mongla Nula and a lock at the eastern end of the MG-canal. Both locks are chosen to be on the southern side of the larger sluice construction.

The navigation lock consists of an approach structure, lock gates, lock heads and a lock chamber and several smaller details such as the construction of a sill. The dimensions of the lock are determined by the water levels, soil conditions and navigation characteristics. In the conceptual design, it is chosen to incorporate a double set of mitre gates at each side of the chamber. The filling and emptying system that is used in the design is openings in the gates. In Figure 4.1, a sketch is shown of how the chamber and double set of mitre gates would look like in a lock.

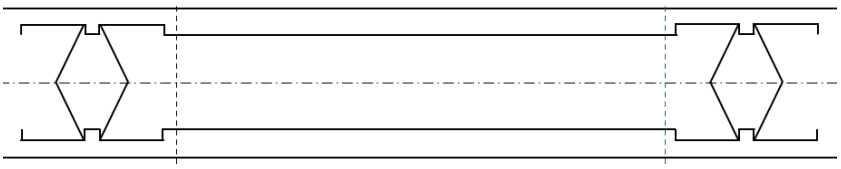

Figure 4.1: Top view of a lock with double mitre gates.

The design of the lock has to withstand the hydraulic loads and the mooring loads. Hydraulic loading conditions differ with the tidal range. The lock will be under critical hydraulic conditions, when the water level difference between the lock chamber and river or channel is the largest. Because the lock first has a long approach structure, it is assumed that the wave forces from the river influencing the chamber, can be neglected. Some boats will need to moor inside the lock chamber when the chamber is levelled, in order to maintain their balance. The loads that come with this need to be held by the chamber walls.

4.2. Tidal conditions

The lock is only opened when vessels need to pass the construction in order to maintain the water level inside the channel and minimise the sediment in it. This means that there will not be a tidal influence on the water between the two locks. However, the tide does strongly influence the design requirements of the lock as it will still be present in the adjacent Pashur river and the Pangunchi and Dharatana river. Because of the tidal movements, the lock can have high water levels from both sides. During high tide, the water level outside the channel is higher and during low tide, the water level inside the channel will be higher.

For this study, certain boundaries are used to describe the water levels. The minimum operational water level at Mongla is set to $-3.0\ mMSL$ and the largest operational water level is set to $+2.0\ mMSL$ (Delta Context & Witteveen+Bos, 2024). The bottom level of the lock is determined by the minimum operation water level on the outside of the lock, the draught of the design ship ($4.2\ m$) and the sill depth ($0.7\ m$). The bottom level is then determined to be $-7.9\ mMSL$. The maximum operational head difference of the lock is $5\ m$.

At Ghasiakhali, the minimum operational water level is set to $-2.0\ mMSL$ and the largest operational water level is set to $+2.0\ mMSL$ (Delta Context & Witteveen+Bos, 2024). The draught of the design ship and sill level remain the same for both lock locations. The lock bottom level then results in a value of $-6.9\ mMSL$. The maximum operational head difference at Ghasiakhali is $4\ m$. The maximum and minimum water levels at the locks are shown in Figure 4.2.

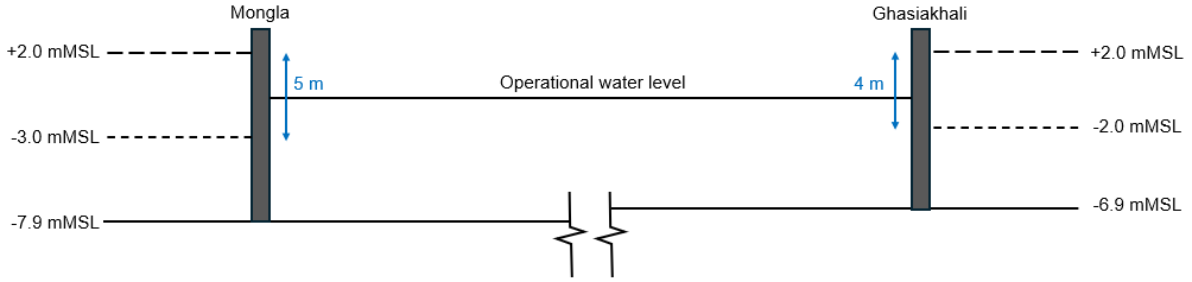

Figure 4.2: Side view of the maximum and minimum water levels in the locked Mongla-Ghasiakhali waterway.

4.3. Sedimentation

The sedimentation in between the two locks will decrease significantly due to the lock constructions and can be assumed zero in the first design phase. In practice, the amount of sedimentation inside the channel strongly depends on the frequency of opening of the lock gates. During every opening, it is inevitable that some sediment enters. Some of this sediment will stay inside the lock construction, and other sediment will be passed down to the river water between the locks. The sediment inside the lock can cause issues for the operation of it, when the amount increases or concentrates at a problematic area.

Another risk of constructing the locks, is that it may probably cause an increase in the sedimentation in the Pashur, Pangunchi and Dharatana river. The most sedimentation in these rivers will concentrate in front of the lock as the flow velocities become very low there. The expected bed level change near the lock entrances after one year of the lock construction is shown in Figure 4.3 (Delta Context & Witteveen+Bos, 2024).

4.4. Navigation

4.4.1. Dimensions

The feasibility study of Delta Context and Witteveen+Bos (2024) has concluded lock dimensions with a length of $110\ m$, a width of $13\ m$ and a depth of $4.2\ m$. With these dimensions, the lock chamber will be able to accommodate two medium vessels or a combination of one large vessel and one or two small ones. To increase the capacity of the waterway, the construction of additional navigation locks can be taken into consideration in the future.

Figure 4.3: Expected bed level change in the Mongla-Ghasiakhali route one year after construction of the two locks.

4.4.2. Operation

Three lock operation scenarios have been identified: a scenario with one way traffic, a scenario with two way traffic and finally a fully operational scenario. The choice of the operational scenario depends on the actual vessel sizes and frequency after the construction of the lock. Two way traffic is more time efficient, but also requires more aids of navigation. The capacity of the lock with regards to the different operating scenarios can be seen in Table 4.1.

Table 4.1: Lock capacity for different operating schemes.

Scenario	Lock operating (out of 24 hours)	Lock cycle [min]	Vessels per cycle	Vessels per day	Vessels per year
One way traffic	9	45	2	24	8,800
Two way traffic	12	60	4	48	17,500
Fully operational	24	60	4	96	35,000

With regards to the sedimentation, there is a balance to be found to determine which operation scenario would be preferable. More lock cycles will cause a higher sediment concentration to appear in the chamber and channel. However, this does not necessarily lead to a higher sediment layer thickness. A higher amount of lock cycles also means more sediment is able to pass through the system without being able to settle due to the presence of a long resting period.

5

Methodology

Now that the area and conceptual design are known, this chapter will give insight into the methodology to design the lock chamber in such a way that it can deal with high suspended sediment concentrations and large amounts of sedimentation. The first step that needs to be taken in order to make a proper design, is defining how much sedimentation will occur and where it will concentrate. After this, different design options are presented and their responses to sedimentation are analysed. The subquestions that need to be answered using the methodology originate from the problem analysis in Chapter 2.

5.1. Sediment transport and sedimentation

1) How much sedimentation will occur in a lock chamber and channel, during an operational and tidal cycle, and where will it concentrate?

To answer the first subquestion, the water and sediment exchange processes need to be analysed. The water and sediment exchange system around a lock chamber is complex as there are multiple turbulent water processes present. Furthermore, the scale in which the solution is needed is quite small in comparison to solutions provided by existing hydrodynamic and morphological models. Some hydrodynamic and morphological models can simulate multiple water exchange causes simultaneously. The models that were considered to be used were, among others, Delft3D and Flow-3D. None of the models however, could meet the requirement of operating on a small scale while still simulating complex three-dimensional flow patterns. Not being able to use an existing hydrodynamic and morphological model means it is recommended to look into the separation of the turbulent water processes and possibly making a choice of neglecting the processes with considerably small influences.

Sediment is transported when water volumes are exchanged. The water exchange processes occurring in a lock chamber which is open, resemble the ones which would occur in a harbour. Therefore, a literature study on harbour siltation is done to determine the most critical water exchange processes with regards to sedimentation.

When the most important sediment transport and sedimentation processes around a lock chamber are identified, a sediment balance can be set up. The schematized box method assumes a rectangular box with one opening to a waterway, as a harbour. The situation has a good resemblance to the lock chamber situation. With the formulas from the schematized box method, the sediment volume and sediment layer thickness that are in the lock after a certain period of time can be calculated.

One operational cycle of a lock can be schematized into different phases. For each phase, a new sediment balance equation needs to be set up, using the schematized box method. One phase can be divided into multiple smaller time steps. The second phase begins with the same water and sediment conditions as the last step of the phase before. When using small time steps, the calculation can become very long. Therefore, the program Python is used to structure the repetition of the calculations. After one operational cycle is simulated, the steps can be repeated to simulate one tidal cycle. The simulation of a tidal cycle strongly depends on how frequent the lock operates, which in turn depends

on the vessel movements near the channel. The calculations can be done by assuming the most critical conditions. The simulations can be repeated to also represent one month. These results can in turn be extrapolated to come to the values for one year of operation.

After the simulations are completed, the sediment concentrations and sediment layer thicknesses inside the lock chamber and the channel are visualized in multiple graphs.

5.2. Design considerations

There are two types of designs that can be optimised regarding a specific lock situation: the structural design and the design of the lock maintenance. In order to discuss the design options, a list of the functional requirements for the structural and maintenance design, regarding a lock that faces high sediment transportation, is first set up. After this, the different design options can be presented per subcategory and they can be assessed using the list of functional requirements.

2) How can sedimentation be reduced through improvement of lock design and operation?

The main features of the structural design that are analysed are the approach structure, the lock gates, the lock chamber and the filling and emptying system. The lock gates are assessed based on some standard lock gate requirements, but also specifically on their sediment characteristics. It is important here to analyse the sediment streams around a lock gate when it is opening and closing. Eventually, the best lock gate type and filling and emptying system for the case study is determined through the assessment based on all of the functional requirements. The analysis also considers smaller modifications to the lock's structural design and their potential impact on reducing sedimentation. Additionally, the study examines how optimising lock operation, such as adjustments in opening and closing procedures, can help minimise sediment build-up and improve overall efficiency.

3) How frequent is maintenance required in a lock dealing with high sediment concentrations and what steps can be taken to optimise the maintenance process?

The maintenance design of the system will focus on the maintenance dredging, as reducing this was a large part of the goal of the lock design. The initial dredging volume will be compared to the new estimated dredging volume and a conclusion can be drawn about the possible improvements and deteriorations. A clear distinction should be made in the dredging in the lock chamber and in the channel. After the simulations have been done, the maintenance chapter should be able to give a first indication on how frequently maintenance would be necessary in both the chamber and channel. Next to the maintenance dredging, other maintenance works will also shortly be discussed and possible alternative routes for during the maintenance are determined.

6

Water exchange processes

Factors that can influence the sediment transport and sedimentation in and near a lock chamber are the filling and emptying system, the gate movements, boat movements and the density currents. The water exchange mechanisms fueling the sediment movements are similar to the water exchange movements in harbour basins. The processes that have the largest effects on sedimentation in harbour basins are the filling and emptying during a tide, the horizontal eddy circulation at the entrance generated by the difference in flow direction and the vertical density currents due to water density differences (Eysink, 1989; Langendoen, 1992; van Rijn, 2016; Weber-Shirk et al., n.d.). Previous reports on harbours have paid little attention to the influence of boat movements as other effects were larger. However, it is expected that these boat movements can have a much larger effect in lock chambers than in harbours. This is due to the smaller ratio of the water volume that can be flushed by a boat and the total water volume in which the boat can move. The horizontal eddy circulation at the harbour entrance is excluded in the quantitative analysis, because a proper designed lock entrance will already have reduced the effect at the front so that it will not have a direct effect at the entrance of the lock chamber. The water exchange movements induced by gate operations were not mentioned in harbour siltation studies as these studies did not go into harbours which were closed by sluices and locks. The choice of the gate system can have a large influence on how sediment responds to gates that are moving. Therefore, it is chosen to only include this process in a qualitative way in the later stage of design considerations.

6.1. Operational phases

The operational cycle of a lock can be separated into different operational phases, each of which has its own water exchange process. Before going into the specifics of each water exchange process, an overview of the phases in which they occur will be given in this paragraph. There are two different operational cycle schemes that need to be discussed. The first scenario happens when the first boat wants to move from the high, sediment containing, water side on the left of the lock chamber to the low water side on the right. The second scenario occurs when a boat first wants to move from the low water side on the right of the chamber towards the high, sediment containing, water on the left. The most critical conditions for each scenario will now be discussed and their operational schemes are explained.

6.1.1. Scenario 1

The first scenario is the most critical when looking at the sedimentation potential, when the water inside the chamber starts at the low water level. This is because the chamber first needs to be filled with water with suspended sediment in it. The operational scheme in this scenario consists of ten phases. Figure 6.1 gives an overview of the phases. The last step is there to indicate at which step the next operational cycle starts.

The first phase of the operational cycle in this case is the filling of the lock chamber from the left side. After the water level inside the chamber matches the high water level on the left side, the gates on the left are opened, and the second phase begins. In phase 2, 5 and 9, the gates are open so that boats can travel through the lock head. However, because two water bodies with different densities are

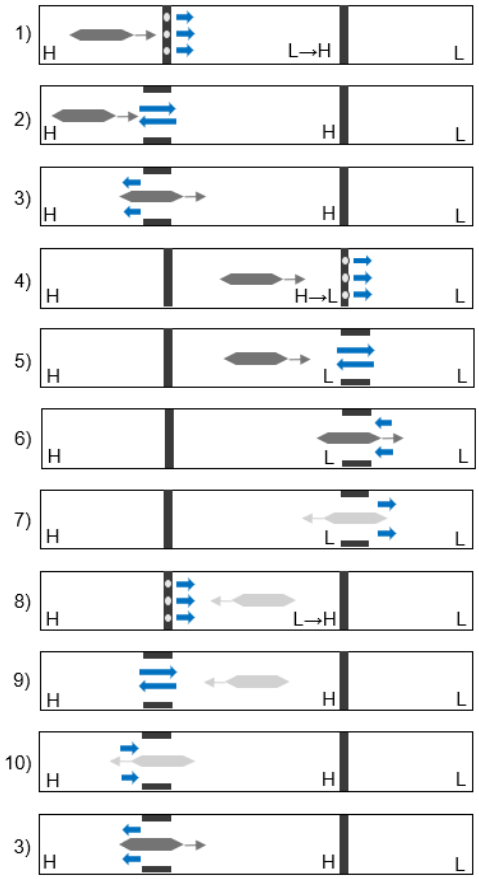

Figure 6.1: Operational phases scenario 1, where the first vessel moves from high to low water.

now in connection with each other, density currents will first be induced. Boats will generally wait on the decrease of the turbulence due to these density currents, before moving in or out of the chamber. Therefore, it can be assumed that the water exchange processes occur non-simultaneously. In phase 3, the first boat travels from the left, high water, side into the lock chamber. In the fourth phase, boat 1 is in the lock chamber, the gates are closed again and the chamber is partially emptied to level the water inside with the water on the right, low water, side of the system. When the water is levelled, the gates on the right side are opened. In the phase 5, the water bodies are exposed to density currents. In the sixth phase, boat 1 leaves the lock on the right side. The seventh phase is the start of the passage of boat 2. Here, boat 2 travels from right to left into the lock chamber. After this, the gates are closed again on both sides in phase 8. The chamber is then filled with water from the left side to increase its level. When the high water levels are equal or nearly equal, the gates on the left side are opened in phase 9. In this phase, the density currents cause a water exchange process. In phase 10, boat 2 leaves the chamber to the left, causing another type of water exchange process. As it is assumed that the operation is continuous during the operating hours of the lock, the operating cycle will directly be repeated. However, the first two phases of the cycle can now be skipped, because the water level inside the chamber is already high and density currents have already occurred. This means the cycle is repeated, beginning with phase 3.

6.1.2. Scenario 2

The second option for the operational scheme, is that a boat wants to move from low water on the right of the lock chamber to high, sediment containing, water on the left. An overview of the second option is shown in Figure 6.2. Before the first operational cycle of the lock, it is assumed that the water inside the chamber and inside the channel (low water side) is fresh and does not contain suspended sediment. In case of the operational cycle in scenario 1, it was more critical to let the cycle begin with the filling of the chamber. In the second scenario, boat 1 is coming from the low water channel. As it is assumed

that the water bodies of the chamber and channel have the same characteristics at the beginning, it is not more or less critical to start with a high or low water level inside the chamber when a boat comes from the channel. Therefore, the shortest scheme is chosen, beginning with a low water level in the lock chamber. In that case, there are eight operational phases. The last step in Figure 6.2 is, once again, to indicate with which step the next cycle begins.

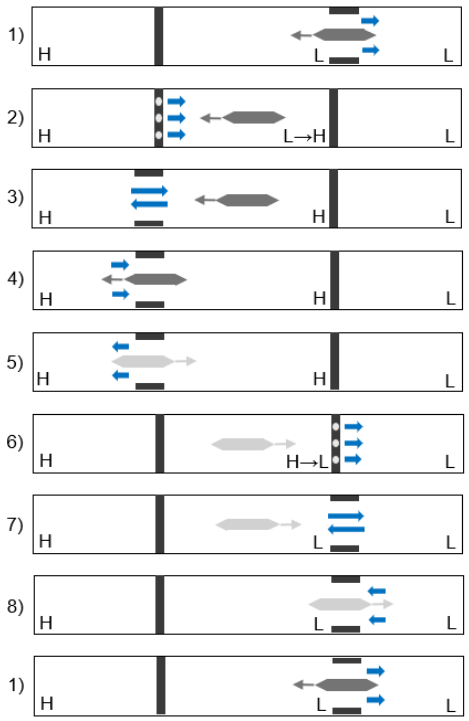

Figure 6.2: Operational phases scenario 2, where the first vessel moves from low to high water.

In the first phase, the water level in the chamber is low and the gates on the right side are already opened. There are no density currents as the characteristics of the water bodies on both sides are equal. Boat 1 moves from the right side into the chamber in the first phase. When the boat in the chamber and the gates on both sides are closed, the second phase occurs. In this phase, the chamber is filled until the water level is equal or almost equal to the water level on the left, high water, side. In phase 3, the gates on the left are open and density currents occur between the left high water side and the water in the lock chamber. When these density currents are in equilibrium, boat 1 travels out of the lock to the left in phase 4. In phase 5, boat 2 is introduced and will travel into the chamber from left to right. Water travels in the opposite direction. In the sixth phase, boat 2 is inside the chamber and the gates on both sides are closed. The water in the chamber is levelled by discharging some of it to the right, low water, side. When the water levels of the chamber and the channel are about equal, the gates on the right side are opened and phase 7 begins. The water exchange process in phase 7 is induced by the density currents. In the eighth phase, water is moved due to boat 2 travelling from the lock towards the right, low water, side. One operational cycle is now complete and the cycle can be repeated. A second operational cycle will begin with phase 1 again, allowing a boat to pass from the low water side into the lock chamber.

6.2. Filling and emptying

The water exchange volume due to the filling and emptying system of a lock is strongly dependent on the type of filling and emptying system that is introduced. The filling and emptying systems that can be used are openings in gates, flow through culverts and partially opening the main gate itself. The filling and emptying through the partial opening of the main gate is often used for locks with a large head difference to speed up the processes (Glerum & Vrijburcht, 2000). The disadvantages of the method is that it is not suitable for mitre, pivot or rolling gates and that the flow needs refraction bars. Refraction

bars can be implemented right after the opening to reduce the flow velocity of the water coming in or out of the chamber when it would be filled or emptied. However, it is hard to minimise this effect when there is a larger head difference. The unfavourable flow patterns that can otherwise be induced, can cause negative effects on the sediment distribution and boat stabilities.

The filling and emptying by flow through culverts is normally used for medium to large lock heads (Chen, 2015). The culverts can provide a good distribution of flow in- and outlet through the side walls or bottom floor. The locking process can therefore be faster than the locking through openings in gates and boats are usually hindered less during the process (Daniel & Paulus, 2019). However, a great disadvantage of culverts outside lock chambers is its proneness to sediment deposits in them and to debris accumulation at their intakes.

Gate openings are normally used for water heads up to about $6\ m$ (Glerum & Vrijburcht, 2000). This option is the least expensive and often the most favourable with regards to its maintenance aspects. The risks for vessels are somewhat higher for gate openings than for culverts as there is less space for a balanced distribution of the flow (Daniel & Paulus, 2019). In the case study, a large advantage of the gate opening system would be that they generally encounter no problems with sediment deposits in normal conditions and little problems with debris.

With the maximum head difference in the case study of $5\ m$, gate openings are often chosen for the filling and emptying. This is also the most favourable option regarding sedimentation. In the next phases, the calculations are based on the use of gate openings. The maximum required time of filling and emptying was set to $15\ min$ and the therefore needed area of the gate openings at Mongla is $2.0\ m^2$. The maximum velocity through the gate openings can be determined by using the head difference. Subsequently, the discharge through the openings can be calculated with the maximum velocity, area of the openings and the discharge coefficient. The formulas for the calculations are stated as Equations 6.1 and 6.2.

$$v_{FE} = \sqrt{2g\Delta h} \tag{6.1}$$

v_{FE}	Filling and emptying velocity	m/s
g	Gravitational acceleration	m/s^2
Δ	Difference	$-$
h	Height of water column	m

$$Q_{FE} = aCv_{FE} \tag{6.2}$$

Q_{FE}	Filling and emptying discharge	m^3/s
a	Area gate openings	m^2
C	Discharge coefficient	$-$

6.3. Density currents

When water with two different densities are brought in contact with each other, vertical circulation currents are generated due to these density differences (Eysink, 1989). The density of a water body depends on its temperature, suspended sediment concentration and salinity. In this case, there is no variation in temperature included, so it is assumed that the density currents are only induced by salinity and suspended sediment concentration differences. When two water bodies with different densities come into contact, the water with a higher density, being heavier, will flow under the water body with a lower density. This interaction generates density currents. Figure 6.3 gives a sketch of how the water exchange volumes due to density differences would look when the high density water is on the left and low density water is on the right.

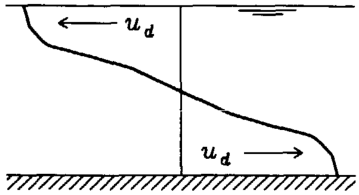

Figure 6.3: Density currents with high density water on the left and low density water on the right (Langendoen, 1992).

The volume of the water exchanged is dependent on the densities of the water bodies, the water depth, the width of the water bodies and the vertical exchange coefficient. The vertical exchange volume on one side can be expressed with Equation 6.3, which is derived by Eysink (1989).

$$V_{vert} = 0.5 f_3 bh \left(\frac{\Delta\rho_w}{\rho_{w,out}} gh\right)^{0.5} dt \tag{6.3}$$

V_{vert}	Water exchange volume density currents	m^3
f_3	Vertical exchange coefficient	$-$
b	Width of chamber	m
h	Height of water column	m
Δ	Difference	$-$
ρ_w	Water density	kg/m^3
g	Gravitational acceleration	m/s^2
dt	Time step	s

As the lock chamber is a relatively short structure, the currents will be reflected back in a short time period. It is assumed that there exists a density equilibrium when the density current in fully reflected back. The time at which the equilibrium starts is thus depending on the speed of the density current. The speed of the density current can be determined using Equation 6.3, but without multiplying the number with time step dt. A sketch of the return current and layered equilibrium is given in Figure 6.4.

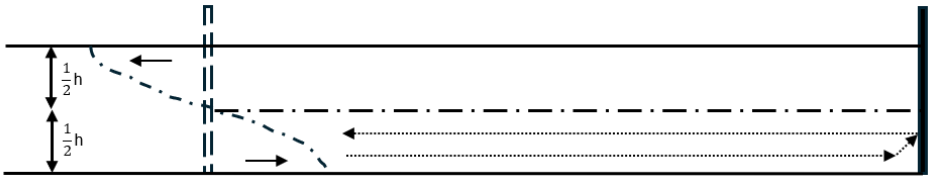

Figure 6.4: Density return current and equilibrium with high density water below and low density water on top.

The time required to reach the density equilibrium can be determined using Equation 6.4. Here, the time is calculated by dividing the total distance the current has to travel by the velocity of the current.

$$t_e = \frac{2L}{v_{vert}} \tag{6.4}$$

t_e	Time to density equilibrium	s
L	Length of chamber	m
v_{vert}	Velocity density currents	m/s

6.3.1. Salinity induced currents

Salt water has a larger density than fresh water and is therefore heavier and will move under the fresh water when they are made into contact. At the start of the calculation, the density of the water outside the locked system is set to $1025\ kg/m^3$ which is often used as a number for the density of sea water. The density of the water inside the lock is first set to $1000\ kg/m^3$. In Figure 6.3, the salt sea water would be on the left and the fresh water on the right.

6.3.2. Sediment induced currents

Water bodies with high suspended sediment concentrations have a larger density than water bodies without suspended sediment in it. The equation used to calculate the density of a suspension is stated below as Equation 6.5. The density of the suspension is depending on the density of the water without suspended particles, the sediment concentration and the density of the suspended particles. The density of the suspended particles is in this case set to $1600\ kg/m^3$.

$$\rho_{w,susp.} = \rho_w(1 - \frac{c}{\rho_d}) + c \tag{6.5}$$

ρ_w	Water density	kg/m^3
c	Suspended sediment concentration	kg/m^3
ρ_d	Sediment density	kg/m^3

The density currents induced by the suspended sediment concentrations move in a similar manner as the salinity induced currents. When looking at Figure 6.3, the water on the left would have a high suspended sediment concentration and the water on the right a low one.

6.4. Boat movements

After the equilibrium in density currents is reached, it is safe for boats to travel to or from the lock chamber. Large and heavy boats can also occupy a large volume underwater. As the water levels near the boat stay equal, boats are transporting water while moving, to account for the volume they occupy underwater. This is called the flushing property of a vessel. The largest design vessel was now assumed to have a length of $75\ m$, a width of $12\ m$ and a draught of $4.2\ m$. This corresponds to a total underwater volume of $3,780\ m^3$. As the width of the lock is not much larger than the width of the design vessel, it is assumed that the maximum speed of the design vessel when coming into or going out of the lock chamber is $3\ km/h$. The speed with which the water is moved by the design vessel is calculated with Equation 6.6. The discharge is then $42\ m^3/s$.

$$Q_{boat} = v_{boat} b_d d \tag{6.6}$$

Q_{boat}	Boat movement discharge	m/s
v_{boat}	Boat velocity	m/s
b_d	Width of design vessel	m
d	Draught of design vessel	m

After about $1.5\ min$, a water exchange volume equal to the total underwater volume is reached. Figure 6.5 presents a sketch of the boat and water movements. When a boat is entering the chamber, water from the chamber is transported outwards. In the case of a boat travelling from the chamber to the channel or an outside river, water from that channel or the river is transported into the chamber. The average velocity of water displacement can be calculated by dividing the discharge by the cross-sectional area of the water body, accounting for the reduction caused by the boat's draught.

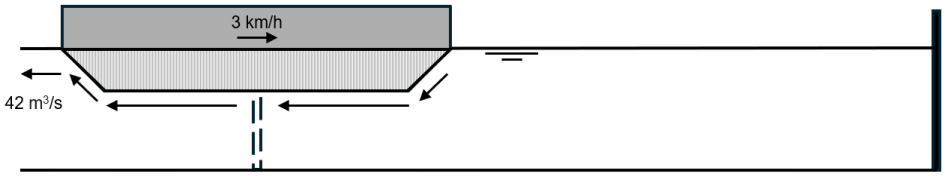

Figure 6.5: Water exchange volume due to boat movements.

6.5. Conclusion

The operational cycle of a lock is divided into phases, each characterised by distinct water exchange processes. These processes include filling and emptying, density currents, and boat movements. Two operational scenarios are considered, differing in the sequence of phases.

The water exchange volume during filling and emptying is calculated based on the use of gate openings. The velocity of the water flowing through the openings depends on the head difference. Density currents arise from differences in salinity and suspended sediment concentration, with higher density water flowing under lower density water. The water exchange volume resulting from density currents depends on the estimated vertical exchange coefficient. Boat movements also contribute to water exchange, as vessels entering or leaving the chamber transport water outward or inward, respectively. The analysis models one large design vessel travelling at a speed of $3\ km/h$.

The study assumes complete mixing of water in both the chamber and the channel. This means that the suspended sediment concentration and salinity are distributed evenly across the entire chamber as well as the channel.

7

Deposition and erosion

Before the water exchange processes can be simulated, a closer look into the vertical movement of suspended sediment and sediment bed particles is needed. This is done by looking at the sedimentation rate of a suspension above a certain bed. Sedimentation can be defined as the net bed level change. The rate of net bed level change is calculated by subtracting the erosion rate from the deposition rate, as can be seen in Equation 7.1 (Winterwerp et al., 2021).

$$S = D - E \tag{7.1}$$

S	Sedimentation rate	$kg/m^2/s$
D	Deposition rate	$kg/m^2/s$
E	Erosion rate	$kg/m^2/s$

7.1. Deposition

In this report, the schematized box method is used to model the water and sediment movements at the lock chamber entrances (van Rijn, 2005). The method focuses on the time-dependent behaviour of suspended sediment concentration in a basin. The basin is modelled as a box, which should be very similar to a lock chamber. The main outputs of the model are the sedimentation volume and thickness inside the basin. These can be expressed using Equations 7.2 and 7.3. In Equation 7.2, the sediment volume is computed by multiplying the water body area inside the so called 'box', with the effective settling velocity of the suspension divided by the sediment density, and the sum of the suspended sediment concentration at a certain time multiplied by a time step. With the water body area, the horizontal surface of the water is meant. For a lock chamber, this area would be the width of the lock multiplied by the length of the lock. The settling velocity of the suspension determines how fast sediments want so settle down. Because the definition of the settling velocity is somewhat complex, this is further described in Paragraph 7.1.1. The sediment density is assumed to be $1600\ kg/m^3$. The suspended sediment concentration for each time step can be determined by using the ratios of different water volumes and their according concentrations. The water volume ratios follow from the water exchange processes analysis.

$$V_s = A\frac{w_{s,eff}}{\rho_d}\Sigma(c\Delta t) \tag{7.2}$$

When the volume of the sediment that will settle is known, the sediment layer thickness can be calculated using Equation 7.3. Here, the sediment volume is divided by the area of the water body. The outcome is then in meters.

V_s	Sedimentation volume	kg/m^3
A	Area water body	m^2
$w_{s,eff}$	Effective settling velocity	m/s
ρ_d	Sediment density	kg/m^3
Σ	Sum	$-$
c	Concentration	kg/m^3
t	Time	s

$$\delta_s = \frac{V_s}{A} \tag{7.3}$$

δ_s	Sediment layer thickness	m

7.1.1. Settling velocity

Before the situations are elaborated, it is important to zoom in on the settling velocity used in Equation 7.2. For the first calculation stage, a constant settling velocity is assumed, but in reality this is depending on sediment characteristics like the floc diameter and the concentration of the suspended sediment. In a later stage of calculations, the suspended sediment concentration over a tidal cycle is incorporated. In this stage, an estimation of the according settling velocities is also used, as this might be of important influence. In Bangladesh, there are very high concentrations of fine sediment in the water coming inland from the tide. The goal of the sluice system is to minimise the concentrations between the locks.

The type of settling of the suspended particles depends on the concentration of the water body. Until a suspended sediment concentration of about $2.8\ kg/m^3$, the settling is unhindered and is primarily depending on the floc diameter (Winterwerp & van Kesteren, 2004). The settling velocity of the sediment in the water body can then be treated as the settling velocity of individual mud flocs in still water. Figure 7.1 presents a graph with data and model outputs on the settling velocity of individual mud flocs in still water for different floc diameters. In reality, the mud flocs will not be in still water. However, this can be a good first estimate of the upper boundary of the settled sediment. As mentioned in Chapter 3, the median sediment grain size in Mongla is $46\ \mu m$ and near Ghasiakhali this is $52\ \mu m$. These values correspond to a settling velocity of individual mud flocs of $0.17\ mm/s$ and $0.19\ mm/s$ respectively (using a fractal dimension of mud flocs, n_f, of 2.0).

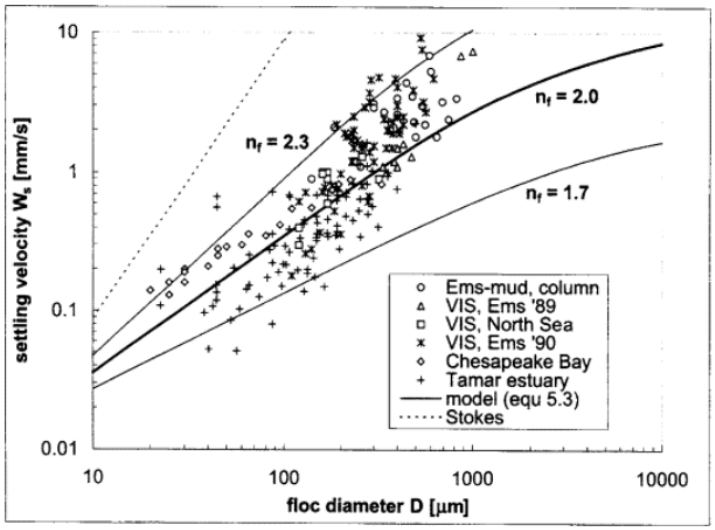

Figure 7.1: Settling velocity of individual mud flocs in still water and floc size (Winterwerp & van Kesteren, 2004).

From about $2.8\ kg/m^3$ to $100\ kg/m^3$, there is hindered settling where the velocity is primarily depending on the sediment concentration. Hindered settling is the process where the concentrations are high and

the flocs start to hinder each other in their settling, reducing the settling velocity. In Figure 7.2, a graph is shown with data and model outputs on the settling velocity in the hindered settling regime for different sediment concentrations.

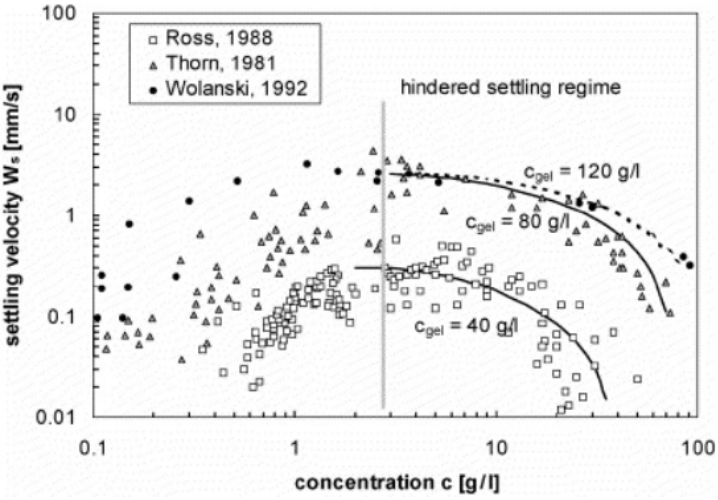

Figure 7.2: Settling velocity in hindered settling regime and sediment concentrations (Winterwerp & van Kesteren, 2004).

Figure 7.2 shows that the gelling concentration influences the settling velocity greatly. The gelling concentration is the sediment concentration at the transition from a water-supporting system to a sediment-supporting system (Kämpf & Myrow, 2014). According to Camenen and van Bang (2011), the estimation of the gelling concentration in case of cohesive sediments is fundamental in determining the sedimentation. However, the article also shows the difficulty of the determination of the variable. In the hindered settling regime, a low gelling concentration computes a lower settling velocity and represents a more critical condition for the sedimentation between the two locks. A higher gelling concentration with a higher settling velocity gives a more critical condition for the area inside the lock chamber as more sedimentation would occur here.

7.2. Erosion

The deposition is an upper limit for the calculation of the sedimentation. In reality, sediment may resuspend due to erosion. There has been a lot of research regarding the erosion processes of a bed (Mitchener & Torfs, 1996; van Rijn, 2020; Winterwerp et al., 2021). Still, it is often stated that the erosion of a certain natural bed remains hard to predict. Erosion and the resuspension of sediment particles in the bed are depending on the bed characteristics and certain erosion event properties which can enhance local flow velocities. The sediment that has eroded can either stay in the suspension or settle again in a further spot.

In the Mongla-Ghasiakhali waterway in Bangladesh, there is a natural bed of cohesive sediment with a bed composition of about 90% clay and silt and 10% sand. Properties of a cohesive bed that are important for predicting erosion, are the mixture contents of the bed, the history, the mineral composition, the organic content, and the pore water composition (Mitchener & Torfs, 1996; Winterwerp et al., 2021). To test a suspended sediment dynamics approach, a sufficiently long time series is required (Tognin et al., 2024). Specific events can enhance erosion processes, when they increase the near-bed flow velocity. The events occurring in a lock chamber which is under operation, that can increase this near-bed flow velocity are listed in Table 7.1.

The filling and emptying of a lock chamber happens through the lower part of the gates. During the filling of the chamber, the velocities induced by the process, can erode the settled sediment at the bottom, when these are high enough. The sediment can then be transported further away from the gate through which the filling is happening. When the chamber is emptied, the process can cause the same effect near the entrances of the lock chamber on the western or eastern side of it. A large amount of settled sediment in front of the lock gates, is able to obstruct the gates from opening. However, when the gates do open, they are able to push a possible sediment layer away and cause resuspension of a

Table 7.1: List of events that can enhance erosion processes.

Number	Erosion event
1	Filling/emptying process
2	Opening and closing of the lock gates
3	Density currents
4	Boat induced turbulence

part of it. During the movements of density currents, a high density water volume travels in the lower part of a water column, thus inducing a flow velocity near the bed that can in turn stir up an erosion process. At last, boat activity can cause an increase in turbulent water movements which can lead to more erosion. Verney et al. (2007) has shown that an erosion event can clearly be correlated with a boat passage. In the study of Safak et al. (2021), an increase in sediment transport due to boat traffic of 12% was found.

Whether erosion will really occur, depends on the actual bed-shear stress and the critical erosion bed-shear stress. Paragraph 7.2.1 presents several approaches to estimate the critical erosion bed-shear stress. In Paragraph 7.2.2, the method on how to calculate the applied bottom shear stress is presented. Equation 7.4 describes that erosion occurs if the applied bottom shear stress exceeds the critical shear stress for erosion.

$$\tau_b > \tau_{ce} \tag{7.4}$$

τ_b	Applied bottom shear stress	N/m^2
τ_{ce}	Critical shear stress for erosion	N/m^2

Mitchener and Torfs (1996) have presented a relation to describe the erosion rate, shown in Equation 7.5. It is also found that a mean value for the erosion constant (m_e) with $10-50\%$ sand, is $0.0002\ kg/N/s$. The erosion constant found for a 0% sand bed varies from 0.0004 to $0.0006\ kg/N/s$. The sand content of the bed material in the Mongla-Ghasiakhali waterway is about 10%. This is on the lower side of the $10-50\%$ range. For the first calculations, it is assumed that the erosion constant has an average value of $0.0003\ kg/N/s$.

$$E = \frac{dm}{dt} = m_e(\tau_b - \tau_{ce}) \tag{7.5}$$

$\frac{dm}{dt}$	Erosion rate	$kg/m^2/s$
m_e	Erosion constant	$kg/N/s$

The volume of the erosion can be determined by multiplying the erosion rate with the time step and area, and dividing this by the density of the bed material. The calculation step is shown in Equation 7.6. After this, the layer depth for where erosion occurs can be calculated in the same manner as in Equation 7.3.

$$V_e = A_e \frac{E}{\rho_d} \Sigma \Delta t \tag{7.6}$$

V_e	Erosion volume	kg/m^3
A_e	Erosion area	m^2

7.2.1. Critical bed-shear stress

Mitchener and Torfs (1996) have presented an approach to approximate the critical shear stress for erosion depending on the bulk density of an undisturbed sediment bed. Figure 7.3 presents the relation they found. The specific dry bulk density of the bed in Bangladesh is not known. Because the bed mainly consists of silt material, a bulk density of $1300\ kg/m^3$ is assumed here (Dong et al., 2013). The bulk density gives a critical shear stress for erosion of about $1\ N/m^2$ using the graph.

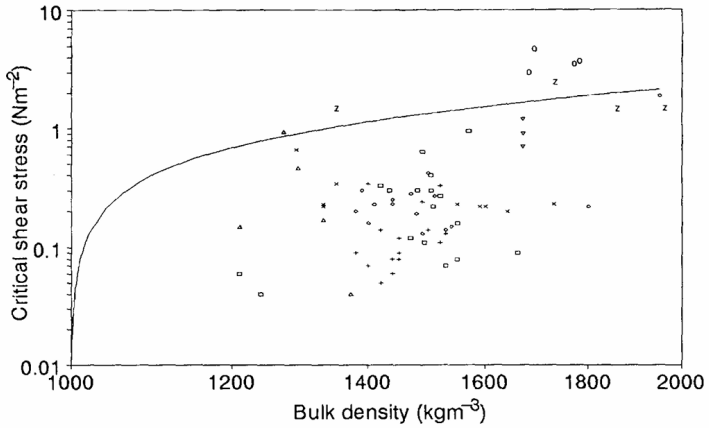

Figure 7.3: Critical bed-shear stress for erosion against the bulk density of a natural undisturbed sediment bed (Mitchener & Torfs, 1996).

The material properties of the bed used in the experiments of Jacobs (2011) are similar to the ones in the Mongla-Ghasiakhali case. The materials are dense and have a high silt percentage and a medium clay content. In the study of Jacobs (2011), a critical bed-shear stress for erosion of $1\ N/m^2$ was found.

According to van Rijn (2020), the critical bed-shear stress for mass and surface erosion of a mud-sand mixtures is depending on its dry bulk density and percentage of fines. The study has shown that with a percentage of fine bed material of 90%, a critical bed-shear stress of about $2\ N/m^2$ is found.

Recently, a new study has been conducted in which different bed samples with mud-sand mixtures have been taken and tested in a laboratory to determine its critical bed-shear stress (van Rijn et al., 2024). In the tests that were done, the bed samples are placed at the bottom of a scaled model and the current velocity is increased gradually until erosion could be observed. One group of bed samples they used, came from a site in the Bay of Bengal in Bangladesh. The samples from the Bay of Bengal in Bangladesh that were tested had a clay and silt content of 94%, a sand content of 6% and a dry density of $1260\ kg/m^3$. The contents of the bed in the Mongla-Ghasiakhali waterway were about 90% clay and silt and 10% sand. Thus, these contents are very similar to the ones of the Bay of Bengal samples in the study. The critical bed-shear stress for erosion for the bed that is studied in van Rijn et al. (2024), has been determined to be $1.5\ N/m^2$.

The approximated values for the critical bed-shear stress for a bed with similar properties as the bed in the Mongla-Ghasiakhali waterway are 1 to $2\ N/m^2$. As the latest study, van Rijn et al. (2024), has determined the critical bed-shear stress of bed samples in the same region as the case study of this report, it is assumed that this critical stress value will be most similar to the actual critical stress value for the erosion of the bed in the case study. On top of this, the value of $1.5\ N/m^2$ is also an average number in the earlier mentioned range that includes other studies. In the next phases, the critical bed-shear stress for erosion, τ_{ce}, is therefore set to the value of $1.5\ N/m^2$.

7.2.2. Applied bottom shear stress

In the study of van Rijn (1993), a formula for the applied time-averaged bed-shear stress has been derived. The formula is shown in Equation 7.7. The applied bottom shear stress that can be computed

with this, is depending on the density of the water, the gravitational acceleration, the depth-averaged velocity of the water and the Chézy coefficient.

$$\tau_b = \rho_w g \frac{\overline{u}^2}{C_h^2} \tag{7.7}$$

ρ_w	Water density	kg/m^3
g	Gravitational acceleration	m/s^2
$\overline{u}$	Depth-averaged velocity	m/s
C_h	Chézy coefficient	$m^{1/2}/s$

The basis of determining the depth-averaged velocity varies per water exchange process. The bed will only erode when a certain water velocity is reached. It is very likely that such a critical velocity only occurs near the heads of the navigation lock. For the erosion that can be induced by the filling and emptying system, it is assumed that the bed will only erode until a distance of $30\ m$ from the lock head. For the density currents, erosion is assumed to occur over the full length of the chamber. When there are only vessel movements causing erosion, it is assumed that they can erode the bed over a distance of $50\ m$ from the lock head.

A large uncertainty in defining the applied bottom shear stress can be caused by the uncertainty in the Chézy coefficient. During the operation of a navigation lock, the water depth can have large variations, including water depths that are considered to be shallow. Therefore, it is useful to use a Chézy value which is depending on the water depth. The formula for the Chézy coefficient depending on the depth that is often used in such cases is stated in Equation 7.8. The Chézy coefficient is then also depending on the Manning coefficient. Under the conditions of the case study, the Manning coefficient is often between 0.01 and $0.015\ m^{1/3}/s$. There will be more erosion, when the applied bottom shear stress is higher and thus when the Manning coefficient is higher. The sedimentation situation in the lock is most critical when there is minimal erosion. Therefore, the value for the Manning coefficient that will be used for now is $0.01\ m^{1/3}/s$.

$$C_h = \frac{1}{n} h^{1/6} \tag{7.8}$$

n	Manning coefficient	$m^{1/3}/s$
h	Height of water column	m

7.3. Sedimentation

The largest sedimentation occurs when there is deposition and no erosion. This happens when the water velocities are low. The water exchange processes can however induce high local flow velocities around the navigation lock heads. Not taking into account the erosion due to these higher local floc velocities, can lead to a design which is too conservative. In the later steps of this report, a distinction will be made between results that have included erosion processes and results that have not.

8

Sediment balance

The amount of sedimentation inside a lock chamber during an operating cycle is an important piece of information that is required to define the possible sedimentation problems inside the chamber. There are two different operation cycle scenarios identified in Chapter 6 with either ten or eight phases. The operational phases of the scenarios are set up to present the most critical conditions. For this same reason, the first calculations have been made using a maximum head difference and a maximum density difference.

8.1. Operational scenario 1

8.1.1. Phase 1: Filling from sea to chamber

The first phase of scenario 1 for which a sediment balance was set up is when the lock is filled with water from the sea side. Phase 1 occurs when boats are waiting on the sea side of the channel and the water inside the lock chamber is low and has to be levelled to let the boats into the chamber. It is estimated that the process can take up to $14\ min$. A schematization of the phase is given in Figure 8.1.

Figure 8.1: Sediment balance scheme for scenario 1, phase 1.

The formulas that were used in the calculation of the sediment processes during the first phase are given below. The index 'i' in the formulas refers to a certain time step. The calculations can be done for one time step, and then repeated using a loop over 'i' to compute the sedimentation over a longer time period. The formulas of the model calculations are now further explained.

The first step is to set the water exchange volume for the time step due to filling ($\Delta V_{F,i}$) equal to the discharge through the gate openings from the previous time step ($Q_{F,i-1}$). This value is then multiplied by the time step duration (dt). The water exchange volume due to density currents is neglected in this situation, as the contact surface between the two water bodies with different densities is rather small and the filling of the chamber already causes a force of water from left to right.

$$\Delta V_{F,i} = Q_{F,i-1} dt \tag{8.1}$$

Now that the water exchange volume is known, the new head difference between the river and lock chamber (Δh_i) can be calculated. This is done by taking the old head difference (Δh_{i-1}) and subtracting the height difference caused by the water exchange volume of that certain time step. The height difference is equal to the water exchange volume ($\Delta V_{F,i}$) divided by the horizontal surface area in the lock (A). The formula is valid under the condition that the newly computed head difference remains

positive. This is because the goal of the situation is to achieve water levelling. Once the water is levelled, the gates will be closed, and the head difference is assumed to be zero.

$$\Delta h_i = max(\Delta h_{i-1} - \frac{\Delta V_{F,i}}{A},\ 0) \tag{8.2}$$

With the new head difference, a new flow velocity ($v_{F,i}$) and discharge ($Q_{F,i}$) through the gate openings can be determined using the equations below. The equations are based on Equations 6.1 and 6.2.

$$v_{F,i} = \sqrt{2g\Delta h_i} \tag{8.3}$$

$$Q_{F,i} = aCv_{F,i} \tag{8.4}$$

Then, when the head difference is above zero, the total volume inside the lock chamber ($V_{in,i}$) is updated with the water exchange volume. When the head difference is not above zero, the volume inside the lock chamber remains the same. The value for the volume inside the chamber is needed for the calculation of the concentration in the chamber.

$$V_{in,i} = \begin{cases} V_{in,i-1} + \Delta V_{F,i}, & \Delta h_i > 0 \\ V_{in,i-1}, & \Delta h_i \leq 0 \end{cases} \tag{8.5}$$

The new water density and suspended sediment concentration of the water inside the chamber ($\rho_{in,i}$ and $c_{in,i}$ respectively) are calculated using volume ratios. The formulas consist of two similar parts that are added up. The formula for the concentration has an extra part. The first similar part is the ratio of the water that has come from the sea side into the lock chamber ($\frac{\Delta V_{F,i}}{V_{in,i}}$) multiplied by the density or suspended sediment concentration of the outside water (ρ_{out}, c_{out}). The second similar part consists of the ratio of the water that was already in the lock chamber and remains there ($\frac{V_{in,i}-\Delta V_{F,i}}{V_{in,i}}$), multiplied with the inside water density or suspended sediment concentration at the time step just before the current time step ($\rho_{in,i-1}$, $c_{in,i-1}$). The extra part in the formula for the concentration is the subtraction of the sediment that is settling down at a time step. This reduces the suspended sediment concentration in the water. The reduction is calculated by multiplying the change in sedimentation volume that has already included erosion processes ($\Delta V_{se,i-1}$) with the sediment particle density (ρ_d) and dividing this product by the water volume in the chamber ($V_{in,i}$).

$$\rho_{in,i} = \frac{\Delta V_{F,i}}{V_{in,i}}\rho_{out} + \frac{V_{in,i} - \Delta V_{F,i}}{V_{in,i}}\rho_{in,i-1} \tag{8.6}$$

$$c_{in,i} = \frac{\Delta V_{F,i}}{V_{in,i}}c_{out} + \frac{V_{in,i} - \Delta V_{F,i}}{V_{in,i}}c_{in,i-1} - \frac{\Delta V_{se,i-1}\rho_d}{V_{in,i}} \tag{8.7}$$

The density of the water, assuming no suspended materials are present, is in every time step converted to the density of the water with a certain suspended sediment concentration. This is done by using Equation 6.5 from Chapter 6. How this equation is dependent on time step 'i' is indicated below.

$$\rho_{in,susp,i} = \rho_{in,i}(1 - \frac{c_{in,i}}{\rho_d}) + c_{in,i} \tag{8.8}$$

After the suspended sediment concentration at a time step is known, the volume of the sediment that will settle in that time step ($V_{sed,i}$) can be calculated. This calculation is done based on Equation 7.2. After this, the accumulated sediment volume in the lock ($\Sigma V_{sed,i}$) is updated by adding the new value.

$$V_{sed,i} = A\frac{w_{s,eff}}{\rho_d}c_{in,i}dt \tag{8.9}$$

$$\Sigma V_{sed,i} = \Sigma V_{sed,i-1} + V_{sed,i} \tag{8.10}$$

The sediment layer thickness in the chamber ($\delta_{sed,i}$) can be determined based on Equation 7.3 from Chapter 7. The last step is to add the sediment layer thickness to the accumulated one ($\Sigma\delta_{sed,i}$). The steps of the calculation are shown below.

$$\delta_{sed,i} = \frac{V_{sed,i}}{A} \tag{8.11}$$

$$\Sigma\delta_{sed,i} = \Sigma\delta_{sed,i-1} + \delta_{sed,i} \tag{8.12}$$

The sedimentation volume and sediment layer thickness that have now been calculated, do not take erosion into account yet. Because the case of no erosion gives the most critical sedimentation case for inside the lock chamber and the erosion parameters are based on a few uncertain assumptions, it is important to also consider the case of no erosion. However, when the erosion is large, it is also important to understand when and to what extent erosion could occur. That is why, in the next explanation and formulas, the sedimentation volume and sediment layer thickness are computed when there is erosion present.

The computation of the depth-averaged velocity in the chamber near the left gate during the filling process ($\overline{u}_{F,i}$) is needed in order to determine the applied bottom shear stress in this area. This velocity is estimated by dividing the discharge through the gate openings due to filling in the chamber ($Q_{F,i}$) by the cross sectional area of the water body which it will immediately meet when entering this. The cross sectional area of the water body consists of the width (W) multiplied by the water level in the chamber at that time ($h_{in,i}$).

$$\overline{u}_{F,i} = \frac{Q_{F,i}}{W h_{in,i}} \tag{8.13}$$

After the depth-averaged velocity near the openings is known, the Chézy coefficient ($C_{h,i}$) and the applied bottom shear stress near this area ($\tau_{b,i}$) can be calculated based on Equations 7.8 and 7.7 respectively. The specifics of the equations are shown below.

$$C_{h,i} = \frac{1}{n} h_{in,i}^{1/6} \tag{8.14}$$

$$\tau_{b,i} = \rho_{in,susp,i} g \frac{\overline{u}_{F,i}^2}{C_{h,i}^2} \tag{8.15}$$

Now, the erosion rate in the area where the depth-averaged velocity is considered to be present. Erosion only occurs when the applied bottom shear stress is larger than the critical bed-shear stress. When this is the case, the erosion rate can be calculated using the earlier discussed Equation 7.5.

$$E_i = \begin{cases} m_e(\tau_{b,i} - \tau_{ce}), & \tau_{b,i} > \tau_{ce} \\ 0, & \tau_{b,i} \leq \tau_{ce} \end{cases} \tag{8.16}$$

The volume of the sediment that is eroded in the area can be computed by using Equation 7.6 from Chapter 7. This equation first takes the area in which erosion occurs (A_e) and then multiplies this with the erosion rate, E, divided by the density of the suspended particles, ρ_d, and with the time step dt.

$$V_{e,i} = A_e \frac{E_i}{\rho_d} dt \tag{8.17}$$

After the volume of eroded material is known, the total sedimentation volume including the consideration of erosion ($\Sigma V_{sed,e,i}$) can be calculated by taking the total sedimentation volume ($\Sigma V_{sed,i}$) and subtracting the erosion volume ($V_{e,i}$).

$$\Sigma V_{sed,e,i} = \Sigma V_{sed,i} - V_{e,i} \tag{8.18}$$

The last step in the calculation of the sedimentation for phase 1, is to calculate the sediment layer thickness which includes erosion processes. It is assumed that erosion will only occur near the gate openings. However, there are also other turbulent water streams which can lead to the redistribution of the layer thickness of the bottom sediment. Next to this, sediment can slip into the eroded zone when the layer thickness here is much lower than the non-eroded zone. Due to these effects, and for simplicity, the average sediment layer thickness inside the lock chamber over its full horizontal area is computed, this is referred to as $\Sigma\delta_{sed,e,i}$. The thickness is determined by dividing the total sedimentation volume including the consideration of erosion ($\Sigma V_{sed,e,i}$) by the whole horizontal area of the chamber (A).

$$\Sigma\delta_{sed,e,i} = \frac{\Sigma V_{sed,e,i}}{A} \tag{8.19}$$

8.1.2. Phase 2: Density currents sea side

The second phase occurs when the gates of the chamber are opened on the sea side. The water levels are equal, but there is a difference in density of the water bodies. The difference in density induces density currents which also transport sediment. The time for the occurrence of the phase is set to $4\ min$. Figure 8.2 gives a schematic overview of the phase.

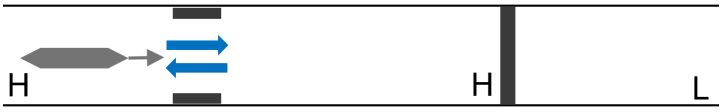

Figure 8.2: Sediment balance scheme for scenario 1, phase 2.

The formulas for the calculation of this sediment transport and according sediment thickness layer are given below. The index 'i' refers to a certain time step again. The steps will now be further explained.

The water exchange volume that is induced by the density currents ($V_{vert,i}$) is based on the earlier mentioned Equation 6.3. One density current moves from left to right and the other one moves in the opposite direction. There is no volume exchange due to boat movement taken into account yet, because it is assumed that the vessels will wait until the density currents are in equilibrium before moving into the chamber. The time to reach the density equilibrium is calculated using Equation 6.4.

$$V_{vert,i} = 0.5 f_3 bh\left(\frac{\Delta\rho_{out,susp,i-1}}{\rho_{out}} gh\right)^{0.5} dt \tag{8.20}$$

The next step is calculating the new water density and suspended sediment concentration inside the lock chamber. It is assumed that when the outside water density is larger than the inside water density, there are indeed density currents. The inside density cannot surpass the outside water density due to natural limitations. This boundary can be seen in the right part of Equation 8.21 and 8.22. When the densities of the two water bodies become nearly the same, there are no density currents present. In this case, the water density inside the chamber is set equal to the value of the water density inside the chamber of one earlier time step. The water densities, in this case, are including the effect that suspended sediment can have on the density. The calculation of the water density including this effect is done in the same manner as for phase 1 (Equation 8.8). The suspended sediment concentration when there are no density currents is equal to the concentration of one time step earlier minus the reduction of the sediment that was first in the suspension and has settled in the last time step. This reduction is calculated in the same manner as for Equation 8.7.

The water density and suspended sediment concentration in the chamber when there are density currents, can be calculated using volume ratios. The ratio of volume of the water coming from the sea side into the lock with regards to the total volume inside ($\frac{V_{vert,i}}{V_{in}}$) is multiplied by the water density or suspended sediment concentration of the water body coming from the outside (ρ_{out} and c_{out} respectively). The second term in the equations, which is added up to this first part, is the volume ratio of the water that was already and remains inside the chamber with respect to the total volume inside ($\frac{V_{in}-V_{vert,i}}{V_{in}}$), multiplied by the water density or suspended sediment concentration of the water in the chamber at

one earlier time step ($\rho_{in,i-1}$, $c_{in,i-1}$). In the equation for the suspended sediment concentration, a reduction term to account for the settled sediment of one earlier time step needs to be included again.

$$\rho_{in,i} = \begin{cases} \frac{V_{vert,i}}{V_{in}}\rho_{out} + \frac{V_{in}-V_{vert,i}}{V_{in}}\rho_{in,i-1}, & \rho_{out,susp,i} > \rho_{in,susp,i-1} \\ \rho_{in,i-1}, & \rho_{out,susp,i} \leq \rho_{in,susp,i-1} \end{cases} \tag{8.21}$$

$$c_{in,i} = \begin{cases} \frac{V_{vert,i}}{V_{in}}c_{out} + \frac{V_{in}-V_{vert,i}}{V_{in}}c_{in,i-1} - \frac{\Delta V_{se,i-1}\rho_d}{V_{in,i}}, & \rho_{out,susp,i} > \rho_{in,susp,i-1} \\ c_{in,i-1} - \frac{\Delta V_{se,i-1}\rho_d}{V_{in,i}}, & \rho_{out,susp,i} \leq \rho_{in,susp,i-1} \end{cases} \tag{8.22}$$

The water density difference of the outside water body and the water body inside the chamber ($\Delta\rho_{out,susp,i}$) is needed for the computation of the water exchange volume. The difference is computed by taking the water density outside ($\rho_{out,susp}$) and subtracting the water density inside ($\rho_{in,susp,i}$).

$$\Delta\rho_{out,susp,i} = \rho_{out,susp} - \rho_{in,susp,i} \tag{8.23}$$

After this, the sedimentation without erosion can first be calculated using the same formulas as for phase 1: Equations 8.9 to 8.12. For the calculation with erosion, the depth-averaged flow velocity near the lock head due to the density currents, $\overline{u}_{dens,i}$, is important. The flow velocity is assumed to only occur in the specific erosion area (A_e). The depth-averaged velocity is then determined by dividing the vertical exchange volume ($V_{vert,i}$) per time step (dt) by the width of the chamber (W) and half of the inside water depth at that time ($h_{in,i}$).

$$\overline{u}_{dens,i} = \frac{V_{vert,i}/dt}{0.5Wh_{in,i}} \tag{8.24}$$

Once the depth-averaged flow velocity in the erosion area is known, the sedimentation volume and sediment layer thickness including erosion processes can be calculated using the same equations as for phase 1: Equations 8.14 to 8.19. Finally, the sediment volumes and sediment layer thicknesses are obtained for when there is erosion, as well as the situation for when there is no erosion.

8.1.3. Phase 3: Boat from sea to chamber

In the third phase, a vessel moves from the sea side to the right, into the lock chamber. The process is assumed to take up to $6\ min$. During the vessel movements, water is transported from the lock chamber to the sea side. The density of the water inside the chamber is not affected by this.

Figure 8.3: Sediment balance scheme for scenario 1, phase 3.

The important change in conditions during this process is in the total volume of water present in the chamber ($V_{in,i}$). There is a maximum water exchange volume which is equal to the underwater volume of the design vessel ($V_{boat,max}$). Water will only be exchanged when this maximum volume is not yet reached. Otherwise, the volume inside the chamber remains the same as the volume of one step earlier ($V_{in,i-1}$). The water which is exchanged during a time step of $10\ sec$ is referred to as ΔV_{boat}. The total water volume which is exchanged during a certain time step is called $V_{boat,i}$. In the equations below, the calculation of the water volume inside the chamber and the water exchange volume due to boat movements is shown. The d_i in the equations is the number of the step for which the calculation is done.

$$V_{in,i} = \begin{cases} V_{in,i-1} - \Delta V_{boat}, & \Delta V_{boat}d_i < V_{boat,max} \\ V_{in,i-1}, & \Delta V_{boat}d_i \geq V_{boat,max} \end{cases} \tag{8.25}$$

$$V_{boat,i} = \begin{cases} \Delta V_{boat} d_i, & \Delta V_{boat} d_i < V_{boat,max} \\ V_{boat,max}, & \Delta V_{boat} d_i \geq V_{boat,max} \end{cases} \tag{8.26}$$

The suspended sediment concentration is only affected by the concentration of a time step earlier ($c_{in,i-1}$) and the reduction due to sediment that was initially in the suspension and has now settled. This reduction is again calculated by taking the sedimentation volume including erosion of one earlier time step ($\Delta V_{se,i-1}$), multiplying it with the sediment density (ρ_d) and dividing this by the water volume in the chamber ($V_{in,i}$).

$$c_{in,i} = c_{in,i-1} - \frac{\Delta V_{se,i-1} \rho_d}{V_{in,i}} \tag{8.27}$$

After the concentration calculation, the steps in Equations 8.9 to 8.12 can be repeated to calculate the sedimentation volume and sediment layer thickness in the chamber when there is no erosion.

To calculate the sedimentation including erosion, the depth-averaged flow velocity near the boat movement, $\overline{u}_{boat,i}$, needs to be calculated. This only occurs in the estimated area of erosion (A_e) for the specific water exchange process. The velocity can be determined by dividing the water volume (ΔV_{boat}) which is exchanged per time step (dt) by the cross sectional area of the water body without the presence of a vessel ($W h_{in,i}$) minus the underwater volume which is taken up by the vessel itself ($b_d d$).

$$\overline{u}_{boat,i} = \frac{\Delta V_{boat}/dt}{W h_{in,i} - b_d d} \tag{8.28}$$

When the velocity in the erosion area is calculated, the sedimentation volume and sediment layer thickness including erosion can be determined in the same manner as for the previous phases (Equations 8.14 to 8.19).

8.1.4. Phase 4: Emptying from chamber to channel

Phase 4 is similar to phase 1, but now the chamber is emptied instead of filled, to lower the water level inside the lock chamber. The density of the water in the chamber remains the same. Parameters that do change are the head difference, emptying velocity and discharge, and the total volume of water inside the chamber. The time in which phase 4 occurs is again set to $14\ min$. The situation takes place when boats want to pass from west to east and are already in the chamber. The situation is visualized in the scheme in Figure 8.4.

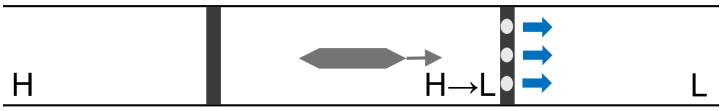

Figure 8.4: Sediment balance scheme for scenario 1, phase 4.

The formulas for the sedimentation calculation are very similar to the equations used in phase 1: Equations 8.1-8.19. One of the differences is that now the emptying volume and discharge is used, instead of the filling one. The difference is distinguished through the use of different subscriptions. The other difference is the sign in Equation 8.5, which is now negative instead of positive. Because the set of equations are almost the same as for phase 1, only the new equation for the volume inside the lock chamber is stated below.

$$V_{in,i} = \begin{cases} V_{in,i-1} - \Delta V_{E,i}, & \Delta h_{c,i} > 0 \\ V_{in,i-1}, & \Delta h_{c,i} \leq 0 \end{cases} \tag{8.29}$$

The sediment concentration inside the chamber is only depending on the settling of the sediment. The concentration can be calculated using Equation 8.27.

It is assumed that there is no erosion of the bed inside the chamber due to the emptying process. This is due to the fact that the inlets of the gate openings are not very close to the bed and when bed material starts to erode and move towards the channel side, the material encounters the gate first and a large part will settle again.

8.1.5. Phase 5: Density currents channel side

Phase 5 occurs when the gates of the lock are open on the channel side and vessels are not moving yet. The main flow that occurs and influences sediment concentrations is induced by the density currents due to density differences of the water bodies. It is assumed that the process of the density currents reaching an equilibrium can take up to $4\ min$. In Figure 8.5, a schematic overview of the phase is presented.

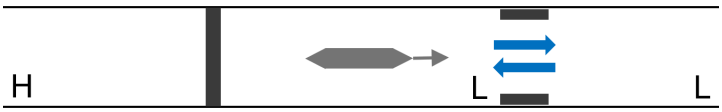

Figure 8.5: Sediment balance scheme for scenario 1, phase 5.

The sediment concentrations, volume and layer thickness can be calculated by using almost the same equations as for phase 2. A difference is that in phase 2, the density difference was between the water on the sea side and the water inside the chamber ($\Delta\rho_{out,susp,i}$), and in phase 5, this difference is between the water inside the chamber and the water in the channel ($\Delta\rho_{c,susp,i}$).

$$\Delta\rho_{c,susp,i} = \rho_{in,susp,i} - \rho_{c,susp,i} \tag{8.30}$$

The other equations needed for the sedimentation calculation of phase 5 remain the same as the equations used in phase 2.

8.1.6. Phase 6: Boat from chamber to channel

In the sixth phase, a boat moves from inside the chamber into the channel on the right side. During the boat movements, water is transported into the lock chamber. In Figure 8.6 a schematic overview of the phase with its water exchange direction is shown. The phase is assumed to occur in a period of $6\ min$.

Figure 8.6: Sediment balance scheme for scenario 1, phase 6.

The equations that are used to model the sediment transport and sedimentation process during phase 6 are similar to the ones used in phase 3. The equations that are adapted for phase 6, are the equation for the water volume inside the chamber ($V_{in,i}$) and the equation for the suspended sediment concentration inside ($c_{in,i}$). Now, the volume is increased during the process instead of decreased. The new formula for the water volume inside the chamber is stated below.

$$V_{in,i} = \begin{cases} V_{in,i-1} + \Delta V_{boat}, & \Delta V_{boat} d_i < V_{boat,max} \\ V_{in,i-1}, & \Delta V_{boat} d_i \geq V_{boat,max} \end{cases} \tag{8.31}$$

The suspended sediment concentration inside the chamber is calculated by taking the water volume ratios dependent on the water exchange volumes due to the boat movements.

$$c_{in,i} = \frac{\sum \Delta V_{boat}}{V_{in,i}} c_{ch,i-1} + \frac{V_{in,i} - \sum \Delta V_{boat}}{V_{in,i}} c_{in,i-1} - \frac{\Delta V_{se,i-1}\rho_d}{V_{in,i}} \tag{8.32}$$

After adapting the formulas for the water volume and suspended sediment concentration inside the chamber and changing the information on the outside water to information about the water in the channel, the rest of the equations of phase 3 can be used to complete the sediment calculation.

8.1.7. Phase 7: Boat from channel to chamber

Phase 7 occurs when a boat moves from the channel side into the lock chamber. The boat movement induces a water exchange volume from inside the lock chamber to the channel. The time in which phase 7 occurs is set to $6\ min$. A schematic overview of the phase is given in Figure 8.7.

Figure 8.7: Sediment balance scheme for scenario 1, phase 7.

The construction of the equations and water exchange volume conditions are similar to the ones of phase 3. An important feature that needs to be changed is that you now need the information about the water body in the channel (next to the information about the water body in the chamber) instead of the information about the water body on the sea side. There is no significant change in the equations or signs in the equations that are changed with respect to the equations in phase 3.

8.1.8. Phase 8: Filling from sea to chamber

In phase 8, the lock chamber is filled, with a boat already in the chamber, to change the water level inside it from low water to high. The time in which phase 8 occurs is again estimated to be $14\ min$. A schematic overview of the phase can be seen in Figure 8.8.

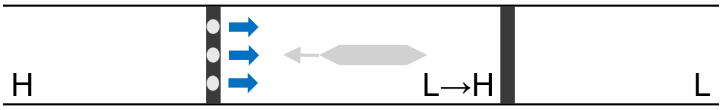

Figure 8.8: Sediment balance scheme for scenario 1, phase 8.

The sediment balance equations that can be used to simulate phase 8 are the same equations that are used to simulate phase 1 of scenario 1.

8.1.9. Phase 9: Density currents sea side

After the filling of the chamber in phase 8, the gates are opened on the left side of the chamber and density currents between the sea side and the water in the chamber can occur. The time in which phase 9 occurs is set to $4\ min$. Figure 8.9 shows an overview of the phase and its water exchange directions.

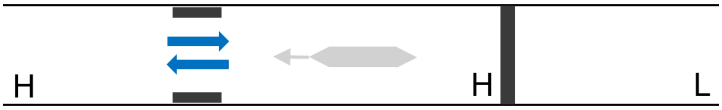

Figure 8.9: Sediment balance scheme for scenario 1, phase 9.

The equations that help simulate the phase during its period are the same equations that were used for phase 2.

8.1.10. Phase 10: Boat from chamber to sea

In the last phase of operational scenario 1, a boat leaves the chamber towards the sea side. The boat movement causes a water volume from the sea side to enter the chamber. An overview of the phase is given in Figure 8.10. The phase occurs for a period of about $6\ min$.

For the method of calculating the sediment transport and sedimentation during phase 10, almost all of the same equations as for phase 3 can be used. The exception is in Equation 8.5. In this equation, the

Figure 8.10: Sediment balance scheme for scenario 1, phase 10.

sign changes for phase 10 because there is now water coming into the chamber instead of leaving the chamber. The equation that should replace Equation 8.5 is Equation 8.31.

8.1.11. Conclusion

Each phase of operational scenario 1 has slight changes in the construction of the sediment balance equations. However, there are also a lot of equations that are repeated. Because it is easy to get lost in the repetitions and slight variations of the equations used in each phase, an overview of which set of equations to use in each phase is presented in Appendix A. The equations in the appendix are listed per phase and are set in the order in which they should be used.

8.2. Operational scenario 2

The second operational scenario consists of the same kind of phases as scenario 1, but now in a different order. The schematic overview of the phases of scenario 2 can be seen in Figure 6.2. It is unnecessary to explain the specific set of equations of the sediment balance calculation for each phase of scenario 2, as they are already explained in the phases of scenario 1. What is needed however, is an overview of which phase of scenario 1 corresponds to the phases of scenario 2. Then, the same set of equations can be used for these phases. The overview of the corresponding phases of the scenarios is given in Table 8.1, in which the phases of scenario 2 are first listed, and then the corresponding phases of scenario 1 are given.

Table 8.1: Phase comparison scenario 2 and 1.

Phases scenario 2	Corresponding phases scenario 1
1	7
2	8
3	9
4	10
5	3
6	4
7	5
8	6

9

Cyclic sedimentation

This chapter will go into the integration of the subsequent phases from Chapter 8 into one model so that it correlates to one operating cycle of the lock. An operational cycle can occur following the phases of operational scenario 1 of Table 6.1 or the phases of operational scenario 2 of Table 6.2. Using an operating scheme of Table 4.1, the operation can be simulated during one tidal cycle. Depending on the operating scheme, this will include multiple operational cycles. The simulations are done for the scheme with 12 lock operating hours (two way traffic) and 24 lock operating hours (fully operational). During one operational cycle, the water level on the outside of the lock and the suspended sediment concentration of the water outside can be assumed constant. During a tidal cycle, the water level and suspended sediment concentration will vary in time. However, the variation of these variables is not known at the time. Therefore, these are first assumed to be constant as well. After one operational cycle and one tidal cycle is simulated, a longer time period including multiple tidal cycles can be simulated. This is done in Paragraph 9.3. There are model checks introduced after every paragraph to make a quick estimate about whether the outcomes of the model are reasonable.

9.1. Operational cycle

The first operational cycles are computed using the maximum head difference of the case study of $5.0\,m$. The maximum head difference gives the most critical scenarios for the phases with a filling/emptying water exchange volume. Next to this, the first calculations are done by assuming the largest density differences as this gives the most critical scenarios for the phases with density currents. Therefore, the initial density of the water in the channel is assumed to be $1000\ kg/m^3$ and that of the water outside the lock system $1025\ kg/m^3$. This is excluding the influence of suspended sediment concentrations on the water density. The discharge coefficient is assumed to be 0.6 and the vertical exchange coefficient 0.3. The suspended sediment concentration in the water from the sea side is first set to $3\ kg/m^3$ and the concentrations inside the lock chamber and in the channel are set to zero. The sediment balance calculations are first done with a settling velocity of $0.17\ mm/s$. After this first calculation, the maximum suspended sediment concentration is determined for the operational cycle. When the maximum concentration is larger than $2.8\,kg/m^3$, an appropriate reduction of the settling velocity should be applied due to hindered settling, on the basis of Figure 7.2. The source code of the calculation in Python can be seen in Appendix B. Because the calculation methods for the two scenarios are very similar, only the code for scenario 1 is presented here. The outcomes of the simulations for the two operational scenarios are now analysed separately.

9.1.1. Operational scenario 1

The suspended sediment concentrations inside the lock chamber during one operational cycle, that will occur under the conditions mentioned above, are given in Figure 9.1a. It can be seen that there is a parabolic increase in concentration during the first two phases. This is due to the filling of the chamber and the water exchange volume containing sediment during the period in which the gates are open. In phase 3, water volume from inside the chamber is transported towards the sea side, due to boat

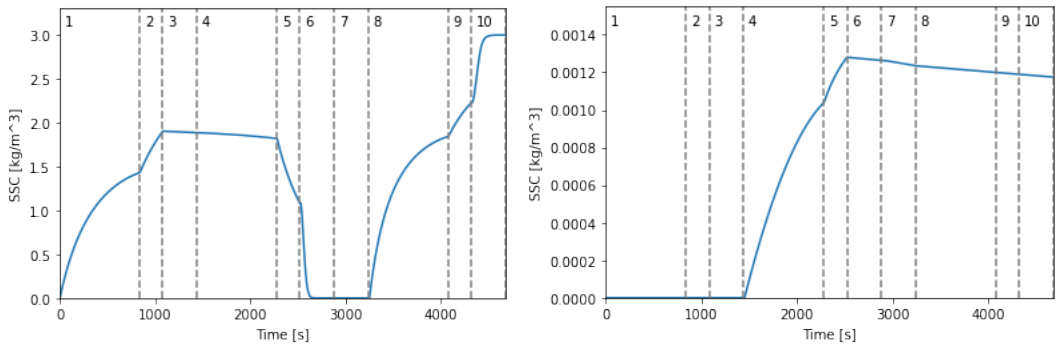

(a) lock chamber

(b) channel

Figure 9.1: Suspended sediment concentration for one operational cycle, scenario 1.

movements. The concentration inside the chamber remains almost constant in this case. The slight decrease is due to the settling of suspended sediment. In phase 4, the chamber is emptied through gate openings. The decrease in suspended sediment concentration is again only caused by the settling of a part of the sediment. In the fifth phase, there is a parabolic decrease of the concentration, as there will be an exchange of water volume with a water body containing a lower salinity. In phase 6, there is also a decrease in the concentration inside the chamber, caused by the water exchange volume due to boat movements going from the channel (lower concentration) towards the chamber (higher concentration). In phase 7, there is, just like in phase 3, only water going out of the chamber. The suspended sediment concentration remains constant here. The eighth phase resembles phase 1 of the scenario. Here, the chamber is filled with water from the sea side that has a high concentration and a parabolic increase can be seen. In phase 9, there is also water from the sea side transported into the chamber due to density currents. Here, the graph also shows a parabolic increase in sediment concentration in the chamber. In the last phase, water from the sea side is transported into the chamber due to boat movements. There is an increase in suspended sediment concentration, until the maximum water exchange volume due to the design vessel is reached. Then, the concentration remains roughly constant.

In the next figure, Figure 9.1b, the suspended sediment concentration inside the channel in between the two locks is presented during one operational cycle. In the first three phases, there is no connection between the water inside the chamber and the water inside the channel, so the suspended sediment concentration in the channel remains at a constant value of zero. In the following two phases, phase 4 and 5, the suspended sediment concentration curve follows a same kind of parabolic increase as the first two phases of the curve for the suspended sediment concentration inside the lock chamber, as these two processes are repeated, but now with different water body characteristics. In phase 6 and 7 there are water volumes exchanged between the chamber and the channel. However, the suspended sediment concentrations of both water bodies is close to zero. That is why there is only a small decrease shown in the suspended sediment concentration graph in the channel during phase 6 and 7. This decrease is also due to the settling of a part of the sediment that was first in the suspension. In the last three phases, there is no connection again between the lock chamber and the channel, so the concentration inside the channel only shows a small decrease due to the settling.

Excluding erosion

The sediment layer thickness inside the lock chamber during one operational cycle is plotted in Figure 9.2a. It can be seen that the layer thickness has a slight parabolic increase in the first two phases, and is then linear until phase 6. The parabolic increase is due to the increase of the suspended sediment concentration inside the chamber at the same time. The linear increase during phase 3 and 4 occurs as the concentration then remains constant. In phase 5 and the beginning of phase 6, the increase in layer thickness is a bit weakened. This is logical, as the concentration decreases in these phases, but the suspended sediment staying inside the lock chamber keeps settling. The layer thickness in the middle of phase 6 and in phase 7 remains constant, because the sediment concentration inside the chamber is then close to zero. During phase 8 to 10, the sediment layer thickness inside the chamber is increasing parabolically again, as the concentration in the chamber increases as well. The sediment layer thickness at the end of the operational cycle, without taking erosion into account, is $6.93 * 10^{-4}\ m$

for scenario 1.

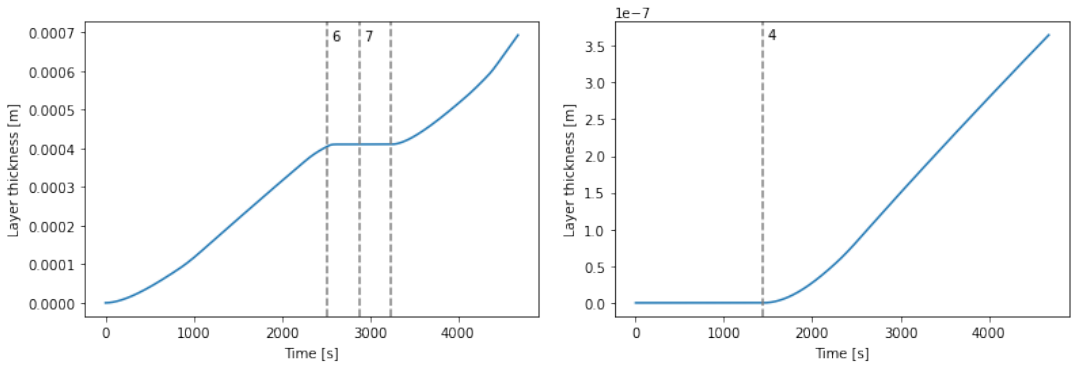

(a) lock chamber **(b)** channel

Figure 9.2: Sediment layer thickness without erosion for one operational cycle, scenario 1.

Figure 9.2b shows the growth of a sediment layer inside the channel between the two locks. During the three phases, there is no sediment layer as there is no suspended sediment in the water yet. From the start of phase 4, the graph shows a mildly parabolic growth of the layer thickness, because the concentration in the channel is then also increasing. After phase 5, the concentration in the channel remains constant and this can also be seen in the sediment layer thickness graph, as the increase in thickness is linear from here. The sediment layer thickness in the channel after the simulation, without taking erosion into account, is equal to $3.65 * 10^{-7}\ m$.

Including erosion

When there is erosion present, the suspended sediment concentration graphs do not change. There is only erosion calculated for the sediment layer inside the lock chamber. The sediment layer thickness graph for inside the chamber can change when there is erosion included. However, the simulation has shown that for this situation and these conditions, the graph does not show a visible change. One of the causes for this, can be seen when the figure of the applied bottom shear stress is plotted. This graph is shown in Figure 9.3. With a critical bed-shear stress of $1.5\ N/m^2$, it can be concluded that the value is only exceeded during phase 6 and 7. This is caused by the fact that the water volume inside the chamber is then low and a boat travels near the lock heads with a small space between the bottom of the boat and the bottom of the lock. The erosion volume remains below $2.10 * 10^{-3}\ m^3$. There is no change in the value for the sediment layer thickness in the chamber at the end of the simulation of scenario 1.

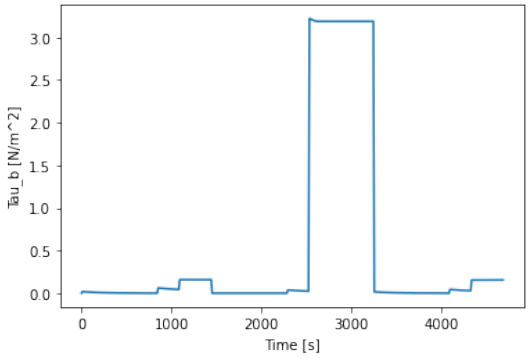

Figure 9.3: Applied bottom shear stress in certain areas of the chamber for one operational cycle, scenario 1.

9.1.2. Operational scenario 2

In operational scenario 2, there are only eight phases. The suspended sediment concentration during one operational cycle for these eight phases inside the lock chamber is shown in Figure 9.4a. During phase 1, the suspended sediment concentration inside the chamber remains zero, because there is

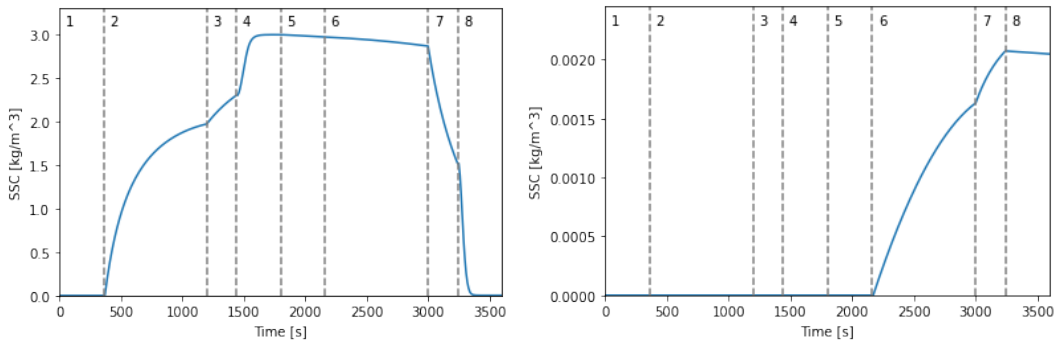

(a) lock chamber **(b)** channel

Figure 9.4: Suspended sediment concentration for one operational cycle, scenario 2.

only an outflow of the water in the chamber due to a boat that is moving into it. In the following three phases, there is an increase seen in the concentration, as there is a water volume coming from the sea side into the chamber in all of these phases. In phase 2, this is due to the filling of the chamber. In phase 3, this is due to the density currents between the water volume on the sea side and the water volume in the chamber. In phase 4, the water volume exchange is due to a boat leaving the chamber. The concentration stops increasing in this phase, when the maximum water exchange volume due to boat movements is reached. The slight decrease in the concentration is due to the settlement of suspended sediment. In phase 5 and 6, there is only water going out of the chamber, so the concentration inside it remains almost constant. The decrease in concentration in these phases follows the same direction as the second part of phase 4, as the decrease is only caused by sediment that is settling here. During the seventh phase, there are density currents between the water in the chamber (higher concentration) and the water in the channel (lower concentration). The concentration inside the chamber then decreases parabolically. In the last phase of the scenario, the concentration in the chamber decreases, because there is water from the channel transported into the chamber due to a boat that is moving outwards.

The suspended sediment concentration inside the channel for one operational cycle in scenario 2 is plotted in Figure 9.4b. In the first phase, there is water transported from the chamber into the channel. However, it is assumed that the starting conditions are that the concentration both inside the chamber and inside the channel are zero. That is why the concentration in the channel also remains zero during the first phase. In the phases 2, 3, 4 and 5, there is no connection of the channel and the chamber with the sea side. Therefore, the concentration during these phases still remains zero. During phase 6, water from inside the chamber, now containing suspended sediment, is discharged into the channel. The concentration inside the channel shows a parabolic increase during this phase. In the seventh phase, there are density currents between the chamber and the channel, thus also transporting more sediment into the channel and letting the concentration increase. In the last phase, phase 8, there is only water transported from the channel into the chamber. There is a small decrease in concentration due to a part of the suspended sediment that is settling.

Excluding erosion

The sediment layer thickness inside the lock chamber for one operational cycle with scenario 2 is plotted in Figure 9.5a. In phase 1, the layer thickness remains zero, as the concentration inside the chamber is also still zero. In the following three phases, there can be a parabolic increase in layer thickness seen in the graph. There is a parabolic increase, as the concentration in the chamber also increases in phases 2, 3 and 4. During phases 5 and 6, the concentration inside the chamber remains almost constant and the increase in layer thickness is linear. During phase 7 and the beginning of phase 8, the increase in layer thickness is weakened as the concentration decreases. During the latter part of phase 8, the layer thickness remains the same, due to the concentration inside the chamber that is close to zero. The sediment layer thickness in the chamber at the end of the simulation of one operational cycle with scenario 2 (not including erosion) is $7.32 * 10^{-4}\ m$.

The simulated sediment layer thickness inside the channel for one operational cycle in scenario 2 is plotted in Figure 9.5b. It can be seen that the layer thickness remains zero during the first five phases.

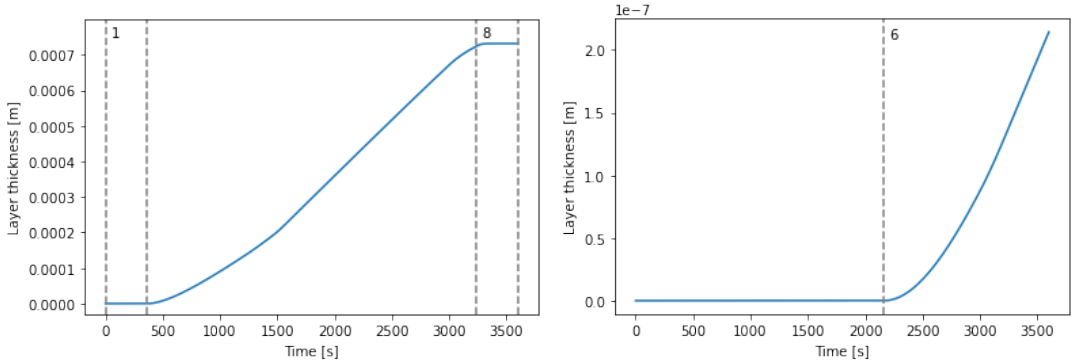

(a) lock chamber **(b)** channel

Figure 9.5: Sediment layer thickness without erosion for one operational cycle, scenario 2.

This is due to the fact that there is no suspended sediment concentration in the channel during this period in scenario 2. During phase 6 and 7, there is a parabolic increase in the layer thickness in the channel, as there is also an increasing suspended sediment concentration. In the last phase, the suspended sediment concentration remains constant and the layer thickness graph shows a linear increase. At the end of the simulation of the operational cycle of scenario 2, the sediment layer thickness (excluding erosion processes) is equal to $2.14 * 10^{-7}\ m$.

Including erosion

The sediment layer thickness in the chamber for one operational cycle with scenario 2 slightly changes when erosion is taken into account. The change is not visible when both cases are plotted in the same graph, but the change can be explained using another graph. In Figure 9.6 the applied bottom shear stress during the phases of scenario 2 is plotted. The graph shows that the critical bed-shear stress for erosion of $1.5\ N/m^2$ is only exceeded during phase 1 and phase 8 of the scenario. The erosion volume remains below $5.20 * 10^{-3}\ m^3$ during the cycle. The value for the sediment layer thickness in the chamber at the end of the operational cycle for scenario 2 is $7.30 * 10^{-4}\ m$.

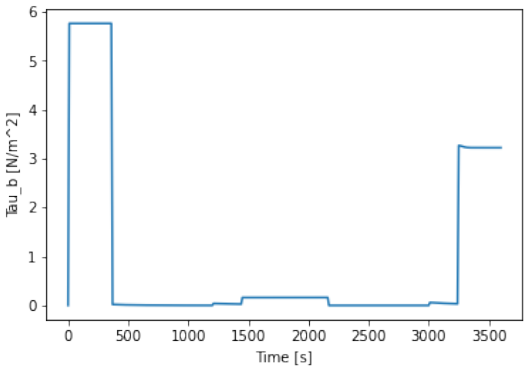

Figure 9.6: Applied bottom shear stress in certain areas of the chamber for one operational cycle, scenario 2.

9.1.3. Model check

The highest possible concentration inside the chamber is equal to the $3\ kg/m^3$ concentration of the water on the seaward side, because the chamber is fully exposed to the much larger water volume on this side. This is different for the channel between the locks. After one operational cycle, only one chamber water volume reduced by the draught volume of the boat(s) inside the chamber can enter the channel. This is a volume of about $10,500\ m^3$ with a maximum concentration of $3\ kg/m^3$. If this is all transported into the channel, the maximum concentration in the channel for the first operational cycle is $2.90 * 10^{-3}\ kg/m^3$. Figures 9.1 and 9.4 show that the upper limits for the suspended sediment concentrations is not exceeded.

The operational cycle for scenario 1 takes $78\ min$ and the operational cycle for scenario 2 takes $60\ min$. When the settling velocity is set to a constant value of $0.17\ mm/s$ and the maximum concentration that was determined above is also taken as a constant, a quick calculation can be done to estimate the upper limit of the sediment layer thicknesses. A first estimate is acquired by multiplying the settling velocity with the operational time. The maximum layer thickness in the system is then $7.96 * 10^{-1}\ m$ for scenario 1 and $6.12 * 10^{-1}\ m$ for scenario 2. This is a rough estimate which is not yet depending on the suspended sediment concentration of the water in the chamber and channel. Better estimates are calculated using Equation 7.2 and 7.3. The maximum sediment layer thickness in the chamber would then be $1.49 * 10^{-3}\ m$ for scenario 1 and $1.15 * 10^{-3}\ m$ for scenario 2. The upper limit for the sediment layer thickness in the channel is $1.44 * 10^{-6}\ m$ for scenario 1 and $1.11 * 10^{-6}\ m$ for scenario 2. Both Figure 9.2 and Figure 9.5 show that none of these four upper limits are exceeded. This confirms that the model is working correctly. The check for the sediment layer thicknesses for each scenario can also be seen in Table C.1.

9.2. One tidal cycle

A tidal cycle can be simulated in different ways depending on the operational schemes from Table 4.1. For the first calculation, the operating scheme of two way traffic is used with lock operating hours of 12 out of 24 and an average locking time of $60\ min$. Therefore, there are 12 operational cycles in this tidal cycle, followed with a resting period of $12\ hrs$. The second calculation is done using the fully operational scheme. The lock is constantly operating in this case. The average locking time remains $60\ min$. The scheme consists of 24 operational cycles and no resting period.

During a tidal cycle, the water levels and suspended sediment concentration outside the lock system will vary. This variation is not known for the case study, but will be important to include in a later design stage, once this is measured. For now, the maximum head difference of $5.0\ m$ is taken and a suspended sediment concentration of $3\ kg/m^3$ is used. The density of the water in the channel and inside the chamber is first assumed to be $1000\ kg/m^3$ and that of the water on the sea side $1025\ kg/m^3$. The discharge coefficient is again assumed to be 0.6 and the vertical exchange coefficient 0.3. The settling velocity is calculated in the same manner as for an operational cycle. It is chosen not to incorporate the source code of this calculation in the appendices, as it was very extensive. The code can be requested by contacting the author of the report.

9.2.1. Two way traffic

Operational scenario 1

The suspended sediment concentration inside the lock chamber and the channel for one tidal cycle with 12 operating hours and scenario 1 is given in Figure 9.7. In Figure 9.7a, it is seen that inside the lock chamber, the increase in suspended sediment concentration is strongly dependent on the concentration of the water from the sea side. When the water inside the chamber is connected with the sea side, the concentration increases significantly until it almost reaches the $3\ kg/m^3$ concentration of the outside water. When the chamber is connected to the channel, it passes along sediment, causing the concentration in the chamber to decrease to a value close to zero. The concentration fluctuates between 0 to $3\ kg/m^3$ during the first $12\ hrs$ of the tidal cycle. At the end of the first 12 hours, the concentration in the chamber is close to $3\ kg/m^3$. There is no connection between the chamber and the sea side or channel side for the following $12\ hrs$. The decrease in the concentration for this period is only due to the settling of sediment particles that were first suspended. The concentration decreases to a value of $1.42\ kg/m^3$.

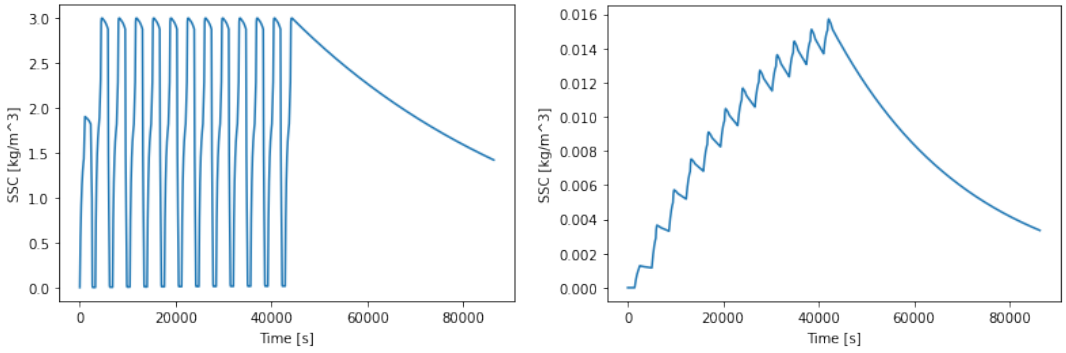

(a) lock chamber **(b)** channel

Figure 9.7: Suspended sediment concentration for one tidal cycle, two way traffic, scenario 1.

Figure 9.7b shows the progression of the suspended sediment concentration inside the channel of the tidal cycle with 12 operating hours and scenario 1. It is assumed that the channel can not pass sediment on to more upstream parts of the waterway. There is an increase in the concentration during the first $12\ hrs$, because sediment is transported from the sea and chamber side into the channel when the chamber and channel are in connection with each other in every operational cycle. The concentration inside the channel stays relatively small compared to the concentrations in the lock chamber, as this is divided over a much larger area. The same holds for the sediment layer thickness. In the second part of the tidal cycle, the concentration in the channel is only decreasing, because the connection with

the sea side via the chamber is closed. The decrease is due to the settling of sediment that was first suspended.

The settled and suspended sediment volumes during the tidal cycle is presented in Figure 9.8a for the chamber and in Figure 9.8b for the channel. These graphs are an important check to verify that there is no extra sediment added in the system that should not be there. In the non-operational part of the cycle, the total sediment volume inside the chamber and channel should stay constant, because the system is closed. This means that the settled sediment volume would increase with the same rate as the suspended sediment volume would decrease with. Figure 9.8 verifies that this part of the model is working correctly.

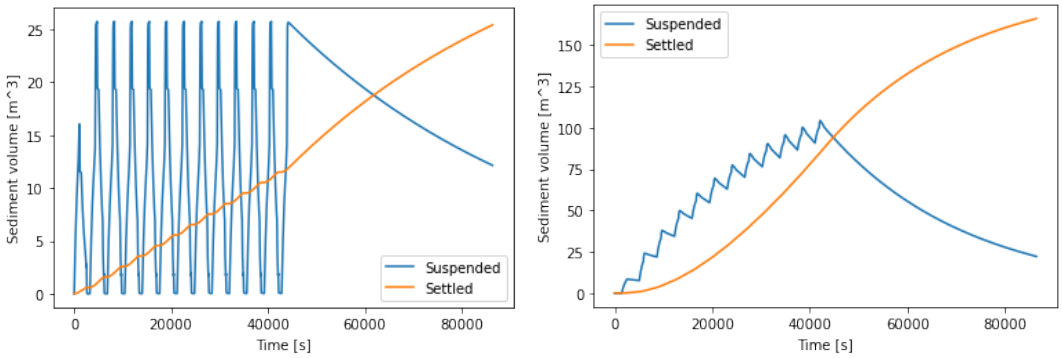

(a) lock chamber **(b)** channel

Figure 9.8: Settled and suspended sediment volume for one tidal cycle, two way traffic, scenario 1.

The emergence of the sediment layers in the lock chamber and in the channel during a tidal cycle, are shown in Figure 9.9a and 9.9b, respectively. It can be seen in the graph of the lock chamber, that the increase in layer thickness is somewhat steeper for the second part of the cycle than for the first part. This is because during the first part, the concentration varied from 0 to $3\ kg/m^3$, while at the end of the 12 operating hours the concentration is close to $3\ kg/m^3$ and decreases to $1.42\ kg/m^3$. In the second half of the tidal cycle, in which the lock is not moving for $12\ hrs$, the sediment concentrations are decreasing and the sediment layer thickness continues to grow with a slightly negative parabolic rate. The sediment layer thickness inside the chamber at the end of the tidal cycle for operational scenario 1 is equal to $1.78 * 10^{-2}\ m$.

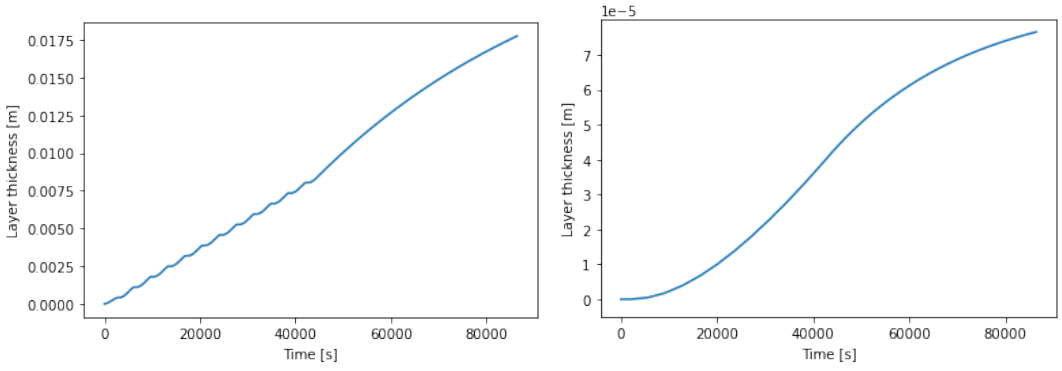

(a) lock chamber **(b)** channel

Figure 9.9: Sediment layer thickness for one tidal cycle, two way traffic, scenario 1.

In Figure 9.9b, the development of the sediment layer thickness in the channel during one tidal cycle with scenario 1 is shown. As the suspended sediment concentration in the channel is still increasing in the first $12\ hrs$, the layer thickness shows a positive parabolic increase. During the second half of the cycle, the concentration in the channel is decreasing, and the layer thickness graph shows a negative parabolic growth. The total layer thickness in the channel after one tidal cycle is $7.65 * 10^{-5}\ m$ for

operational scenario 1. This is assuming that the settled sediment in the channel is distributed equally over the whole channel.

Operational scenario 2

The suspended sediment concentration graphs of scenario 2 are similar to the ones of scenario 1. In Figure 9.10a, the concentration inside the chamber is shown. It can be seen that the concentration varies again from $0\ kg/m^3$ when the chamber is in connection with the sea side and $3\ kg/m^3$ when the chamber is connected to the channel. One large difference compared to scenario 1 is that, at the end of the first $12\ hrs$ of the tidal cycle, the suspended sediment concentration is nearly $0\ kg/m^3$ instead of approximately $3\ kg/m^3$. There is no visible decrease in the concentration in the next non-operational part of the cycle as this is already very low.

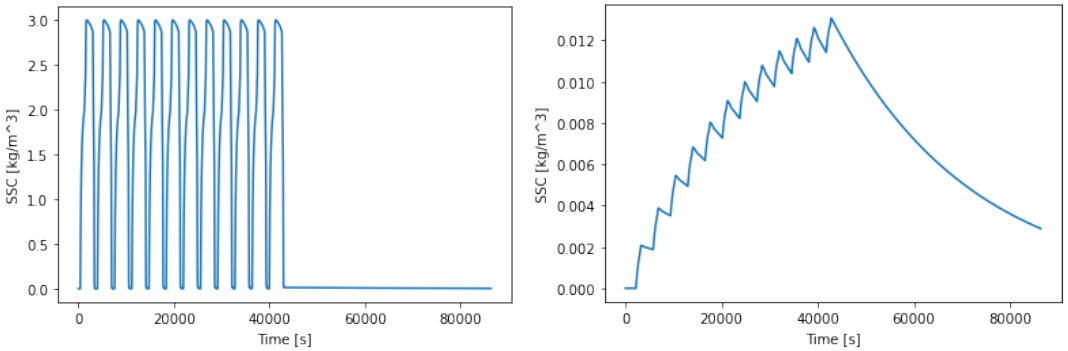

(a) lock chamber **(b)** channel

Figure 9.10: Suspended sediment concentration for one tidal cycle, two way traffic, scenario 2.

Figure 9.10b shows a step by step progression during the operational hours of the suspended sediment concentration in the channel for operational scenario 2. The concentrations are much smaller in the channel than inside the chamber. The concentration in the channel starts decreasing when the system is in a closed position. This decrease is again assumed to only be caused by the settling of sediment particles that were initially in the suspension.

The interim check regarding the sediment volumes in the system is also done for this scenario. In Figure 9.11, the settled and suspended sediment volumes in the chamber and channel during one tidal cycle are presented. It can be seen in Figure 9.11a that the settled sediment volume in the chamber is not visibly increasing in the second part of the tidal cycle. This is because there is not much sediment present in the suspension from that point that can settle. The total sediment volume in the channel is smaller for scenario 2 than for scenario 1. The volumes presented in Figure 9.11b do follow a same course as the lines in Figure 9.8b.

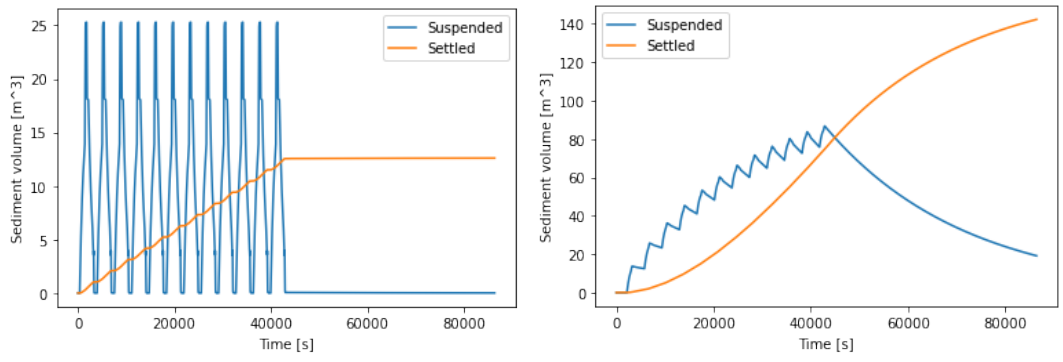

(a) lock chamber **(b)** channel

Figure 9.11: Settled and suspended sediment volume for one tidal cycle, two way traffic, scenario 2.

The development of sediment layer thicknesses in both the lock chamber and the channel during a full

tidal cycle is shown in Figure 9.12. In Figure 9.12a, it can be seen that in the first part of the tidal cycle with scenario 2, the layer thickness in the lock chamber shows a similar increase in the thickness as in Figure 9.9a which shows the increase during scenario 1. However, there is a large difference in the course of the second part of both graphs. In scenario 1, the concentration in the chamber at the end of a tidal cycle is about $3\ kg/m^3$. The concentration in the chamber at the end of a tidal cycle with scenario 2 is, however, close to $0\ kg/m^3$. This means that there is a much slower increase in sediment layer thickness in the second part of the tidal cycle with scenario 2 than with scenario 1. The sediment layer thickness in the lock chamber at the end of the tidal cycle with scenario 2 is $8.81 * 10^{-3}\ m$.

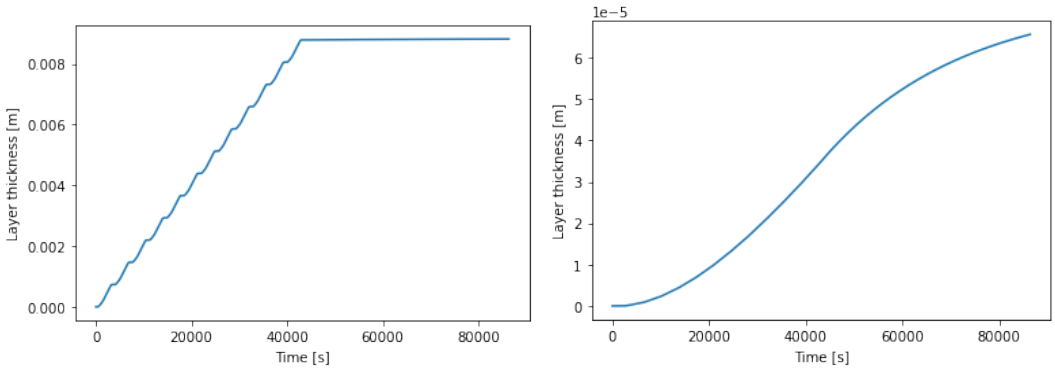

(a) lock chamber **(b)** channel

Figure 9.12: Sediment layer thickness for one tidal cycle, two way traffic, scenario 2.

During the tidal cycle, the sediment layer thickness in the channel first increases with a positive parabolic rate, as can be seen in Figure 9.12b. The increase is parabolically, as the concentration inside the channel is increasing. After the operational part of the cycle, the graph shows a negative parabolic increase in sediment layer thickness during the next $12\ hrs$ of the non-operational part of the cycle, as the sediment concentration is simultaneously decreasing. The layer thickness in the channel is $6.56 * 10^{-5}\ m$ at the end of the full tidal cycle with scenario 2.

9.2.2. Fully operational

Operational scenario 1

There is no non-operational period in the operation scheme with 24 operational hours. This means that the tidal cycle does not have a period in which the suspended sediment volume only decreases while the settled sediment volume would increase with the same rate. Instead, the suspended sediment volume in the chamber keeps varying from about $0\ kg/m^3$ to $3\ kg/m^3$. The settled sediment volume in the chamber is increasing step by step. The growth of the sediment layer thickness in the chamber for scenario 1 is shown in Figure 9.13a. The total sediment layer thickness at the end of the $24\ hrs$ is $1.66 * 10^{-2}\ m$.

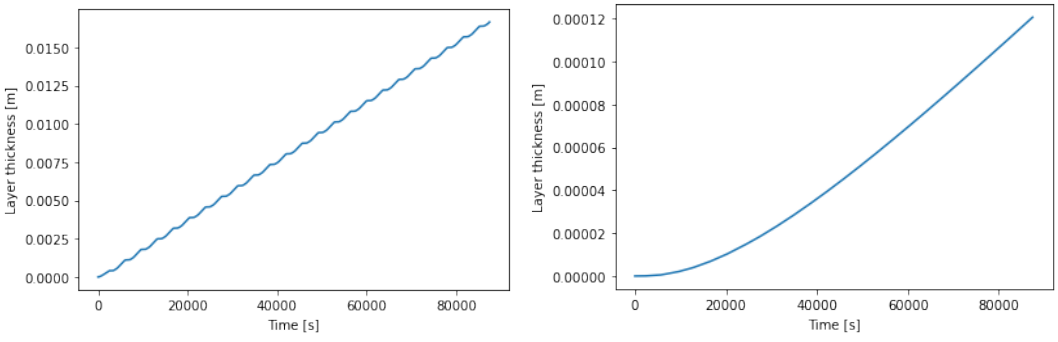

(a) lock chamber **(b)** channel

Figure 9.13: Sediment layer thickness for one tidal cycle, fully operational, scenario 1.

The suspended sediment volume inside the channel keeps increasing during the fully operational tidal cycle. The rate of increase gradually decreases over time. The settled sediment volume and sediment layer thickness in the channel are both increasing parabolically. As the rate of increase of the suspended sediment is decreasing in time, the sediment layer thickness curve is becoming less parabolic in time. The sediment layer thickness curve for in the channel is shown in Figure 9.13b . The layer thickness at the end of the cycle is $1.21 * 10^{-4}\ m$ when the sediment would be distributed equally in the channel.

Operational scenario 2

There is not a visible difference in the course of the sediment layer thickness graphs for scenario 1 and 2 for the fully operational case. There is, however, a difference in the overall rate of increase of the layer. The sediment layer thickness graphs for scenario 2 are shown in Figure 9.14. The layer thickness in the chamber for scenario 2 after one fully operational tidal cycle is $1.76 * 10^{-2}\ m$. In the channel, the layer thickness after the cycle would be $9.88 * 10^{-5}\ m$ when the sediment would be distributed evenly.

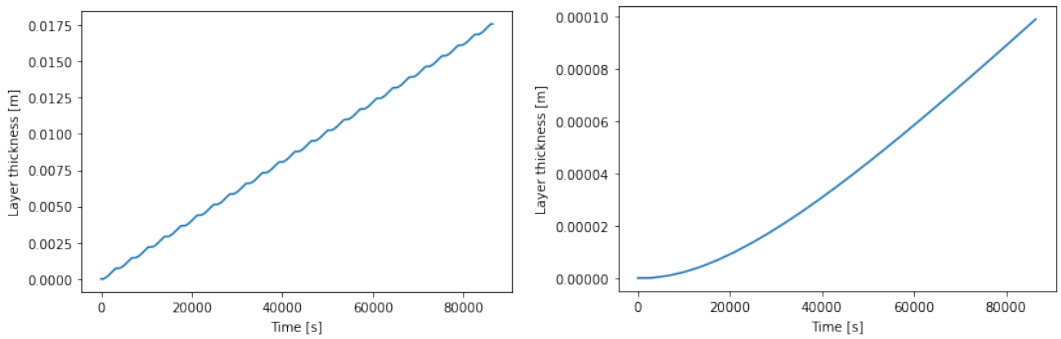

(a) lock chamber **(b)** channel

Figure 9.14: Sediment layer thickness for one tidal cycle, fully operational, scenario 2.

9.2.3. Model check

The maximum suspended sediment concentration during a tidal cycle is $3\ kg/m^3$ in both the two way traffic case and the fully operational case. The upper limit for the suspended sediment concentration inside the channel for the two way traffic scheme, can be determined by assuming that 12 chamber water volumes reduced by the draught volume of the boat(s) with a concentration of $3\ kg/m^3$ are exchanged with the water in the channel. The upper limit for the concentration in the channel is then $3.48 * 10^{-2}\ kg/m^3$ for both operational scenario 1 and 2 of the two way traffic scheme. Figures 9.7 and 9.10 show that this condition is fulfilled. The upper limit for the suspended sediment concentration in the channel for the fully operational scheme is calculated in the same way, but then taking 24 chamber water volumes instead of 12. The maximum concentration for both scenarios is $6.97 * 10^{-2}\ kg/m^3$ for this operation scheme.

An estimate for the upper limit of the sediment layer thicknesses can be calculated by using Equations 7.2 and 7.3 and assuming a constant maximum suspended sediment concentration which is calculated above and a constant settling velocity of $0.17\ mm/s$. The maximum sediment layer thickness inside the chamber for both schemes is determined to be $2.75 * 10^{-2}\ m$. The upper limits for the sediment layer thicknesses in the channel are different for the two schemes, as the schemes also have a different maximum suspended sediment concentration. The upper limit for the layer thickness in the channel for the two way traffic scheme is $3.19 * 10^{-4}\ m$. For the fully operational scheme, the upper limit for the layer thickness is $6.40 * 10^{-4}\ m$. All of the sediment layer thickness graphs in the previous paragraphs remain under the limits that are calculated. The model still satisfies the upper limit checks. An overview of all the sediment layer thickness checks is also given in Table C.2.

9.3. Multiple tidal cycles

The sedimentation process in the lock during one tidal cycle can be repeated to simulate a longer time period. Repeating the same data over multiple tidal periods, can be a good first estimation, but it is essential to remember that the actual situation will differ.

The two scenarios that were considered, differ in where the first boat of the operational part of the cycle comes from. Whether a boat comes from the left or the right can differ each day, but it can also happen that vessels almost always want to travel from the left to the right (or the other way around) in the morning. The actual specific order of each day cannot be fully known, but it is possible to find out what one of the most critical options would be. In order to do this, four different kind of series are analysed. The series differ in the sequence of four options that can happen. There are two different situations under scenario 1: one where the starting water level is low (1.1) and one where this is high (1.2). In both cases, the first boat of the operational part of the tidal cycle wants to move from the sea side to the channel (left to right). The water level at the end of these situations is high. Next to these, there are also two situations that can be considered for scenario 2: one beginning with a low water level (2.1) and one beginning with a high one (2.2). The first boat wants to travel from the channel to the sea (right to left) in both these situations and the water level at the end of the tidal cycles is low. Table 9.1 gives an overview of the four situations.

Table 9.1: Directions and water levels of tidal cycle situations.

Situation	Direction of first vessel	Water level at start and end
1.1	Sea -> Channel	Low -> High
1.2	Sea -> Channel	High -> High
2.1	Channel -> Sea	Low -> Low
2.2	Channel -> Sea	High -> Low

Now that the situations have been presented, the four series types that are considered are analysed. In series A, it is assumed that a boat always travels from the sea to the channel at the start of a new tidal cycle. The first situation is situation 1.1. As this situation ends with a high water level, the following situations of this series are all of the type of situation 1.2. For series B, the assumption is made that a boat always wants to travel from the channel to the sea at the start of a new tidal cycle. The starting situation is situation 2.2. After this, the water level in the chamber is low and the following tidal cycle situations are all of type 2.1. For series C and D, it is assumed that the direction of the first boat of a new tidal cycle alternates per cycle. In series C, the first tidal cycle starts with a boat moving from the sea to the channel (1.1) and the second tidal cycle starts in the opposite direction (2.2). In the series D, the first tidal cycle starts with a boat from the channel to the sea (2.2) and the second tidal cycle with a boat from the sea to the channel (1.1). Table 9.2 presents an overview of the situation sequence of all series.

Table 9.2: Multiple tidal cycles series with their situation sequences.

Series	Situation sequence
A	1.1 -> 1.2 -> 1.2 -> 1.2 -> etc.
B	2.2 -> 2.1 -> 2.1 -> 2.1 -> etc.
C	1.1 -> 2.2 -> 1.1 -> 2.2 -> etc.
D	2.2 -> 1.1 -> 2.2 -> 1.1 -> etc.

9.3.1. Monthly prediction

Two way traffic

The simulation of multiple tidal cycles will first be done for 30 days with 12 operating hours. Figure 9.15a presents the sediment layer thicknesses development during $30\ days$ inside the chamber for the four series with the two way traffic operation scheme. It can be seen that the sediment layer thickness in the chamber will be the largest when multiple tidal cycle series A would occur. Here, the sediment layer thickness after $30\ days$ would be $5.32 * 10^{-1}\ m$. The sediment layer thickness graphs for series C and D are very similar to each other. Series B gives the least critical sediment layer thickness case for in the chamber with $2.65 * 10^{-1}\ m$.

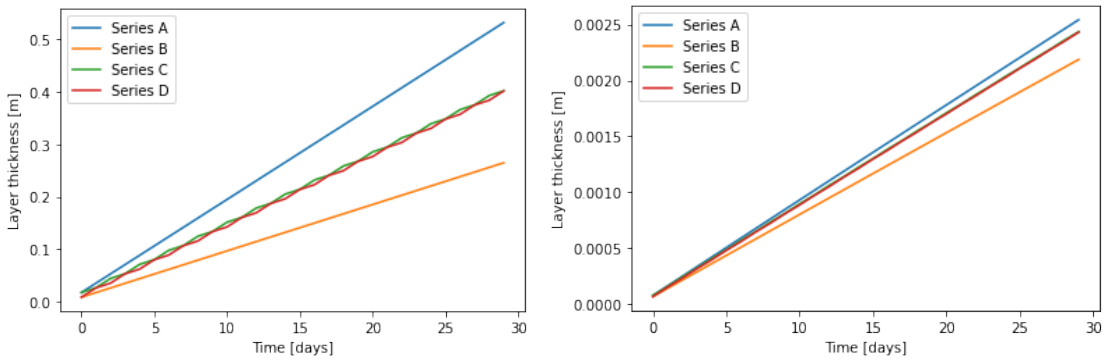

(a) lock chamber **(b)** channel

Figure 9.15: Sediment layer thicknesses over $30\ days$, two way traffic, different multiple tidal cycle series.

The layer thicknesses in the channel have a different order of magnitude than the ones in the chamber. Nevertheless, they are still very important for the design of the lock and the determination of what the most critical operational series would be. In Figure 9.15b, the sediment layer thicknesses in the channel over a period of $30\ days$ for the two way traffic operation scheme are presented. This is again, assuming the settled sediment in distributed equally over the whole channel area. The most critical sediment layer thickness situation for the channel is the same as the one for the chamber, this is series A. The total sediment layer thickness in the channel for series A after 30 days is equal to $2.54 * 10^{-3}\ m$. The least critical case occurs again for series B with $2.19 * 10^{-3}\ m$. The graphs for series C and D are, once more, very similar to each other. The layer thickness values over time remain between the values for series A and B.

Fully operational

The situation with 24 operating hours is for almost all cases more critical than the situation with 12 operating hours. The only case for which this is not true, is the sediment layer thickness that can be developed inside the chamber with series A. The sediment layer thicknesses in the chamber during the first $30\ days$ for all series with the fully operational scheme are given in Figure 9.16a. The largest sediment layer thickness development now occurs for series B. The total thickness would then be $5.28 * 10^{-1}\ m$ after $30\ days$. The values for the sediment layer thicknesses are quite close to each other. Series A has the lowest sediment layer thickness with $5.02 * 10^{-1}\ m$.

For the channel, the layer thicknesses are approximately one hundred times smaller than for the chamber. The sediment layer thicknesses for inside the channel during $30\ days$ with a fully operational scheme are given in Figure 9.16b. The most critical situation occurs with series A. The sediment layer thickness in the channel is in that case $5.05 * 10^{-3}\ m$ after $30\ days$. The lowest sediment layer thickness occurs for series B and is $4.14 * 10^{-3}\ m$.

Erosion influence

The erosion constant strongly depends on the type of sediment that is settling in the chamber and channel. In the Mongla-Ghasiakhali waterway, this is primarily a combination of the materials silt and sand. While there have been a lot of studies on the erosion of sand, the erosion of silt remains difficult to predict. The specific composition of the sediment that would settle is not known. This means that the erosion constant also remains hard to predict. The erosion constant for the simulations was first

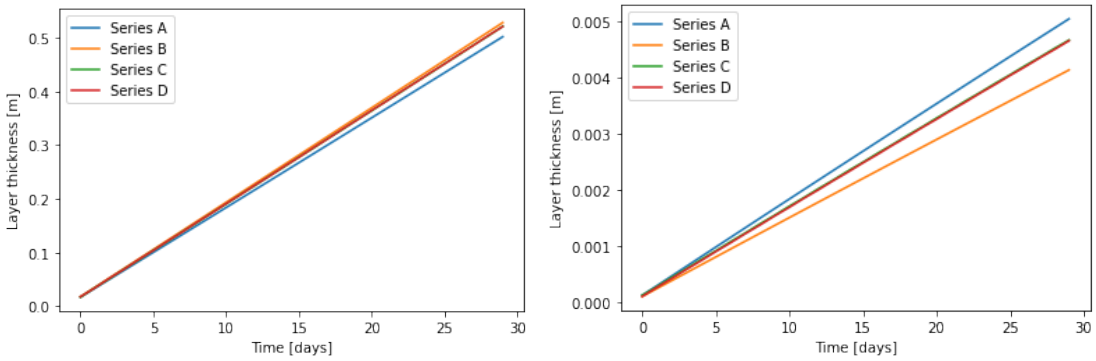

(a) lock chamber **(b)** channel

Figure 9.16: Sediment layer thicknesses over $30\ days$, fully operational, different multiple tidal cycle series.

set to 0.0003. The most favourable situation with regards to the minimisation of the sediment layer thickness in one month, would be the one with the two way traffic scheme following series B. The simulation of this scenario is also done with different values for the erosion constant. The results of the simulations can be seen in Figure 9.17. It is observed that there is not a real visible change in the sediment layer thickness inside the channel. The cause of this could be that the erosion volume remains small with respect to the surface area of the channel. It can, however, be seen that there is a difference in the developed sediment layer thickness in the chamber for different erosion constants. The sediment layer thickness in the chamber decreases with an increasing erosion constant. This is logical, as more of the settled sediment in the chamber will erode with a higher erosion constant. The eroded sediment is resuspended and can either settle again in the chamber or in the channel or stay resuspended. Because of this new distribution of sediment volume, the volume of settled sediment in the chamber is able to decrease.

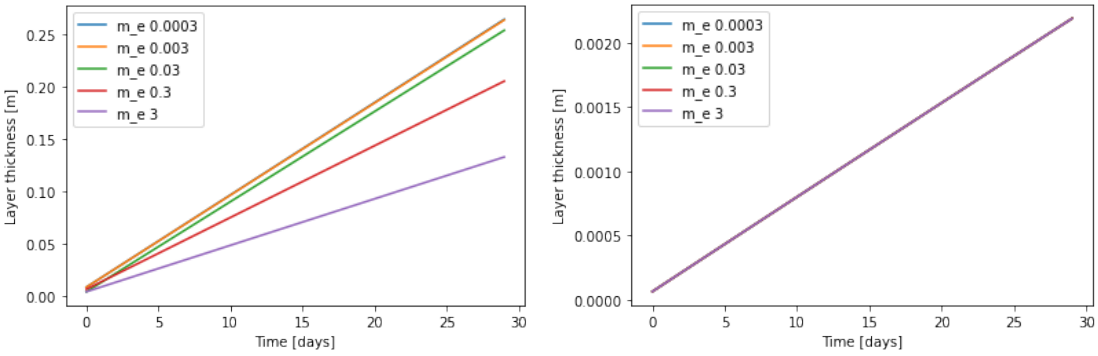

(a) lock chamber **(b)** channel

Figure 9.17: Sediment layer thicknesses over $30\ days$, two way traffic, series B, different erosion constants.

9.3.2. Yearly prediction

Two way traffic

For the yearly sedimentation prediction of the two way traffic case, only operational series A and B are considered as these are the two extreme cases. The lines in Figure 9.15 are quite linear and can therefore be extrapolated to estimate the sediment layer thickness progression over one year. This computed thickness for the sediment layer would only occur when the concentration of the water on the sea side remains $3\ kg/m^3$ during the whole year and the maximum head difference of $5\ m$ also remains present during this time. The sediment layer thickness in the chamber after one year under these same conditions, assuming the progression of the layer continues in the same manner, would be about $6.50\ m$ for series A and $3.22\ m$ for series B. The sediment layer thickness in the channel after one year under the same conditions is $3.11 * 10^{-2}\ m$ for series A and $2.67 * 10^{-2}\ m$ for series B.

Fully operational

The sediment layer thickness lines for the fully operational scheme, seen in Figure 9.16, are also linear and can be extrapolated to estimate the layer thickness in the chamber and channel after one year of operating. The series A and B are again extrapolated because they give the extreme cases. It should be noted that the result of the cases would only occur when the concentration of the water on the sea side is constantly $3\ kg/m^3$ and the water level difference remains $5\ m$ during the whole period. The estimated sediment layer thickness in the chamber after one year of operating under these conditions is then $6.12\ m$ for series A and $6.45\ m$ for series B. The sediment layer thickness in the channel after one operational year under the described conditions is $6.22 * 10^{-2}\ m$ for series A and $5.12 * 10^{-2}\ m$ for series B.

9.3.3. Model check

The maximum suspended sediment concentration in the lock chamber is still assumed to be $3\ kg/m^3$. For the monthly prediction of the two way traffic scheme, the upper limit for the concentration in the channel can be calculated by assuming that 30 times 12 chamber water volumes are exchanged with the water in the channel and that the water volume of the chamber constantly has a concentration of $3\ kg/m^3$ when the exchange takes place. The maximum concentration is then $1.05\ kg/m^3$ in the channel. For the monthly prediction of the fully operational scheme, it is assumed that 30 times 24 chamber water volumes with a concentration of $3\ kg/m^3$ are exchanged. Then, the upper limit for the concentration in the channel is $2.09\ kg/m^3$. When the same method is used to calculate the concentration in the channel after one year, this outcome would exceed $3\ kg/m^3$, which is not possible. Therefore, the upper limit for the suspended sediment concentration after one year is set to $3\ kg/m^3$ for both the two way traffic scheme and the fully operational scheme.

The upper limit values for the sediment layer thickness in the chamber and channel can again be estimated using Equation 7.2 and Equation 7.3. In these formulas, the maximum suspended sediment concentration that was previously calculated is used. The maximum sediment layer thickness inside the chamber is then $8.26 * 10^{-1}\ m$ for one month. This holds for both the two way traffic scheme and the fully operational scheme, as the maximum suspended sediment concentration in the chamber is assumed to have the same value in these cases. The upper limit for the sediment layer thickness in the channel for the two way traffic scheme is estimated to be $2.89 * 10^{-1}\ m$ for one month. For the fully operational scheme, the maximum layer thickness in the channel is $5.76 * 10^{-1}\ m$ for one month. The maximum value for the layer thickness in the chamber and channel for one year is estimated to be $10.1\ m$ for both the two way traffic and fully operational scheme. None of the upper limits for the sediment layer thicknesses in the chamber and channel that are mentioned above are exceeded in the model simulation. This is a good sign for the correctness of the model.

In the area analysis in Chapter 3, it was mentioned that there is currently an average volume of $2.2\ Mm^3$ sediment dredged annually to maintain navigability in the channel. This corresponds to a sediment layer thickness in one year of $1.01\ m$, when the sediment would be distributed equally over the length and width of the channel. With the construction of the two navigation locks, the sediment layer thickness in the channel should be lower than this, because the locks reduce the amount and velocity of the amount of sediment coming into the channel. Therefore, the $1.01\ m$ is also an upper limit for the sediment layer thickness in the channel after one year. The limit is not exceeded in the model simulations. The model checks for one month are summarized Table C.3. The model checks for the situation after one year are presented in Table C.4.

9.4. Conclusion

The outcomes of the sedimentation model are based on a constant water level on the sea side and in the channel, a constant head difference between these two, a constant water density on the outside of the system and a suspended sediment concentration of the water on the sea side that remains constant. The water levels, head difference and water density have been chosen to represent a situation with maximum water exchange volumes. The suspended sediment concentration that was used is an average value.

The operational cycle is simulated with two different scenarios. The suspended sediment concentration in the chamber is highly dependent on the concentration in the water to which it is connected every time. The concentration at the end of one operational cycle with scenario 1 is close to $3\ kg/m^3$, while the concentration at the end of one operational cycle with scenario 2 is close to $0\ kg/m^3$. The sediment layer thicknesses in the chamber and channel for each scenario are given in Table 9.3. It is notable that while the sediment layer thickness in the chamber is lower in scenario 1 and higher in scenario 2, the sediment layer thickness in the channel shows an opposite difference.

Table 9.3: Sediment layer thickness per case.

Case			SLT chamber $[m]$	SLT channel $[m]$
Operational cycle		Scenario 1	$6.93 * 10^{-4}$	$3.65 * 10^{-7}$
		Scenario 2	$7.30 * 10^{-4}$	$2.14 * 10^{-7}$
Tidal cycle	Two way traffic	Scenario 1	$1.78 * 10^{-2}$	$7.65 * 10^{-5}$
		Scenario 2	$8.81 * 10^{-3}$	$6.56 * 10^{-5}$
	Fully operational	Scenario 1	$1.66 * 10^{-2}$	$1.21 * 10^{-4}$
		Scenario 2	$1.76 * 10^{-2}$	$9.88 * 10^{-5}$
One month	Two way traffic	Series A	$5.32 * 10^{-1}$	$2.54 * 10^{-3}$
		Series B	$2.65 * 10^{-1}$	$2.19 * 10^{-3}$
	Fully operational	Series A	$5.02 * 10^{-1}$	$5.05 * 10^{-3}$
		Series B	$5.28 * 10^{-1}$	$4.14 * 10^{-3}$
One year	Two way traffic	Series A	6.50	$3.11 * 10^{-2}$
		Series B	3.22	$2.67 * 10^{-2}$
	Fully operational	Series A	6.12	$6.22 * 10^{-2}$
		Series B	6.45	$5.12 * 10^{-2}$

In the two way traffic operation scheme, the concentration of the water in the chamber at the end of the first operating hours is very important for the eventual suspended sediment concentration and sediment layer thickness in the chamber. As mentioned earlier, scenario 1 and 2 differ in their chamber concentrations at the end of an operational cycle. Scenario 1 has a high end concentration in the chamber and therefore also has a higher sediment layer thickness in the simulation of one tidal cycle with the two way traffic scheme in the chamber. The sediment layer thicknesses are summarized in Table 9.3. The sediment layer thickness in the channel is overall higher for the fully operational scheme than for the two way traffic scheme. This is logical, as the chamber is transporting sediment from the sea side into the channel, a double amount of times.

For the channel, it is preferred to have a two way traffic scheme rather than a fully operational one. This gives a lower sediment layer thickness for one tidal cycle, but also for the simulation of one month and one year. The advice would be to start with the introduction of the two way traffic scheme and only use a fully operational scheme when the capacity of the lock is constantly lacking significantly. It is also clear that, when a two way traffic scheme is chosen, series B would be preferred when looking at the sediment layer thickness in the chamber. Series B consists of operational cycles of scenario 2, so with

a low concentration at the end of each operation. This can lead to almost half of the sediment layer thickness in the chamber than series A, consisting of scenario 1 cases, would lead to. It is not necessary to only use scenario 2 cases when you want the sediment layer thickness in the chamber reduced. The last cycle of the two way traffic operation scheme is the one that matters most. The scenarios can be alternated, but the last operating cycle needs to be kept as a 'flushing cycle' like scenario 2. This will reduce the suspended sediment concentration in the chamber during the non-operational period of the tidal cycle, which can cause a significant reduction in the sediment layer thickness here.

Once the two way traffic scheme is used and every operating part of the tidal cycle is ended with a 'flushing cycle', the most representative values for the sediment layer thicknesses in the chamber and channel are the ones for the two way traffic scheme and series B from Table 9.3. The sediment layer thickness in the chamber after one year would then be $3.22\ m$ and the sediment layer thickness in the channel after one year would be $2.67 * 10^{-2}\ m$. This corresponds to a total sedimentation volume in one year of about $6.25 * 10^{4}\ m^3$.

One of the limitations of the model that should be noted is that the simulation only uses one large design vessel. Smaller vessels can decrease the water exchange processes as they have a smaller draught. However, they can also increase the sediment exchange as there remains a larger water volume with sediment inside the chamber when a boat travels from the sea side to the channel. Another limitation is that the model is based on a two-dimensional approach. In reality, vertical sedimentation rates would actually be larger than for this two-dimensional case.

10

Structural design

The previous chapters have provided insight into the scope of the sedimentation problem in a navigation lock. The objective of this report is to develop tools that improve the design of a navigation lock operating in conditions of high sediment transport. Rather than providing a complete sluice design, the focus is placed on addressing sedimentation-specific challenges in a navigation lock design. This chapter focuses on tools regarding the structural design and Chapter 11 focuses on the maintenance design.

Multiple sources (Hoekstra, 2015; Kirby, 2011; Navigation channel sedimentation task committee, 2023) state that there are three preventive sedimentation strategies: keep sediment out, keep sediment moving, and keep sediment navigable. Keeping the sediment out entails that the inlet of water with high suspended sediment concentrations is minimised. With the option of keeping the sediment moving, the suspended sediment is being passed through the channel while minimising the settlement inside it. Minimising the settlement can for example be done by raising the flow velocities in quiescent areas. Keeping the sediment navigable means, for example, increasing the depth of the lock and channel, so that boats are still able to travel through them when sedimentation has occurred. The design choices presented in this chapter are based on all three preventive sedimentation strategies.

The main features of the structural design of a navigation lock are the approach structures, the lock heads with lock gates, the lock chamber and the filling and emptying system. Next to these, the lock consists of several smaller components which can each affect the sedimentation in a negative or positive manner. First, a general explanation of the functional requirements will be given. Subsequently, the lock design features will be explored in greater detail across several paragraphs.

10.1. Functional requirements

Before going into the different parts of the design and their design options, it is important to specify the functional requirements for the structural design of the lock. There are functional requirements regarding the economic efficiency of the design and regarding different aspects of the safety of the structure. Next to this, a design specifically made to reduce sedimentation in a system, will have a few extra requirements regarding this topic. Some of the functional requirements have a role in all of the main features of the structural design of a lock, but others only play a part in a few of them. The functional requirements listed in Table 10.1 are now clarified.

A lock approach is the navigation area between the connected waterway and the lock system. In this area, ships need to be able to decrease their speed and moor to a guiding structure when this is necessary. The connection should be navigable safely and therefore, the income of transverse currents should be minimised. In case of high suspended sediment concentrations, the approach can also bear the function of diverting the flow such that the sediment inlet is minimised. The loading jetties between the rectangular lock approach part and the lock chamber are there to guide the vessels and enable a smooth connection. The layout of the lock approach can be seen in Figure 10.1. In Table 10.1, the requirements for the lock approach can be found as numbers 1, 4 and 7.

Table 10.1: Functional requirements for the structural design of a lock facing high sediment transportation.

Number	Functional requirement
1	Cost efficient, stable and constructable design
2	Minimising the waiting time for vessels
3	Minimising the filling and emptying time
4	Safe and navigable lock approach that can guide vessels
5	Chamber which can safely accommodate one or multiple ships
6	Prevent high water velocity currents due to filling/emptying
7	Minimising sediment inlet in lock system
8	Gate operation able to flush sediment
9	Tight sealing of the gates

Lock gates play a crucial role in the design of a navigation lock and therefore need to meet multiple of the requirements. The gates should be able to operate under a certain amount of time, which is determined by the desirable transfer time and required capacity. The operation should not induce currents that can influence the safety of the vessels negatively. When the gates are open, all ships that are present in the area should be able to safely pass the lock head. When the gates are closed, they should be sealed tight to ensure no streams of water or sediment can still pass through. With regard to sedimentation, the gates should be designed in such a way that sedimentation near the lock gates will not be able to disturb the movements. Flushing can be an effective solution to mitigate the risk of sedimentation. The aforementioned requirements are represented by numbers 1, 2, 7, 8 and 9 of Table 10.1.

The chamber of a lock is required to safely accommodate one or multiple ships during the filling and emptying process. The number of ships the chamber should accommodate depends on the vessel frequency and size, and the acceptable waiting time in the waterway channel. The chamber should be equipped with mooring facilities to stabilise the vessels during filling and emptying when necessary. The depth of the chamber may be increased in advance to account for a certain sediment layer thickness. The requirements are listed as numbers 1, 2 and 5 in Table 10.1.

Filling and emptying systems were already shortly introduced in Chapter 6. The filling and emptying process should be as fast as is safely possible. This means that the filling or emptying should not induce water velocities that can negatively impact vessel stabilities. The system should not be prone to sedimentation accumulations. The requirements applicable to the filling and emptying system are numbers 1, 3 and 6 of Table 10.1.

Flushing

In Chapter 9, it is found that the sedimentation in the chamber and channel strongly depends on the sequence of the operational phases. The sedimentation in the chamber significantly decreases when the operational cycle ends with a flushing cycle, flushing more sediment into the channel. Subsequently, the sedimentation in the channel increases. The effectiveness of a flushing cycle is depending on the time that the sediment is present in the chamber. It is either preferable to minimise the time inside the chamber to minimise the sedimentation possibilities in it, or to lengthen this in order to minimise the passing through capacity of the sediment through the lock chamber. The latter option increases the flushing cycle effectiveness. The choice of minimising or maximising the time inside the chamber depends on the preference regarding the location of the dredging works.

The operation of the gates can also flush sediment out of the system in a different manner. More on this will be explained in Paragraph 10.3.

10.2. Approach structure

The approach structure of a lock is meant to guide the ships to and from the waiting area and chamber. With regards to sediment transportation, the approach structure is especially important on the outside of the lock system (on the west at Mongla and on the east at Ghasiakhali). The functional requirements of an approach structure are making the transition of the rivers navigable, contributing to a safe and speedy entry of vessels and facilitating mooring spaces for vessels (Chen, 2015; Glerum & Vrijburcht, 2000). In a holding basin, vessels can wait and line up before they can enter the lock chamber. To prevent sedimentation on the lock sill, holding basins must have a greater depth than the sill depth (Rijkswaterstaat, 2020). At the end of the holding basin, the approach structure often has a funnel structure leading to the chamber which ensures the ships have visual and physical guidance when needed to enter the lock safely. Figure 10.1 shows the layout of a typical approach structure. In Figure 10.2 a picture of the lock approach at Engelen, Netherlands, can be seen.

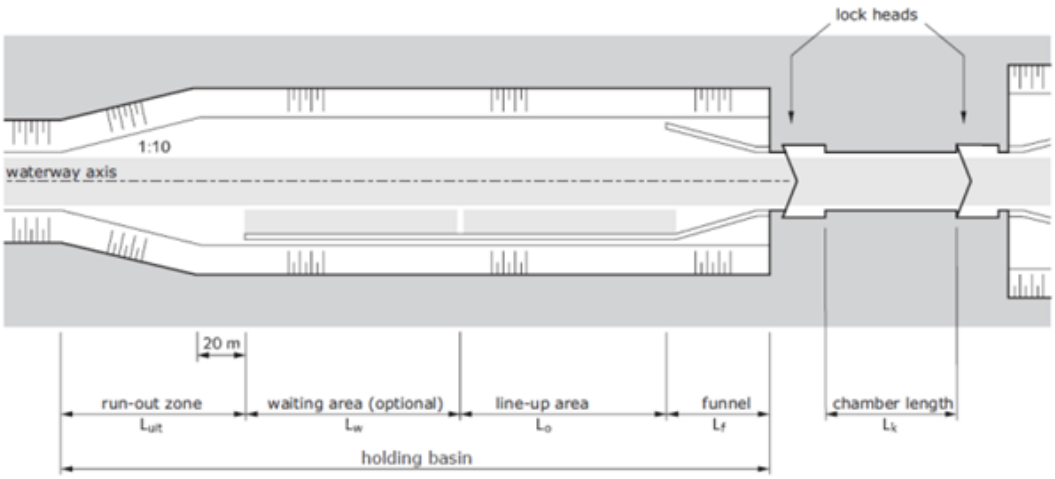

Figure 10.1: Lock approach structure (Rijkswaterstaat, 2020).

Figure 10.2: Lock approach at Engelen, Netherlands (Glerum & Vrijburcht, 2000).

As this report focuses more on the inside of the lock chamber and channel, there are no further steps

taken in determining and optimising the alternatives for the approach structures. The effect that different approach structures can have on the sediment transport and sedimentation is recommended to take into account in a future study.

10.3. Lock gates

There are fifteen possible gate types identified through a literature study (Chen, 2015; Daniel & Paulus, 2018, 2019; Glerum & Vrijburcht, 2000). Not every gate type is fit to be used in a navigation lock. There are already a lot of navigation locks constructed around the world. The first step in the choice of the gate type is therefore to look at the history of the gate types and their use in reference projects. By doing this, it can be concluded that a group of five gate types are generally not used in navigation locks: drum and roller gates, horizontally hinged sector gates, barge gates, bear-trap and roof gates, and inflatable gates (Daniel & Paulus, 2018, 2019). Five other gate types that are sometimes used in navigation locks, but often not the preferred option, are: single-leaf gates, hinged crest or other flap gates, radial (or tainter) gates, visor gates, and vane gates. The five options that are often used in navigation locks are: mitre gates, vertical lift gates, rotary segment gates, vertically hinged sector gates and rolling and sliding gates. All of the gate types are given in Table 10.2.

Table 10.2: Gate types and their previous usage in navigation locks.

Almost never used	Sometimes used	Often used
Drum and roller gates	Single-leaf gate	Mitre gate
Horizontally hinged sector gate	Hinged crest or other flap gate	Vertical lift gate
Barge gate	Radial (or tainter) gate	Rotary segment gate
Bear-trap and roof gate	Visor gate	Vertically hinged sector gate
Inflatable gate	Vane gate	Rolling and sliding gate

Now that the options are known, the gate types can be analysed and assessed based on the functional requirements for the structural design of the lock. The general aspects of each gate type are not discussed. For these details, the information provided by Daniel and Paulus (2018, 2019) and Glerum and Vrijburcht (2000) can be consulted. In Appendix D, an overview of the lay-outs of the ten gate types which are sometimes and often used for navigation locks are shown. The gate movements can also be seen in the Figures 10.3-10.11, along with their sediment streams during the operation. These figures are explained later on.

Some of the mentioned lock gates have clear disadvantages for the specific application with regards to sedimentation and variable water heads. All of the gate types that are almost never used for locks, except for barge gates, can only control the flow in one direction. They can carry a water head only on one side and are not suited for alternating flows (Daniel & Paulus, 2019). The same case holds for a hinged crest of other flap gate which is more often used in spillways. Near a navigation lock, which is also subjected to a flow following tidal variations on one side, the water head is constantly alternating. The gates of a navigation lock need to account for this and also need to be able to control the flow in both directions as this is the only way to ensure the safe passage of ships. Barge gates are often not considered for navigation locks, because they are not suitable to operate frequently. The gate structure is heavy and has a very long opening and closing time. Additionally, the five gate types that are generally not used for locks and the hinged crest or other flap gates do not have a specific advantage with regards to sediment transport and sedimentation. Therefore, these will not be analysed in further detail. In the next part, the other gate types will be analysed to a greater extent, beginning with the sediment considerations.

10.3.1. Sediment considerations

Inlet in opened condition

Sediment can only enter the lock system either when the gates are opened or when the water in the chamber is being levelled. The optimisation of this second situation is discussed in Paragraph 10.5.

The sediment inlet while the gates are opened, can be influenced by the type of gates. One of the largest variables here is the time that is required for the gates to be fully opened. When this time is large, the water from the sea side, with a high sediment concentration, has a longer period to enter the chamber during density currents. The closing of the gates and the opening of the gates on the other side will also take longer, when the same gate type is implemented on both sides. The sediment will therefore be able to settle more inside the chamber. The time inside the chamber will directly influence the suspended sediment concentration that the water in the chamber has when it is in connection with the channel. On the one hand, it is possible that more sediment has entered the chamber with a longer gate opening/closing time resulting in a higher concentration of sediment in the chamber. On the other hand, the sediment has a longer period to settle, which would cause a decrease in the suspended sediment concentration in the chamber. It can be concluded that the total sediment volume entering the lock system will probably increase when the opening/closing time of the gate increases.

Gate types with low to moderate opening/closing times are the mitre gate, vertical lift gate, radial (or tainter) gate and the vertically hinged sector gate. Single-leaf gates and rolling and sliding gates generally have a high opening/closing time due to their weight and size. There is not much specific information regarding the opening and closing times of the remaining gate types when they are used in navigation locks.

Sediment movements during opening/closing

It is predicted that sediment will accumulate in front of lock gates as the flow velocity is near zero here. Some gates are able to flush a part of this sediment away during their operation. Other gate types can increase the inlet of sediment by their operation. For this property, it is important to understand the movement of each gate type.

A single-leaf gate, a mitre gate and a vane gate all turn around a vertical axis, pushing the gate doors to the high water side. In these cases, the sediment that has accumulated in front of the doors, is pushed back. A large part of the sediment that is pushed back will erode and be resuspended into the water in front of the gate. During this process, the concentration of the water in front of the gate can increase. An advantage of these gate types is that the accumulated sediment is not let directly into the chamber or channel, thus directly increasing the sediment layer thickness in these areas. When the layer of sediment in front of the gate is very large, the gate might start experiencing trouble pushing this away and fully open. The force opening the gates acts at the top of them, while the resistant force, induced by sediment accumulation, acts near the bottom. This force distribution causes the gates to experience an increase in stress internally. Consequently, the doors become more susceptible to fatigue. If these gates would be implemented in an environment with high sediment concentrations, this should be a point of attention.

The sediment streams induced by the opening and closing of a single-leaf gate is shown in Figure 10.3. On the left side of the figure, the gate is opened and on the right, the gate is closed. The yellow arrows represent the horizontal movement of the sediment that remains settled on the ground. The blue arrows indicate the movement of sediment that was first settled and is now resuspended due to the gate movements.

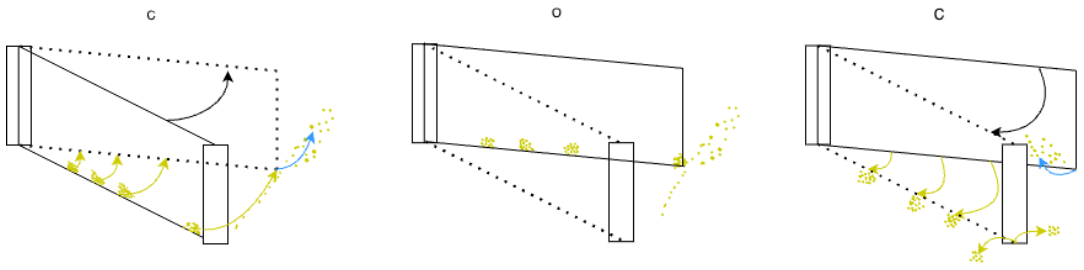

Figure 10.3: Sediment movements single-leaf gate.

The sediment movements around a mitre gate when it is opened or closed are shown in Figure 10.4. The sediment following the yellow arrows stays settled again, and the sediment following the blue arrows will resuspend. When there is a same amount of sediment in front of a single-leaf gate and a

mitre gate, the mitre gate will have less difficulties with pushing the sediment away, as the span of the gate is halved.

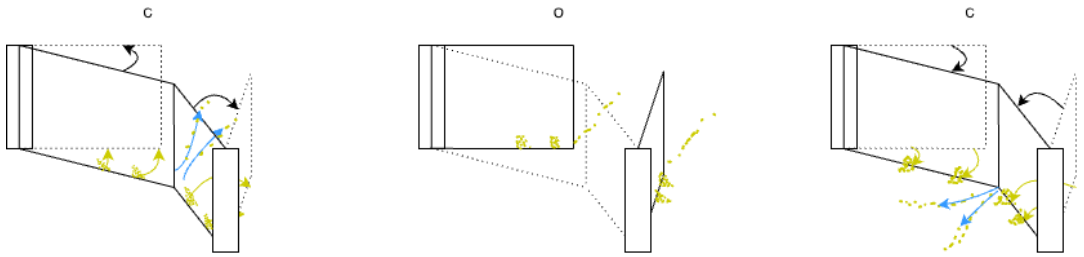

Figure 10.4: Sediment movements mitre gate.

Figure 10.5 shows the sediment movements during the opening and closing of a vane gate. The movements look a lot like the movements of a mitre gate. Only now, the sediment can be collected in the gate chambers of the lock heads. This sediment volume can be replenished during every gate opening cycle. The accumulation can cause problems for the gate operation.

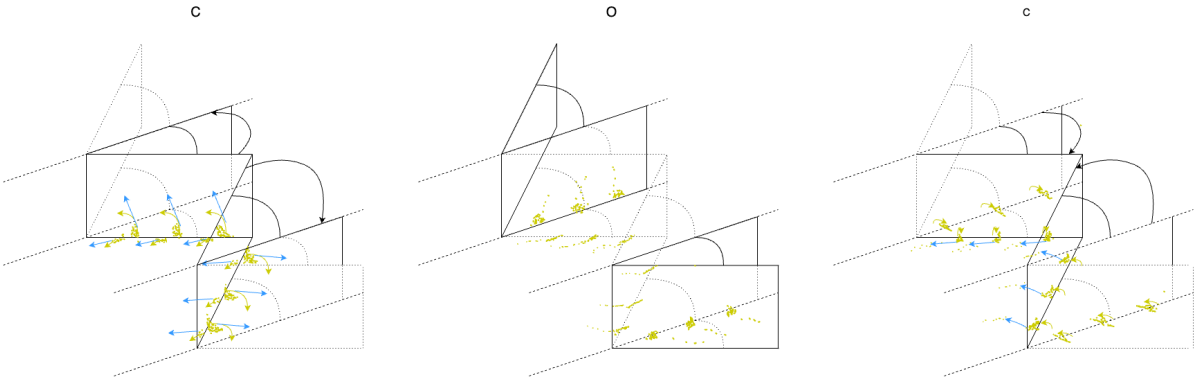

Figure 10.5: Sediment movements vane gate.

The vertical lift gate, radial (or tainter) gate and the visor gate all operate vertically. When these gates are opened, they cause friction between the gate and the sediment in front of the gate. A part of the sediment will be able to erode and be resuspended, but another part of the sediment layer might also be able to directly enter the chamber or channel and enhance the layer thickness in these. A danger of this is that the sediment should not end up in the connection between the gate and the bottom or sill. This can hinder the sealing functionality of the gate. An advantage of the gates is however, that when they are closed, the movement of the gates can flush the sediment near the connection away again to both sides of the gate.

The sediment movements around a vertical lift gate when the gate is opened and closed are shown in Figure 10.6. On the left of the figure, it can be seen that some of the sediment that was first settled in front of the gate will move horizontally towards the gate opening, because their resistant wall is removed. Another part of the sediment is sucked upwards due to the gate movement and will resuspend in the water. When the gate is closed on the right side of the figure, the sediment that was able to gather around the gate opening is pushed away to both sides of the gate. A part of the sediment will move horizontally and another part is partially pushed upwards due to the turbulence and will be able to resuspend in the water.

The sediment movements around a radial (or tainter) gate when it is opening and closing can be seen in Figure 10.7. Just like for the vertical lift gate, it can be seen on the left side of the figure that one part of the settled sediment will move towards the gate opening when the gate is opened and another part is sucked upwards and will resuspend. When the gate is closing (on the right), the sediment is flushed away. Some of the sediment is only pushed away horizontally, and the other part is also moving upwards due to the turbulence. This part is able to settle again later or will be resuspended in the water.

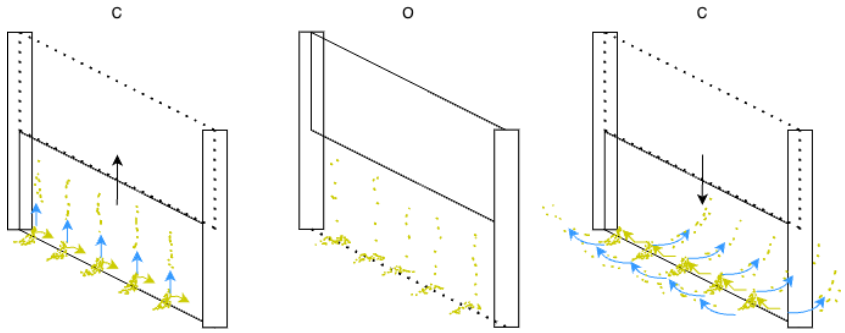

Figure 10.6: Sediment movements vertical lift gate.

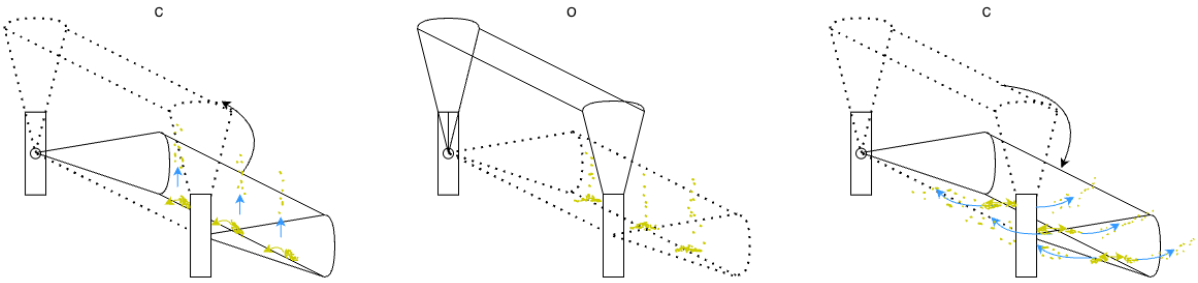

Figure 10.7: Sediment movements radial (or tainter) gate.

Figure 10.8 shows the sediment streams during the opening and closing of a visor gate. When the gate is opened on the left side of the figure, a part of the settled sediment is moved towards the connection area of the gate and the bottom of the lock. Another part is moved upwards to the bottom of the gate. A part of this last sediment will be resuspended into the water. The sediment that has gathered near the connection area is pushed towards both sides of the gate when it is closing again. The sediment can either move horizontally and stay settled or also move upwards and get resuspended into the water.

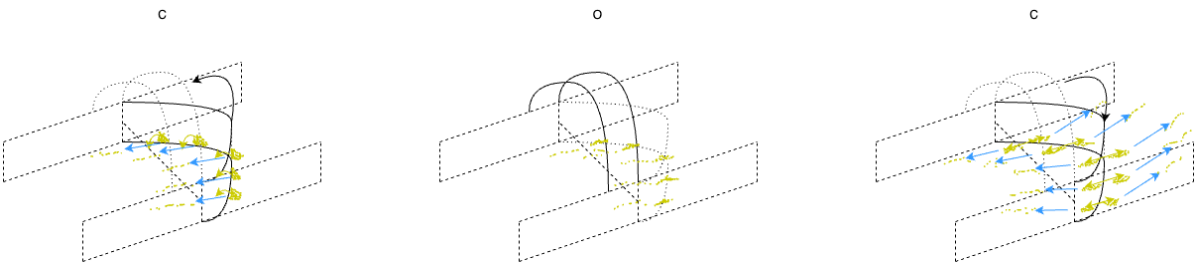

Figure 10.8: Sediment movements visor gate.

A rotary segment gate is a separate case with regards to the flushing of sediment. When the gate is closed, sediment can also accumulate in the rotating hole behind the gate. When the gate is then opened, it will scoop up this sediment and let a large part erode and be resuspended. The gate might endure problems in opening again when a lot of the sediment is settled on top of the gate when it is down. However, this amount is assumed to be limited, as the boat movements will help let this settled sediment erode again. During the closing of the gate, it can suck in some sediment in the hole behind it. On the other hand, the gate will push the sediment right in front of the gate away. The sediment movements during the opening and closing are shown in Figure 10.9.

The vertically hinged sector gate and rolling and sliding gate move horizontally without pushing sediment back. Just like for the vertical lift gate, radial (or tainter) gate and the visor gate, a part of the sediment will be able to erode and be resuspended while opening the gates, but another part of the sediment layer might also be able to directly enter the chamber or channel and enhance the layer

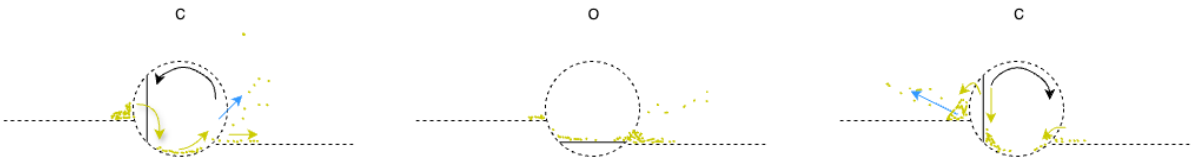

Figure 10.9: Sediment movements rotary segment gate.

thickness in these.

The sediment streams induced by the opening and closing of a vertically hinged sector gate are shown in Figure 10.10. During the opening of the gate, sediment can be moved more to the sides of the lock chamber, as this is also the direction in which their resistant walls are moving. During the closing of the gate, the sediment near the sides of the lock chamber are moved towards the middle again. A part of this sediment will also move upwards due to the turbulence and get resuspended.

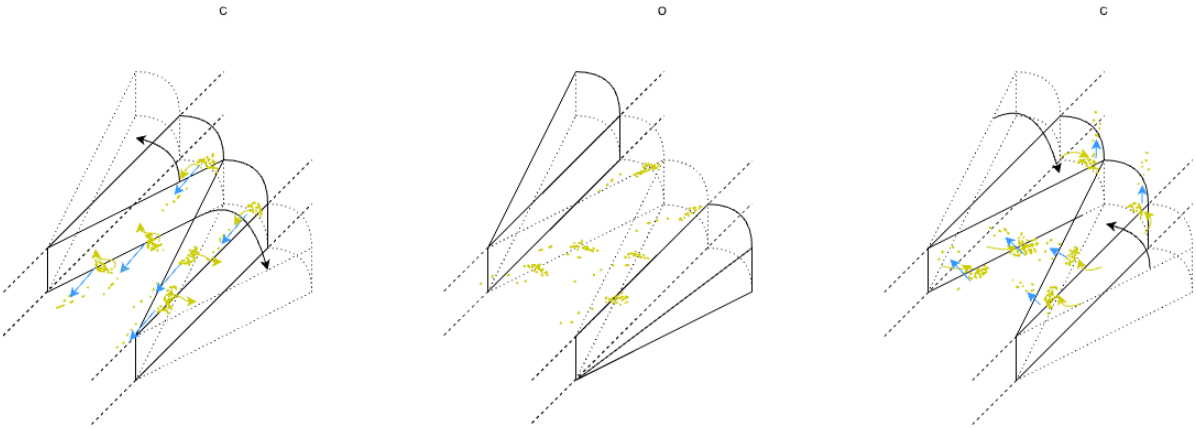

Figure 10.10: Sediment movements vertically hinged sector gate.

In Figure 10.11, the sediment movements during the opening and closing of a rolling/sliding gate are shown. Sediment will move towards the gate chamber and gate opening when the gate is opened. There is a danger of having sediment near the connection area. The gate will be able to push a part of this sediment away again when it is closing. During the closing, the sediment is moved sidewards to both sides of the gates, and is also pushed in the moving direction of the gate. Due to the turbulence, a part of the sediment that is pushed away, will be able to resuspend into the water around the gate.

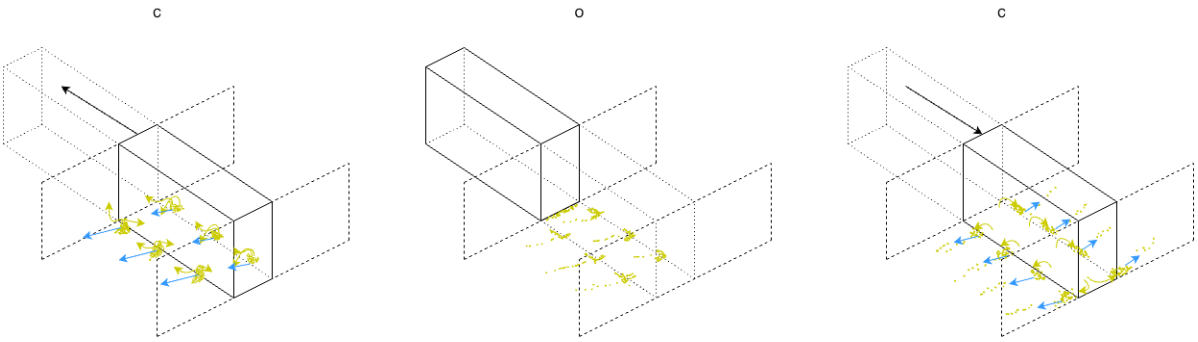

Figure 10.11: Sediment movements rolling/sliding gate.

Flushing

The timing and manner in which lock gates are operated, can significantly influence the flushing of sediment around the gates. Gates are frequently opened and closed before the water levels of the two bodies are fully equalized. This residual difference in water head generates a flow over the sill of the

lock, which facilitates the removal of sediment through flushing. Certain gate operation methods can also enhance the flushing capacity of locks. This is often achieved by closing the gates relatively quickly until a small opening remains, followed by a slower closing phase. During this final, slower movement, the flow near the sill of the lock effectively flushes accumulated sediment. Among the various gate types, the vertical lift gate, radial (or tainter) gate and visor gate can particularly be effective for improving the flushing, as their closing mechanisms bring the opening closer to the bottom of the lock, where sediment tends to accumulate most.

Sealing

A tight sealing of the gate will ensure that no water with sediment can enter the chamber or channel, when the gates are in a closed position. Such a leak can be small, but when a leak is constantly present it can cause a significant increase in sedimentation in the end. The sealing property of gates can be improved by, for example, changing the seals more often or introducing a high-precision sill. There are three gate types that have proven to be difficult to seal in a lock gate operation: rotary gates, vertically hinged sector gates, and rolling and sliding gates. Gate types that are generally sealed quite well because the hydraulic loads working on them increase this property, are single-leaf gates and mitre gates.

10.3.2. Cost, construction, time and safety requirements

Table 10.3 gives a comparison of the different gate types based on the remaining criteria from the functional requirements. The criteria include costs, construction complexity, vessel waiting time and safety of vessels. The scoring of the criteria is based on literature research (Daniel & Paulus, 2018, 2019; Glerum & Vrijburcht, 2000).

Now, an elaboration is given on how each of the criteria is defined. Both costs and complexity are desired to be kept to a minimum. Bangladesh does not have a rich history of implementing navigation locks in their sediment polluted waterways. Because of their lack in experience, the construction of a gate with a relatively low complexity will be beneficial. In a later design stage, a more detailed study should be conducted on the costs of certain gate types. This will give insights into what gates will give the optimal cost to benefit ratio. The waiting time for vessels depends on a few factors: the amount of boats wanting to pass the channel at that time, the state that the lock is in when the vessel arrives, the time required to fill and empty the chamber, and the time required to open and close the gates. Generally, a low waiting time is desired. Maintaining the safety of vessels passing through the gates is of utmost importance. The safety of vessels can be decreased when there is a limited clearance under the gate when it is in an open condition and when they are more susceptible to ship collisions due to the direction and way in which they move. Each gate is assigned a score, varying from '-', '0', '+', for every criterion.

In Table 10.3, it is seen that the radial (or tainter) gate, the mitre gate and the vertical lift gate have the best total score. All three gate types have low to moderate costs and a low vessel waiting time. Additionally, the mitre gate has good properties with regards to the safety of vessels. Radial (or tainter) gates and vertical lift gates score lower on vessel safety due to their limited clearance when they are fully opened. These gate types remain viable options. However, this limitation warrants attention, particularly in the Mongla-Ghasiakhali case, where navigation aids are absent, and fleet information is insufficient.

10.3.3. Conclusion

The opening/closing time of the gates is the most important sediment consideration when the differences between the water bodies outside and inside the chamber are large. When the sediment layer thickness is relatively large, the flushing property is of importance. The tight sealing of the gates is very important when there is a high suspended sediment concentration inside the water in front of the gate.

The gates that have a low to moderate opening/closing time are the mitre gate, vertical lift gate, radial (or tainter) gate and vertically hinged sector gate. A mitre gate is able to push accumulated sediment in front of the gate away and thereby reduces the sediment inlet. The operation can experience trouble when the force needed for this pushing away becomes large due to an increased accumulated sediment volume. The vertical lift gate and radial (or tainter) gate can flush sediment away when they are closed.

Table 10.3: Gate comparison: cost, construction, time and safety.

Gate type	Costs	Construction complexity	Vessel waiting time	Safety of vessels
Single-leaf gate	+	0	-	+
Radial (or tainter) gate	+	0	+	0
Visor gate	0	0	0	-
Vane gate	0	0	0	+
Mitre gate	+	0	+	+
Vertical lift gate	+	0	+	0
Rotary segment gate	0	0	0	-
Vertically hinged sector gate	-	-	+	+
Rolling and sliding gate	-	0	-	-

This is needed, as sediment in the connection between the gate and the bottom or sill can cause various problems. A vertically hinged sector gate is more likely to flush sediment into the lock chamber than outwards. Mitre gates are often sealed well as the loads on the gate increase its sealing function. A vertically hinged sector gate has experienced problems with sealing in the past.

It can be concluded that in the Mongla-Ghasiakhali case, the mitre gate is the best option for reducing the sediment inlet and accumulation, while still fulfilling the other gate requirements. The vertical lift gate and radial (or tainter) gates are also valid options, but would not be chosen here in this stage, because there is not enough information about the heights of the vessels in the waterway.

10.4. Lock chamber

The most important properties of the chamber of a lock are its length, width and depth. These properties are primarily dependent on the vessel sizes, but sedimentation can also play a role in these. It can be chosen to widen or deepen the chamber in order to account for future sedimentation. Otherwise, maintenance dredging would have to be undertaken earlier. More on this is explained in Chapter 11. When the length or width of the chamber is increased, the sediment layer thickness will generally be decreased due to the fact that the sediment volume can be distributed over a larger area. When only the depth of the chamber is increased, the layer thickness will not be immediately increased or decreased, but the system can allow for a greater layer thickness, as there is more clearance in the height. Next to these direct influences, the changes in the chamber dimensions can also affect the sediment movements indirectly.

By increasing the chamber dimensions, the water exchange volume needed to level the water inside the chamber is also increased. However, there is also a larger initial water volume inside the chamber in this case. The ratio between the water exchange volume and the water already inside the chamber only changes when the height of the water column is changed.

When the width of the chamber is increased, the water exchange volume due to density currents is increased as well. However, there is again also a larger volume of fresh(er) water in the chamber. The ratio remains the same in this case. The sediment layer thickness in the lock chamber can also be affected indirectly through the length of the chamber and its influence on the density currents. When the length of the chamber is increased, the time required for the density currents to reach an equilibrium increases as well.

The ratio of water exchange volume due to boat movements of the total water volume inside the chamber decreases when the chamber dimensions increase. This means the boat movements will have a lesser effect on the suspended sediment concentration inside the chamber until the keel clearance is reduced considerably. The reduction of the keel clearance can cause a rise in the erosion rate and can increase the suspended sediment concentration due to the resuspension of particles. A boat will also be able to travel with a greater speed into the lock when the width of the chamber is increased. This change reduces the time in which the total water exchange volume due to boat movements is reached. Higher boat velocities can enhance the erosion and resuspension processes during these movements.

10.5. Filling and emptying system

The most frequently used filling and emptying systems are culverts, openings in lock gates and lock gates themselves (Daniel & Paulus, 2018, 2019; Glerum & Vrijburcht, 2000). Each type has their own advantages and disadvantages. When the different types are known, their efficacy can be assessed using the functional requirements of the structural design of the lock.

Culverts are closable conduits along or below the lock entrance. This option is often preferred in large locks as they have a better flow distribution and can therefore have a lower filling/emptying time without disturbing vessels due to high currents. Culverts do require more space aside or under the lock chamber which in turn requires more excavation of the site. This leads to higher construction costs. Another disadvantage of using culverts is their susceptibility to sediment deposits at their intakes.

Openings in lock gates can distribute the water flow in a less balanced manner than culverts. This results in higher flow velocities and higher loads on vessels. The construction of the openings in the gates do not require additional space or excavations. The openings in gates generally have no problems regarding sediment deposits.

Most gates can also be opened partially to fill or empty the chamber. This operation gives the highest flow velocities and loads on vessels. The operation can only be done for small water head differences, with large opening/closing times or when no boats are present in or near the chamber. The partial opening of a gate is able to flush sediment towards the low water side of the system. The opening can be preferable when you would want to flush some sediment from the lock chamber into the channel so that the sediment layer thickness in the chamber is reduced.

The best option regarding a sedimentation based design of a lock also including the other requirements, is the use of openings in gates. The system will consist of multiple gate openings in the bottom of the

gates. Energy dissipating bars can be included to further distribute the flow when flowing into our out of the chamber. The openings often have a rectangular shape. The filling/emptying system of gate openings can definitely be incorporated in mitre gates as well as in vertical lift gates, but may be more difficult for radial (or tainter) gates due to their curvature.

10.6. Other features

The previous paragraphs went into adapting the design of the main parts of a navigation lock so they can manage the sediment concentrations and sedimentation volume in a better way. Next to this, it is also possible to introduce other (smaller) elements that can improve its ability to deal with sediment even further. The goal of such an element can be to catch sediment, to flush it away or to increase the sealing tightness of the system.

In order to catch the sediment, you need to have room to store this and the sediment itself needs to be appropriate for it. In the Mongla-Ghasiakhali waterway, the sediment is very fine. This can make it hard to catch the sediment. When the sill depth is increased, more sediment can be trapped in front of the lock, thereby reducing the inlet. As mentioned earlier, the depth of the lock chamber can also be increased. This means that the system can allow more sediment to be caught inside the chamber. This sediment does need to be dredged at some point, when the sediment layer starts to become an obstacle for the vessels that are passing through.

The principle of incorporating an additional flushing device would be to increase the bottom flow velocity by releasing water or air from a location near or on the bottom or the lock with a greater speed that the existing flow velocity. Implementing such a system does mean that the design becomes more complex and costly. Therefore, it should only be implemented when the maintenance option does not suffice.

A seal is needed to tighten the lock gate connection. By improving the seal in the connection, less sediment would be able to enter the chamber through leakage, when the gates are supposed to be closed. It is also good to replace the seal more often when you want to ensure its tightness, as the connection can be damaged due to its wear and tear.

10.7. Conclusion

The approach structure is meant to guide ships to and from the waiting area and chamber. To prevent sedimentation on the lock sill, holding basins must have a greater depth than the sill depth. The effect that different approach structures can have on the sediment transport and sedimentation is recommended to take into account in a later study.

The sediment-based characteristics on which the gate types are tested are the opening/closing time of the gates, the sediment movements during the opening/closing, and the flushing and sealing ability of the gates. Using only the sediment considerations, the preferred gate types would be the mitre gate, vertical lift gate and radial (or tainter) gate. These gates have a rather short opening/closing time and a good flushing property during the opening/closing. From these options, the mitre gate should be chosen when the sealing of the gates is very important. After also looking at the other requirements, it can be concluded that in the Mongla-Ghasiakhali case, the mitre gate is the best overall option.

It can be chosen to widen or deepen the lock chamber in order to account for future sedimentation. Otherwise, maintenance dredging would have to be undertaken earlier. When the length or width of the chamber is increased, the sediment layer thickness will generally be decreased due to the fact that the sediment volume can be distributed over a larger area. When only the depth of the chamber is increased, the layer thickness will not be immediately increased or decreased, but the system can allow for a greater layer thickness, as there is more clearance in the height. Next to these direct influences, the changes in the chamber dimensions can also affect the sediment movements indirectly.

The best option for the filling and emptying system, regarding a sedimentation-based design of a lock also including the other requirements, is the use of openings in gates. The construction of the openings in the gates do not require additional space or excavations and the gates generally have no problems regarding sediment deposits. The filling/emptying system of gate openings can definitely be incorporated in mitre gates as well as in vertical lift gates, but may be more difficult for radial (or tainter) gates due to their curvature.

It is also possible to introduce other (smaller) elements that can improve the locks' ability to deal with sediment even further. The goal of such an element can be to catch sediment, to flush it away or to increase the sealing tightness of the system.

11

Maintenance design

11.1. Functional requirements

The functional requirements for the maintenance design of a lock dealing with high sediment concentrations are given in Table 11.1. First of all, the maintenance frequency should be minimised in order to decrease the lifetime costs of the design. It is also important to minimise the time and space in which the maintenance would take place. When the maintenance time is long, a possible alternative route should be provided during maintenance works. At last, the maintenance design should be efficient and durable.

Table 11.1: Functional requirements for the maintenance design of a lock facing high sediment transportation.

Number	Functional requirement
1	Minimising the maintenance frequency
2	Minimising the obstruction time or space during maintenance
3	Provide a possible alternative route during maintenance works
4	Cost efficient and durable design

Maintenance can be required in the chamber as well as in the channel. Maintenance works in the chamber will probably have to be done more frequently than in the channel as the sediment in the chamber is distributed over a smaller area.

It is preferred to carry out the maintenance when the chamber and channel are not operational. This can only be the case when the operational cycle of the lock is less than $24\ hrs$ a day. There is no alternative route needed when it is possible to carry out the maintenance during the standard non-operational time.

11.2. Frequency

11.2.1. Lock chamber

The sediment layer thickness inside the chamber when it has operated one year with the two way traffic scheme and a flushing cycle after every operating $12\ hrs$ is about $3.22\ m$. The frequency with which both the chamber and the channel need to be dredged to maintain navigability is strongly dependent on their bottom levels. The bottom levels were initially set to a value that provides just enough keel clearance for a large design vessel. In the case of sedimentation, however, it would be better to excavate more to start with and lower the bottom level. Lowering the bottom level means that the system can allow for (more) sedimentation before maintenance is really needed. A first estimate of the required lowering can be determined based on the sediment layer thickness calculated in the model. In Paragraph 10.4 it is explained that deepening the lock chamber also has an effect on the sedimentation itself. Therefore, this would need to be recalculated to determine a better estimate of the required excavation. The first

estimate would be that, when you would only want to do maintenance works in the chamber once a year, the lock chamber needs to be excavated with $3.22\ m$ more than is needed for the required keel clearance. This is possible, but it is quite a large excavation. The corresponding volume that would need to be dredged in the chamber is then $4.60 * 10^3\ m^3$. About $1.61\ m$ would need to be excavated when maintenance would be done twice a year and about $1.07\ m$ when you would do maintenance three times a year. When the excavation needs to be lower, the frequency of the dredging that is required will increase. It is assumed that it is not preferable to excavate the chamber more than $3.22\ m$, resulting in a minimum maintenance frequency of once per year.

11.2.2. Channel

The estimated sediment layer thickness in the channel after one year with the two way traffic scheme and a flushing cycle after every operating $12\ hrs$ is about $2.67 * 10^{-2}\ m$. In comparison with the sedimentation in the lock chamber and the situation in the channel before the lock construction, this is not a large number. The channel can be excavated with this amount to prepare for the future sedimentation. The maintenance frequency in the channel can be less than once per year, which would be a certain improvement with respect to the situation in which no locks would have been constructed. The sediment layer thickness in the channel after one year under the described conditions corresponds to a sedimentation volume of $5.79 * 10^4\ m^3$ per year. In the situation before the lock construction, a volume of $2.2 * 10^6\ m^3$ needed to be dredged annually. This corresponds to an allowable sediment layer thickness of about $1.01\ m$ over the channel. When this same amount is allowed now and the sediment layer thickness progression would follow the same linear course as calculated in Chapter 9, the channel would only have to be dredged once every $37\ yrs$. You can also argue the other way around: when the allowed maintenance frequency is once in $20\ yrs$, the sediment layer thickness that is allowed is $5.34 * 10^{-1}\ m$. The low frequency of the dredging options for the channel is a good indication that the locked system effectively protects the channel from sediment.

It should be noted that both in the lock chamber and in the channel, boat movements will have pushed settled sediment to the sides of the chamber and channel. The sediment will be brought into two slopes with the lowest sediment layer thickness in the middle of the chamber and channel. Due to this, the system can allow for a sediment layer thickness that would slightly exceed the required keel clearance, because the layer is not distributed equally. Figure 11.1 shows a sketch of the new distribution of the sediment layer thickness due to boat movements. The sedimentation volume is not changing. The dotted orange line represents the sediment layer when it would be distributed equally and the full orange line presents the new slopes.

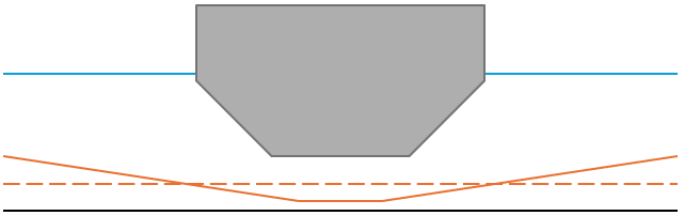

Figure 11.1: Sketch sediment layer thickness slopes.

When the locks would be constructed and a more accurate estimate of the actual sedimentation can be made, it is recommended to look into the optimisation of the maintenance dredging. The important choices that need to be made are then how much the chamber and channel are deepened to allow a certain amount of sedimentation and what the preferred maintenance frequency is.

Maintenance dredging is not the only part of the system that requires periodic care. The navigation lock itself, including the lock heads with gates and the operation mechanisms behind them, also need to be maintained. The frequency of this maintenance is depending on the eventual lock design and operation scheme. Overall, a lock with higher investment costs in the design phase, will require a lower maintenance frequency and therefore lower maintenance costs. Next to this, the fully operational scheme will require a higher maintenance frequency than the two way traffic scheme, because the lock is used more often and therefore also has a higher probability to endure problems such as wear. It

can be beneficial to find an optimum between the investment costs of the design and the maintenance costs. This should be done in a later design phase.

11.3. Duration

The duration of the maintenance dredging is mainly depending on the volume that needs to be dredged and the equipment that is used. Dredging can be performed using equipment either on land or in the water (Land and water, n.d.). Overall, the dredgers in the water are larger and therefore often have a greater capacity than the excavators used for dredging on land. Which type of dredger should be used is also depending on the location of the sediment disposal site and if this is better reachable via land or water. The channel between Mongla and Ghasiakhali is large enough to accommodate a dredging ship and let other vessels still pass by. The channel is $31\ km$ long and the total dredging volume over this area is quite large when the frequency is minimised. Furthermore, it is assumed that an excavator on land will not be able to reach the full $70\ m$ width of the channel. For these reasons, it is logical to let the dredging in the channel be done by a dredging ship. During the dredging of the lock chamber, no navigation through it will be possible. The lock has 12 non-operating hours when the two way traffic scheme is implemented. The maintenance dredging should only be done during these $12\ hrs$ in the night, when it is important not to obstruct the navigation. The dredging can be done by a small or medium dredging boat or by an excavator on land. The lock is only $110\ m$ long and $13\ m$ wide. When the infrastructure around the lock is constructed with maintenance dredging in mind, the lock will be readily accessible to an excavator.

A dredger can be either mechanically or hydraulically driven (Hardya, 2016). A mechanical dredger, equipped with a bucket, works with digging and/or cutting. A hydraulic dredger operates using water power. The hydraulic dredger uses a water jet to extract a mixture of water and soil from the dredging area. Maintenance dredging can be divided into four main phases (Notteboom et al., 2022). The first phase is the excavation of the sediment. This is done with a bucket or with a sucking force. The second phase of dredging is the vertical transport of the sediment. The sediment on the bottom of the chamber or lock needs to be transported to the water or land level of the dredger. In the third phase, the sediment needs to be transported horizontally towards a specific sediment disposal site. The transportation can be done via road or river. After this, the dredged material should be placed for disposal somewhere or placed at a spot where it can be re-used. It is important to analyse the possible re-use of the dredged sediment in a later stage of the study. This can reduce the environmental impact that the dredging works may have.

Between the excavators and boat dredgers and the mechanical and hydraulic ones, there are still a lot of different options with a large capacity range. The capacity of a dredging device is often found in a range varying from $30\ m^3/h$ to $330\ m^3/h$ (Hanowsky et al., 2024; Hardya, 2016; Webb et al., 2015). With this range in capacity, the volume that can be dredged per $12\ hrs$ is $360\ m^3$ to $3,960\ m^3$. When it is assumed that an excavator with a capacity of $100\ m^3/h$ is used to dredge the chamber, it would take the excavator about $14.3\ hrs$ to dredge $1.0\ m$ sedimentation in the chamber. The water dredger which would be used for dredging the channel can, for example, have a capacity of $200\ m^3/h$. It would take one of these dredgers about 45 full days to dredge $0.1\ m$ sedimentation out of the channel.

As there are still parameters unknown with regards to the sedimentation and dredging process, it is not useful to go into more depth about the specific optimisation of the dredging works in the chamber and channel. The first step will be to do more site investigation on the surrounding area and facilities, and on the specific sediment that is suspended in the water near Mongla and Ghasiakhali. This will need to be done in a later stage of the maintenance dredging design.

11.4. Alternative route

The waterway between Mongla and Ghasiakhali is wide enough for boats to travel on one side of it, while another side is being partially dredged. However, when there is only one lock constructed on both sides of the waterway, it is not possible to let water vessels pass the chamber during maintenance. This would not be a problem if all the maintenance works can be done in the non-operational hours of the lock. It would be a problem when the lock is normally in constant operation. A solution to this problem would be to construct a second lock on both sides of the waterway. In this case, one lock can

keep operating when the other one is under maintenance. However, the construction of a second lock on both sides is very costly. This option is preferable only if the annual maintenance costs become so high that, over the lock's lifetime, they exceed the construction costs of building a second lock.

Constructing a second lock is not the only option of providing an alternative route when maintenance needs to be done. It is mentioned in Chapter 3 that in the Mongla-Ghasiakhali case, there is one alternate waterway route possible. This route takes longer and goes through the Sundarbans. The Sundarbans is a protected area, so this would definitely not be preferable. It is also possible to provide a route by constructing more roads. However, companies would then need to invest in vessels for on the road for only a short period of maintenance time. The traffic can also be inhibited during the maintenance. No alternative route is then needed, but boat vessels need to wait a period before they can travel through the channel again. Whether this is acceptable, depends on the time that is needed for the maintenance. It may be preferred to perform the maintenance in steps in this case, to reduce the consecutive amount of time the waterway is obstructed.

11.5. Costs and efficiency

Multiple studies have already been conducted to optimise the maintenance dredging schedule (Bai et al., 2021; Hanowsky et al., 2024; Hardya, 2016; Webb et al., 2015). The costs and efficiency of the maintenance are very much depending on the chosen dredging schedule, but also on the eventual design of the lock system.

The sediment in the Mongla-Ghasiakhali waterway is highly silty and solidifies rapidly. Frequent dredging prevents excessive solidification, making the process more efficient and cost-effective. Delayed dredging increases sediment hardness, raising the cost per cubic meter of removal. Maintenance schedule optimisation should account for the trade-off between minimising dredging volume and reducing overall dredging costs.

The sedimentation analysis concludes that the total dredging volume per year with the two way traffic operation scheme and a flushing cycle is about $6.25 * 10^4\ m^3$ for the chamber and channel together. This is 35 times less than the volume that was required to be dredged before. The locked system can therefore definitely reduce the costs for the maintenance dredging. The total cost of maintenance is difficult to estimate, as the lock itself will require maintenance as well. How the specific costs and efficiency of the maintenance design will look, needs to be determined in a later stage of the study.

11.6. Conclusion

Maintenance works in the chamber will have to be done more frequently than in the channel. The frequency with which both the chamber and the channel need to be dredged to maintain navigability, is strongly dependent on the bottom level of them. The volume that needs to be dredged in the chamber with a two way traffic operating scheme and a flushing cycle is $4.60 * 10^3\ m^3/y$. The minimum frequency of maintenance dredging in the channel is about once per year. The required dredging volume in the channel under the same conditions is $5.79 * 10^4\ m^3/y$. The minimum frequency for this dredging is about once in $37\ yrs$. The maintenance dredging in the channel requires a larger dredger on a boat, while the maintenance dredging in the chamber can be done by an excavator on land. The capacity of a single dredger is typically in between $30\ m^3/h$ and $330\ m^3/h$. It is recommended to look into the optimisation of the maintenance dredging schedule in a later study.

The waterway between Mongla and Ghasiakhali is wide enough for boats to travel on one side of it, while another side is being partially dredged. However, when there is only one lock constructed on both sides of the waterway, it is not possible to let water vessels pass the chamber during maintenance. This is only a problem when the lock is in constant operation. A solution to this problem is constructing a second lock. This option is preferable only if the annual maintenance costs become so high that, over the lock's lifetime, they exceed the construction costs of building a second lock.

The costs and efficiency of the maintenance are very much depending on the chosen dredging schedule, but also on the eventual design of the lock system. The optimisation of the dredging schedule should include the choice between minimising the dredging volume or reducing the overall dredging costs. As the eventual design of the lock system is not completely known yet, the maintenance costs of the

additional parts remain difficult to determine. It is concluded that the maintenance dredging costs of the Mongla-Ghasiakhali waterway are reduced by introducing the two navigation locks.

12

Conclusion

Many rivers, including the Mongla-Ghasiakhali waterway in Bangladesh, are dominated by an asymmetrical tide. When high sediment concentrations are present, this asymmetry, combined with an increased tidal pumping process, can lead to significant sedimentation rates near the tidal meeting zone of the system. The proposed solution is to reduce sedimentation by introducing two sluices with navigation locks on either side of the waterway. This report models the sedimentation within the navigation lock and the channel between the two locks. Based on these results, the optimal adaptations for the structural and maintenance design of the lock dealing with sedimentation are discussed. The research questions regarding the sedimentation quantification, design and operation choices, and the maintenance considerations (established in Chapter 2) will subsequently be answered.

Quantification of sedimentation

The sedimentation in both the lock chamber and the channel behind it is calculated using the schematized box method. The operational cycle of a lock is divided into phases, and for each phase, the sediment balance has been set up. The phases are organised in two different sequences, referred to as scenario 1 and scenario 2. It is assumed that, during each phase, a single water exchange process is active. The considered water exchange processes include the filling and emptying of the lock chamber, the density currents induced by differences in salt content and sediment concentration between the water bodies, and the movement of boats in and out of the chamber.

The sedimentation is determined by quantifying the deposition and erosion. The model developed to simulate the sedimentation within the system is initially run for one operational cycle, followed by one tidal cycle, and eventually for multiple tidal cycles.

In the simulation of the operational cycle under two scenarios, the largest increase in suspended sediment concentration in the chamber occurs during the filling phase, while in the channel, it occurs during the chamber's emptying phase. Scenario 2 produces the largest sediment layer thickness in the chamber, reaching $7.30 * 10^{-4}\ m$ per operational cycle. In this scenario, the concentration in the chamber attains a higher value earlier on, due to a greater ratio of salt water suspension relative to freshwater. This is because a boat is already present in the lock chamber during its initial filling phase. Conversely, scenario 1 produces the largest sediment layer thickness in the channel per operational cycle, with a value of $3.65 * 10^{-7}\ m$. This occurs because sediment enters the channel earlier in scenario 1 than in scenario 2, allowing more time for sediment to settle. There were no significant differences observed between the simulations conducted with and without erosion. This is explained by the assumption of no initial sediment layer thickness at the start of the simulation, resulting in no initial sediment bed volume available for erosion. During the operational cycle, the erodible volume remains relatively small.

The tidal cycle is simulated using a two way traffic scheme with 12 operating hours followed by a resting period, as well as a fully operational scheme. In scenario 2, the cycle concludes with a flushing operation, meaning the chamber is last connected to the channel side rather than the sea side. Conversely, in scenario 1 the chamber is last connected to the sea side. For the two way traffic scheme, scenario 2 is preferred in terms of sedimentation, because it ensures a lower sediment concentration in the chamber

at the end of the 12 operating hours. The lower concentration results is a smaller sediment layer thickness in the chamber. However, this advantage may lead to an increase in sediment layer thickness in the channel. Nonetheless, the impact on the sediment layer thickness in the channel is relatively minor, as the sediment is distributed over a much larger area. The fully operational scheme leads to higher sediment layer thicknesses in the channel and lower ones in the chamber, as it continuously transports sediment from the sea side to the channel side.

The sedimentation after one month is simulated by adding multiple tidal cycles with different scenarios in a specific sequence. Series B, consisting exclusively of tidal cycles from scenario 2, results in the lowest sediment layer thickness in both the lock chamber and the channel for the two way traffic scheme. This outcome is attributed to the flushing cycle and the non-operating hours following it. In the fully operational scheme, differences in sediment layer thicknesses within the chamber between the series are less pronounced, as there is no significant variation in the build-up of the concentration. The average sediment layer thickness with series B and the two way traffic scheme after one month is $2.65 * 10^{-1}\ m$ in the chamber and $2.19 * 10^{-3}\ m$ in the channel. After one year, this results in a sediment layer thickness of $3.22\ m$ in the chamber and $2.67 * 10^{-2}\ m$ in the channel. The total sediment volume after one year is $6.25 * 10^{4}\ m^3$. In conclusion, the sedimentation volume is able to significantly decrease with the introduction of the locked system. However, sedimentation will still take place, in the lock chambers as well as the channel.

Structural design

The structural design choices aim to mitigate sediment accumulation in the system. One key consideration for the approach structure is that the holding basin should be deeper than the sill, to reduce sediment build-up in front of the lock. The mitre gate is identified as the most effective gate type for sediment-rich environments. This gate type has a short opening and closing time, has the ability to push sediment away during operation, and provides strong sealing capabilities. However, as the gate is exposed to increased torsion, it may be subject to fatigue. Other gate types suitable for such environments include the vertical lift gate and the radial (or tainter) gate. Regarding the filling and emptying system, openings in gates are preferred in sediment-rich environments, as they do not typically encounter issues with sediment deposits.

The lock chamber should be deepened to allow for the accumulation of the first sediment layer. Increasing the length and/or width or the lock chamber may reduce the sediment layer thickness, as the surface area on which the sediment volume is distributed increases. These dimensional changes can also indirectly influence the sediment inlet and accumulation within the system, as the water volume in the chamber will also change.

It may be beneficial to install a flushing device at the bottom of the lock chamber, which could flush sediment back to the sea side when the chamber is connected to it. The flushing velocity should be set higher than the velocity induced by the water exchange processes to ensure effective sediment removal.

Maintenance considerations

The maintenance design of the lock and channel is assessed based on its functional requirements, with a focus on the required maintenance dredging in the system. Based on the sedimentation analysis, the total volume that would need to be dredged after one year with the lock system installed is 35 times smaller than in the scenario without the locks. If it is desired to perform maintenance dredging in the chamber only once a year, the chamber will need to be deepened by approximately $3.22\ m$. If the preferred deepening is limited to approximately $1\ m$, maintenance dredging will be required three times per year. When a sediment layer thickness of $1\ m$ is allowed in the channel, maintenance dredging is expected to be needed only once every 37 years. The accumulated volume after this period will be nearly equal to the annual volume that is currently dredged. If it is preferred to lower the level of deepening or perform smaller, more frequent dredging instead of a single large dredging operation, the maintenance frequency should be increased.

The duration of the maintenance works depends on the dredging volume but also on the dredging equipment and its capacity. It is preferable to conduct maintenance dredging in the chamber only during non-operational hours, provided the operation scheme allows for this. A dredging device with a

capacity of $100\ m^3/h$ needs $14.3\ hrs$ to dredge $1\ m$ of sediment in the chamber. The dredging in the channel requires a dredging boat to cover the entire distance. A dredging device with a capacity of $200\ m^3/h$ needs approximately 45 full days to dredge $0.1\ m$ in the channel.

To optimise the maintenance dredging process, it is essential to evaluate the dredging facilities near the site and analyse the specific characteristics of the sediment bed. Additionally, a decision must be made to either minimise the volume of dredging or minimise the associated costs. It can be inferred that the maintenance dredging costs are reduced by the introduction of the locks.

13

Discussion

The model simulations rely on several assumptions and approximations, each of which introduces uncertainty. A key assumption is that the water in the chamber and the channel is initially free of salt and sediment. In reality, these water volumes will always contain some level of salt and sediment, which would reduce the impact of density currents at the start of the simulation.

The suspended sediment concentration of the water on the sea side significantly affects the amount of sediment present in the chamber and channel during each operational cycle. In the model, this concentration is assumed to be constant, but in reality, it fluctuates with the tidal cycle.

Modelling uncertainties

The duration of each operational phase is a significant source of uncertainty in the system's sedimentation rate. These durations are based on the time required for the water exchange processes to fully occur and on the time periods observed in similar projects. Longer durations lead to more sediment accumulation, potentially exacerbating the problem.

The uncertainty in the modelling of the filling and emptying of the lock chamber primarily stems from the head difference between sea side and the channel side. The head difference significantly influences the volume of water that is exchanged during each phase. In the model, this head difference is assumed to be constant, but in reality, it fluctuates with the tidal cycle, further contributing to uncertainty. Additionally, the modelling assumes that density currents during the chamber's filling and emptying can be neglected due to the high velocities typically present during these phases. However, as the velocity decreases towards the end of these phases, sediment-induced currents could potentially form, which the model does not account for.

The modelling of the boat movements raises several discussion points, primarily due to the uncertainty regarding vessel sizes. The simulation currently considers only one large design vessel, which occupies more underwater volume than multiple smaller vessels would. The use of multiple smaller vessels would result in a differing volume ratio during operations, which could lead to a reduction in the sediment intake during the filling and emptying phases. The velocity of smaller vessels is higher than that of a large design vessel, but the total required time for small vessels to enter or exit the chamber may be longer, as some vessels may need to wait for one another. Both the velocity differences and vessel sizes influence the erosion caused by boat movements. A vessel with a larger draught causes more erosion than a smaller one, but smaller vessels travelling at higher velocities can also induce significant erosion due to their speed.

Deposition and erosion considerations

An important but uncertain parameter in the calculation of the deposition is the effective settling velocity of the sediment. The effective settling velocity is depending on the sediment size and concentration. Small changes in these properties can significantly affect deposition. The uncertain parameters in erosion calculations are the critical bed shear stress and the erosion constant, both of which depend on the characteristics of the sediment bed. A higher erosion constant and a lower critical bed shear

stress both lead to increased erosion. In addition to these uncertainties, it is important to note that erosion caused by gate movements is not included in the model. As a result, actual erosion may exceed the model predictions, potentially leading to a reduction in the sediment layer thickness in the chamber and an increase in the sediment layer thickness in the channel.

There is no visible difference in the development of the sediment layer thickness in the chamber for erosion constants of 0.0003 and 0.003. However, if the erosion constant is increased further, a noticeable difference becomes apparent. It remains debatable whether this difference should have been observable with the first increase in the erosion constant.

Two-dimensional approach

The model is a simplified two-dimensional approach used to simulate sedimentation. One of the simplifications involves that settled sediment is distributed evenly. In reality, an uneven sediment distribution can sometimes result in a greater sediment layer thickness. Additionally, extending the simulation to a three-dimensional model could alter the settling dynamics. For instance, the settling velocity might increase in certain conditions. The current model does not account for variations in the settling velocity over the height of the water column, a factor that can significantly influence sedimentation rates. This is particularly relevant during the non-operational part of the tidal cycle when the water movement is minimal. During this period, suspended sediment concentrations in both the chamber and the channel would likely decrease to near-zero levels when the three-dimensional settling velocity is taken into account.

The structural and maintenance design choices for the lock system are based on waterways with high sediment transport and sedimentation, and the specific case of the Mongla-Ghasiakhali waterway. Other waterway case studies may require different design considerations to address their unique sediment transport and deposition characteristics.

14

Recommendations

The scope of this project was to investigate sedimentation within the lock chamber and the channel between the locks when installed on both sides of the waterway. Past human interventions, whose consequences were not fully researched, have contributed to the exacerbation of the sedimentation problem in the waterway of the study. Therefore, it is essential to also assess the potential effects the lock constructions can have on the interconnected waterway system. The construction of the locks is expected to increase sedimentation in the waterways upstream of the locks. Although this effect has not yet been fully analysed, it should be addressed in subsequent research.

Model improvements

The Python model used for the simulations can be further improved in successive analyses. One key improvement would be to account for erosion resulting from gate movements. While this could initially be implemented solely for the mitre gate, a more robust approach would include options for different gate types. This would require either making general assumptions or modelling distinct erosion areas and velocities for each gate type. Additionally, it is recommended to introduce an optional flushing device within the model. This device would generate a flow velocity near the bottom of the lock chamber, aiding in the removal of sediment from the system. It is also important to investigate the sediment distribution in the channel itself, as sediment is expected to accumulate more densely near the locks compared to other parts of the channel.

Further improvements to the model could be identified through a more extensive sensitivity analysis. The first aspect to explore is the model's sensitivity to changes in the erosion constant and its impact on sedimentation. Analysing the model's response to slight variations in lock chamber dimensions would also provide valuable insights. These changes could stem from future modifications, such as deepening the lock chamber to accommodate sediment layer accumulation or adjusting lock dimensions based on new vessel specifications. Understanding how sedimentation behaves in response to these changes would provide valuable insights for future model enhancements.

Field data

The simulation cannot only be improved by adding more processes, but also by incorporating more field data. In the case study, the water head and suspended sediment concentration of the water on the sea side of the system are currently treated as constants, but in reality, they vary with the tidal cycle. Including these variations could enhance the accuracy of the sediment predictions. While the water head and suspended sediment concentration can be estimated, field measurements are necessary to further improve the accuracy of the results. Another area with a lack of field data is the fleet in the region. Obtaining more information about the actual fleet could influence the required lock chamber dimensions and reveal specific operational opportunities.

After implementing the initial improvements and more accurately predicting sedimentation, the maintenance dredging schedule should be optimised. The model indicates that maintenance dredging will

remain necessary throughout the lifetime of the navigation locks. However, the costs associated with maintenance dredging can be minimised by strategically optimizing its schedule.

References

Bai, S., Li, M., Song, L., Ren, Q., Qin, L., & Fu, J. (2021). Productivity analysis of trailing suction hopper dredgers using stacking strategy. *Automation in Construction*, *122*. https://doi.org/10.1016/j.autcon.2020.103470

Brunner, G. (2020). Hec-ras, river analysis system hydraulic reference manual. *6*.

Camenen, B., & van Bang, D. (2011). Modelling the settling of suspended sediments for concentrations close to the gelling concentration. *Continental Shelf Research*, *31*(10), S106–S116. https://doi.org/10.1016/j.csr.2010.07.003

Center for Environmental and Geographic Information Services. (2014). Carryout morphological studies and eia/sia study to restore the mongla-ghasiakhali navigation route.

Chen, S. (2015). *Hydraulic structures*. Springer Berlin, Heidelberg. https://doi.org/10.1007/978-3-662-47331-3

Daniel, R., & Paulus, T. (2018). *Lock gates and other closures in hydraulic projects* (1st ed.). Elsevier.

Daniel, R., & Paulus, T. (2019). *Lock gates and other closures in hydraulic projects*. Elsevier. https://doi.org/10.1016/C2015-0-05399-0

Delta Context & Witteveen+Bos. (2024). Mongla-ghasiakhali canal upgrading project - conceptual study.

Dong, Y., Wu, Y., Yin, J., Wang, Y., & Gou, S. (2013). Investigation of soil shear-strength parameters and prediction of the collapse of gully walls in the black soil region of northeastern china. *Physical Geography*, *32*(2), 161–178. https://doi.org/10.2747/0272-3646.32.2.161

Eysink, W. (1989). Sedimentation in harbour basins: Mall density differences may cause serious effects. *Delft Hydraulics*, (417).

Glerum, A., & Vrijburcht, A. (2000). *Design of locks 1*. Rijkswaterstaat.

Hanowsky, M., Mitchell, K., Kothari, K., Lillycrop, W., & Loney, D. (2024). Optimal scheduling of maintenance dredging in a maritime transportation system. *Maritime Transport Research*, *6*. https://doi.org/10.1016/j.martra.2024.100113

Haque, M., & Sakil, S. (2020). A comprehensive morphological and hydrological analysis of the dharla river, northwestern bangladesh. *Bangladesh geoscience journal*, *26*, 15–40.

Hardya, T. (2016). Analysis of productivity in dredging project a case study in port of tanjung perak surabaya - indonesia. *World Maritime University*.

Hoekstra, R. (2015). Pianc wg-130 - anti-sedimentation measures for marinas and yacht harbours.

Jacobs, W. (2011). Sand-mud erosion from a doil mechanical perspective. *Doctoral Thesis, Technical University of Delft, Department of Civil Engineering, Delft, The Netherlands*.

Kämpf, J., & Myrow, P. (2014). High-density mud suspensions and cross-shelf transport: On the mechanism of gelling ignition. *Journal of Sedimentary Research*, *84*, 215–223. https://doi.org/10.2110/jsr.2014.20

Kirby, R. (2011). Minimising harbour siltation - findings of pianc working group 43. *Ocean Dynamics*, *61*, 233–244. https://doi.org/10.1007/s10236-010-0336-9

Land and water. (n.d.). *Capital and maintenance dredging*. Retrieved January 13, 2025, from https://www.land-water.co.uk/what-we-do/dredging/

Langendoen, E. (1992). Flow patterns and transport of dissolved matter in tidal harbours. *Delft University of Technology*.

Menon, R. (2023, August). *Indo bangladesh protocol route*. Retrieved September 25, 2024, from https://www.linkedin.com/pulse/indo-bangladesh-protocol-route-rajesh-menon

Mitchener, H., & Torfs, H. (1996). Erosion of mud/sand mixtures. *Coastal Engineering*, *29*(1-2), 1–25. https://doi.org/10.1016/S0378-3839(96)00002-6

Navigation channel sedimentation task committee. (2023). *Navigation channel sedimentation solutions*. ASCE. https://doi.org/10.1061/9780784485149

Notteboom, T., Pallis, A., & Rodrigue, J. (2022). *Port economics, management and policy*. Routledge. https://doi.org/10.4324/9780429318184

Rahman, M., Ahsan, M., Hore, S., Sarker, M., & Hoissain, A. K. (2013). Assessing the causes of deterioration of the mongla-ghasiakhali navigation route for restoration of navigability. *Research gate*. https://doi.org/10.13140/RG.2.1.2834.4169

Rashid, H. (1991). *Geography of bangladesh*. University Press.

Rijkswaterstaat. (2020). Waterway guidelines 2020.

Safak, I., Angelini, C., & Sheremet, A. (2021). Boat wake effects on sediment transport in intertidal waterways. *Continental Shelf Research*, *222*. https://doi.org/10.1016/j.csr.2021.104422

Shadid, S. (2010). Recent trends in the climate of bangladesh. *Climate Research*, *42*(3), 185–193. https://doi.org/10.3354/cr00889

The GeoTech: Geotechnical Engineer's Knowledge Base. (n.d.). Silt soil engineering point of view.

Tognin, D., D'Alpaos, A., D'Alpaos, L., Rinaldo, A., & Carniello, L. (2024). Statistical characterization of erosion and sediment transport mechanics in shallow tidal environments - part 2: Suspended sediment dynamics. *Earth Surface Dynamics*, *12*(1), 201–218. https://doi.org/10.5194/esurf-12-201-2024

van Rijn, L. (1993). *Principles of sediment transport in rivers, estuaries and coastal seas*. Aqua Publications.

van Rijn, L. (2005). *Principles of sedimentation and erosion engineering in rivers, estuaries and coastal seas*. Aqua Publications.

van Rijn, L. (2016). Harbour siltation and control measures.

van Rijn, L. (2020). Critical bed-shear stress for mud-sand beds.

van Rijn, L., Albernaz, M. B., Perk, L., Alonso, A. C., van Weerdenburg, R., & van Maren, D. (2024). Critical bed-shear stress of mud-sand mixtures. *Journal of Hydraulic Engineering*, *151*(1). https://doi.org/10.1061/JHEND8.HYENG-14092

Verney, R., Deloffre, J., Brun-Cottan, J., & Lafite, R. (2007). The effect of wave-induced turbulence on intertidal mudflats: Impact of boat traffic and wind. *Continental Shelf Research*, *27*(5), 594–612. https://doi.org/10.1016/j.csr.2006.10.005

Webb, R., Dreher, T., & Fuglevand, P. (2015). Environmental dredging productivity for precision excavator dredges. *Proceedings of the Western Dredging Association and Texas AM University Center for Dredging Studies, Dredging Summit and Expo 2015*.

Weber-Shirk, M., Guzman, J., O'connor, C., Pennock, W., Lion, L., Du, Y., Maisel, Z., Conneely, J., Doyle, A., McGrattan, S., Wood, E., & Pennock, A. (n.d.). The physics of water treatment design. *AguaClara*.

Winterwerp, J., van Kessel, T., van Maren, D., & van Prooijen, B. (2021). *Fine sediment in open water: From fundamentals to modeling*. World Scientific. https://doi.org/10.1142/12473

Winterwerp, J., & van Kesteren, W. (2004). *Introduction to the physics of cohesive sediment in the marine environment*. Elsevier.

A

Set of equations phases scenario 1

Table A.1: Set of equations for the phases of operational scenario 1, in the order in which they should be used.

Phase	Period of time [min]	Set of equations
1	14	8.1 - 8.19
2	4	8.8 8.20 - 8.23 8.9 - 8.12 8.24 8.14 - 8.19
3	6	8.25 - 8.27 8.9 - 8.12 8.28 8.14 - 8.19
4	14	8.1 - 8.4 8.29 8.6 - 8.13
5	4	8.8 8.20 - 8.22 8.30 8.9 - 8.12 8.24 8.14 - 8.19
6	6	8.31 8.26 8.32 8.9 - 8.12 8.28 8.14 - 8.19
7	6	8.25 - 8.27 8.9 - 8.12 8.28 8.14 - 8.19
8	14	8.1 - 8.19
9	4	8.8 8.20 - 8.23 8.9 - 8.12 8.24 8.14 - 8.19
10	6	8.31 8.26 8.32 8.9 - 8.12 8.28 8.14 - 8.19

B

Source code operational cycle scenario 1

```
import numpy as np
import matplotlib.pyplot as plt
import matplotlib.ticker as ticker

# Sediment balance scenario 1
# One tidal cycle (phase 1-10)


# Simulation parameters
timestep = 10 # Time step 10 s
time_steps = np.arange(0, 4681, timestep) # 78 minutes

# 06:00

# Parameters
c_o_0 = 3 # Concentration at some time, place, and averaged depth (kg/m^3)
c_i_0 = 0 # Initial inside concentration (kg/m^3)
c_c_0 = 0 # Initial channel concentration (kg/m^3)

rho_d = 1600 # Density sediment (kg/m^3)
rho_o = 1025 # Mean fluid density outside basin (kg/m^3)
rho_i_0 = 1000 # Initial inside density (kg/m^3)
rho_c_0 = 1000 # Initial channel density (kg/m^3)

rho_o_s = rho_o * (1 - c_o_0 / rho_d) + c_o_0 # Inital density of the water outside including
     suspended sediment contribution (kg/m^3)
rho_i_s_0 = rho_i_0 # Initial density of the water inside including suspended sediment
    contribution (kg/m^3)
rho_c_s_0 = rho_c_0 # Initial density of the water channel including suspended sediment
    contribution (kg/m^3)

D_rho_o_s_0 = rho_o_s - rho_i_s_0 # Initial density difference between outside & inside (kg/m
    ^3)
D_rho_oc_s_0 = rho_i_s_0 - rho_c_s_0 # Initial density difference between outside & inside (
    kg/m^3)

W = 13 # Width channel (m)
L = 110 # Length channel (m)
A = W * L # Area channel (m^2)
a = 2.0 # Area openings F/E (m^2)
Wc = 70 # Width MG-canal (m)
Lc = 31000 # Length MG-canal (m)
Ac = Wc * Lc # Area canal (m^2)

b_d = 12 # Width of design vessel (m)
d = 4.2 # Draught of design vessel (m)
```

```
L_d = 75 # Length of design vessel (m)
v_boat = 3 / 3.6 # Velocity of design vessel (m/s)

g = 9.81 # Gravitational constant (m/s^2)
C = 0.6 # Discharge coefficient (to be checked)
f3 = 0.3  # Vertical exchange coefficient

h_i_0 = 4.90 # Initial water level inside (7.90 + 2) - 5 (m)
h_o_0 = 9.90 # Water level outside(m)
h_c_0 = 4.90 # Initial water level channel (m)
V_i_0 = h_i_0 * A # Initial volume inside basin (m^3)
V_c_0 = h_c_0 * Ac # Initial water volume inside channel (m^3)
D_ho_0 = h_o_0 - h_i_0 # Initial max head difference F/E (m)
D_hc_0 = h_i_0 - h_c_0 # Initial max head difference channel (m)

Vboats = v_boat * b_d * d * timestep # Exchange volume per 10 seconds (m^3)
V_boat_max = L_d * b_d * d # Maximum exchange volume due to design vessel (m^3)

ws_eff_i = 0.00017 # Effective settling velocity (m/s), placeholder value
ws_eff_c = 0.00017 # c_c

V_s_0 = A * (ws_eff_i / rho_d) * c_i_0 * timestep # Initial sediment volume inside basin (m
    ^3)
G_s_0 = V_s_0 / A # Initial sediment layer thickness inside basin (m)
V_s_c_0 = Ac * (ws_eff_c / rho_d) * c_c_0 * timestep # Initial sediment volume inside channel
     (m^3)
G_s_c_0 = V_s_c_0 / Ac # Initial sediment layer thickness inside channel (m)

tau_ce = 1.5 # Critical bed-shear stress (N/m^2)
m_e = 0.0003 # Erosion constant (kg/N/s)
n = 0.01 # Manning coefficient (m^1/3 / s)
u_0 = 0 # Depth-averaged flow velocity at t=0 (m/s)
Ch_0 = (1 / n) * (h_i_0) ** (1/6) # Chezy coefficient (m^1/2 / s)
tau_b_0 = rho_i_s_0 * g * ((u_0 ** 2) / (Ch_0 ** 2)) # Applied bed-shear stress (N/m^2)
A_e_fe = 30 * W # length, area of velocity filling/emptying (m^2)
A_e_dens = 110 * W # length, area of velocity density currents (m^2)
A_e_boat = 50 * W # length, area of velocity boats (m^2)

# Arrays to store results
h_i = np.zeros_like(time_steps, dtype=float) # Water level inside basin (m)
h_o = np.zeros_like(time_steps, dtype=float) # Water level outside (m)
h_c = np.zeros_like(time_steps, dtype=float) # Water level inside channel (m)
D_ho = np.zeros_like(time_steps, dtype=float) # Water level difference outside and inside
    basin (m)
D_hc = np.zeros_like(time_steps, dtype=float) # Water level difference inside basin and
    inside channel (m)
V_i = np.zeros_like(time_steps, dtype=float) # Water volume inside basin (m^3)
V_c = np.zeros_like(time_steps, dtype=float) # Water volume inside channel (m^3)
v_FE = np.zeros_like(time_steps, dtype=float)
Q_FE = np.zeros_like(time_steps, dtype=float)
D_V = np.zeros_like(time_steps, dtype=float)
Vvert = np.zeros_like(time_steps, dtype=float)
Vboat = np.zeros_like(time_steps, dtype=float)
rho_i = np.zeros_like(time_steps, dtype=float)
rho_c = np.zeros_like(time_steps, dtype=float)
rho_i_s = np.zeros_like(time_steps, dtype=float)
rho_c_s = np.zeros_like(time_steps, dtype=float)
D_rho_o_s = np.zeros_like(time_steps, dtype=float)
D_rho_oc_s = np.zeros_like(time_steps, dtype=float)

c_i = np.zeros_like(time_steps, dtype=float) # Suspended sediment concentration inside basin
    (kg/m^3)
c_c = np.zeros_like(time_steps, dtype=float) # Suspended sediment concentration inside
    channel (kg/m^3)
V_s = np.zeros_like(time_steps, dtype=float) # Sediment volume inside basin for each time
    step (m^3)
V_s_sum = np.zeros_like(time_steps, dtype=float) # Accumulated sediment volume inside basin (
    m^3)
G_s = np.zeros_like(time_steps, dtype=float) # Sediment layer thickness inside basin for each
     time step (m)
G_s_sum = np.zeros_like(time_steps, dtype=float) # Accumulated sediment layer thickness
```

```
    inside basin (m)
V_s_c = np.zeros_like(time_steps, dtype=float) # Sediment volume inside channel for each time step (m^3)
V_s_c_sum = np.zeros_like(time_steps, dtype=float) # Accumulated sediment volume inside channel (m^3)
G_s_c = np.zeros_like(time_steps, dtype=float) # Sediment layer thickness inside channel for each time step (m)
G_s_c_sum = np.zeros_like(time_steps, dtype=float) # Accumulated sediment layer thickness inside channel (m)

u = np.zeros_like(time_steps, dtype=float) # Depth-averaged flow velocity near lock heads
Ch = np.zeros_like(time_steps, dtype=float) # Chézy coefficient
tau_b = np.zeros_like(time_steps, dtype=float) # Applied bottom shear-stress
E = np.zeros_like(time_steps, dtype=float) # Erosion rate
A_e = np.zeros_like(time_steps, dtype=float) # Area of erosion (m^2)
V_e = np.zeros_like(time_steps, dtype=float) # Erosion volume (m^3)
V_e_s = np.zeros_like(time_steps, dtype=float)

V_chamb_susp = np.zeros_like(time_steps, dtype=float)
V_chann_susp = np.zeros_like(time_steps, dtype=float)

V_s_sum_s = np.zeros_like(time_steps, dtype=float)
V_s_sum_e = np.zeros_like(time_steps, dtype=float)
V_e_s_tot = np.zeros_like(time_steps, dtype=float)
G_e_s_tot = np.zeros_like(time_steps, dtype=float)

# Initial conditions
D_ho[0] = D_ho_0
D_hc[0] = D_hc_0
v_FE[0] = np.sqrt(2 * g * D_ho[0]) # Max F/E velocity at t0
Q_FE[0] = a * C * v_FE[0] # Max F/E discharge through openings at t0
D_V[0] = 0 # Total volume exchanged (m^3) (max would be: L * W * D_h_0)
rho_i[0] = rho_i_0
rho_c[0] = rho_c_0
rho_i_s[0] = rho_i_s_0
rho_c_s[0] = rho_c_s_0
D_rho_o_s[0] = D_rho_o_s_0
D_rho_oc_s[0] = D_rho_oc_s_0
h_i[0] = h_i_0
h_o[0] = h_o_0
h_c[0] = h_c_0

c_i[0] = c_i_0
c_c[0] = c_c_0
V_s_sum[0] = V_s_0
G_s_sum[0] = G_s_0
V_i[0] = V_i_0
V_c[0] = V_c_0
V_s_c[0] = V_s_c_0
V_s_c_sum[0] = V_s_c_0
G_s_c[0] = G_s_c_0
G_s_c_sum[0] = G_s_c_0

u[0] = u_0
Ch[0] = Ch_0
tau_b[0] = tau_b_0
V_e[0] = 0

# Loop over time steps
# Phase 1 loop (t = 0 to 840 s) # 14 minutes
# Filling from left to right
for i in range(1, 85):  # 840 seconds, timestep = 10s, so 84 steps
    h_o[i] = h_o[i - 1]
    h_c[i] = h_c[i - 1]
    V_c[i] = V_c[i - 1]
    rho_c[i] = rho_c[i - 1]

    D_V[i] = Q_FE[i - 1] * timestep
    D_ho[i] = max((D_ho[i - 1] - D_V[i] / A), 0)
    h_i[i] = h_i[i - 1] + (D_V[i] / A)
    D_hc[i] = h_i[i] - h_c[i]
```

```
    v_FE[i] = np.sqrt(2 * g * np.abs(D_ho[i]))
    Q_FE[i] = a * C * v_FE[i]

    if D_ho[i] > 0:
        V_i[i] = V_i[i - 1] + D_V[i]
    else:
        V_i[i] = V_i[i - 1]

    rho_i[i] = (D_V[i] / V_i[i]) * rho_o + ((V_i[i] - D_V[i]) / V_i[i]) * rho_i[i - 1]
    c_i[i] = (((D_V[i] / V_i[i]) * c_o_0 + ((V_i[i] - D_V[i]) / V_i[i]) * c_i[i - 1]) * V_i[i
        ] - (V_e_s_tot[i - 1] - V_e_s_tot[i - 2]) * rho_d) / V_i[i]
    c_c[i] = (c_c[i - 1] * V_c[i] - V_s_c[i - 1] * rho_d) / V_c[i]

    rho_i_s[i] = rho_i[i] * (1 - c_i[i] / rho_d) + c_i[i]
    rho_c_s[i] = rho_c[i] * (1 - c_c[i] / rho_d) + c_c[i]
    D_rho_o_s[i] = rho_o_s - rho_i_s[i]
    D_rho_oc_s[i] = rho_i_s[i] - rho_c_s[i]

    V_s_c[i] = Ac * (ws_eff_c / rho_d) * c_c[i] * timestep
    V_s_c_sum[i] = V_s_c_sum[i - 1] + V_s_c[i]
    G_s_c[i] = V_s_c[i] / Ac
    G_s_c_sum[i] = G_s_c_sum[i - 1] + G_s_c[i]

    V_s[i] = A * (ws_eff_i / rho_d) * c_i[i] * timestep
    V_s_sum[i] = V_s_sum[i - 1] + V_s[i]
    G_s[i] = V_s[i] / A
    G_s_sum[i] = G_s_sum[i - 1] + G_s[i]

    # Erosion
    u[i] = Q_FE[i] / (W * h_i[i])
    Ch[i] = (1 / n) * h_i[i] ** (1/6)
    tau_b[i] = rho_i_s[i] * g * u[i]**2 / Ch[i]**2

    if tau_b[i] > tau_ce:
        E[i] = m_e * (tau_b[i] - tau_ce)
        V_e[i] = A_e_fe * (E[i] / rho_d) * timestep
    else:
        E[i] = 0
        V_e[i] = 0

    V_s_sum_s[i] = ((A - A_e_fe) / A) * V_s_sum[i]
    V_s_sum_e[i] = (A_e_fe / A) * V_s_sum[i]

    if V_e[i] < V_s_sum_e[i]:
        V_e_s[i] = V_s_sum_e[i] - V_e[i]
    else:
        V_e_s[i] = 0

    V_e_s_tot[i] = V_e_s[i] + V_s_sum_s[i]
    G_e_s_tot[i] = V_e_s_tot[i] / A

    V_chamb_susp[i] = (c_i[i] * V_i[i]) / rho_d
    V_chann_susp[i] = (c_c[i] * V_c[i]) / rho_d

# Phase 2 loop (t = 840 to 1080 s) # 4 minutes
# Density currents left
for i in range(85, 109):
    h_i[i] = h_i[i - 1]
    h_o[i] = h_o[i - 1]
    h_c[i] = h_c[i - 1]
    D_ho[i] = D_ho[i - 1]
    D_hc[i] = D_hc[i - 1]
    V_i[i] = V_i[i - 1]
    V_c[i] = V_c[i - 1]
    rho_c[i] = rho_c[i - 1]

    Vvert[i] = 0.5 * f3 * W * h_o_0 * ((D_rho_o_s[i - 1] / rho_o_s) * g * h_o_0) ** 0.5 *
        timestep

    if rho_o_s > rho_i_s[i - 1]:
        rho_i[i] = (Vvert[i] / V_i[i]) * rho_o + ((V_i[i] - Vvert[i]) / V_i[i]) * rho_i[i -
```

```
            1]
        c_i[i] = (((Vvert[i] / V_i[i]) * c_o_0 + ((V_i[i] - Vvert[i]) / V_i[i]) * c_i[i - 1])
             * V_i[i] - (V_e_s_tot[i - 1] - V_e_s_tot[i - 2]) * rho_d) / V_i[i]
        c_c[i] = (c_c[i - 1] * V_c[i] - V_s_c[i - 1] * rho_d) / V_c[i]
        rho_i_s[i] = rho_i[i] * (1 - c_i[i] / rho_d) + c_i[i]
        rho_c_s[i] = rho_c[i] * (1 - c_c[i] / rho_d) + c_c[i]

        D_rho_o_s[i] = rho_o_s - rho_i_s[i]
        D_rho_oc_s[i] = rho_i_s[i] - rho_c_s[i]
    else:
        rho_i[i] = rho_i[i - 1]
        c_i[i] = (c_i[i - 1] * V_i[i] - (V_e_s_tot[i - 1] - V_e_s_tot[i - 2]) * rho_d) / V_i[
            i]
        c_c[i] = (c_c[i - 1] * V_c[i] - V_s_c[i - 1] * rho_d) / V_c[i]
        rho_i_s[i] = rho_i[i] * (1 - c_i[i] / rho_d) + c_i[i]
        rho_c_s[i] = rho_c[i] * (1 - c_c[i] / rho_d) + c_c[i]

        D_rho_o_s[i] = rho_o_s - rho_i_s[i]
        D_rho_oc_s[i] = rho_i_s[i] - rho_c_s[i]

    V_s_c[i] = Ac * (ws_eff_c / rho_d) * c_c[i] * timestep
    V_s_c_sum[i] = V_s_c_sum[i - 1] + V_s_c[i]
    G_s_c[i] = V_s_c[i] / Ac
    G_s_c_sum[i] = G_s_c_sum[i - 1] + G_s_c[i]
    V_s[i] = A * (ws_eff_i / rho_d) * c_i[i] * timestep
    V_s_sum[i] = V_s_sum[i - 1] + V_s[i]
    G_s[i] = V_s[i] / A
    G_s_sum[i] = G_s_sum[i - 1] + G_s[i]

    # Erosion
    u[i] = (Vvert[i] / timestep) / (W * 0.5 * h_i[i])
    Ch[i] = (1 / n) * h_i[i] ** (1/6)
    tau_b[i] = rho_i_s[i] * g * u[i]**2 / Ch[i]**2

    if tau_b[i] > tau_ce:
        E[i] = m_e * (tau_b[i] - tau_ce)
        V_e[i] = A_e_dens * (E[i] / rho_d) * timestep
    else:
        E[i] = 0
        V_e[i] = 0

    V_s_sum_s[i] = ((A - A_e_dens) / A) * V_s_sum[i]
    V_s_sum_e[i] = (A_e_dens / A) * V_s_sum[i]

    if V_e[i] < V_s_sum_e[i]:
        V_e_s[i] = V_s_sum_e[i] - V_e[i]
    else:
        V_e_s[i] = 0

    V_e_s_tot[i] = V_e_s[i] + V_s_sum_s[i]
    G_e_s_tot[i] = V_e_s_tot[i] / A

    V_chamb_susp[i] = (c_i[i] * V_i[i]) / rho_d
    V_chann_susp[i] = (c_c[i] * V_c[i]) / rho_d

# Phase 3 loop (t = 1080 to 1440 s) # 6 minutes
# Boat into chamber from left
for i in range(109, 145):
    h_i[i] = h_i[i - 1]
    h_o[i] = h_o[i - 1]
    h_c[i] = h_c[i - 1]
    D_ho[i] = D_ho[i - 1]
    D_hc[i] = D_hc[i - 1]
    V_c[i] = V_c[i - 1]
    rho_c[i] = rho_c[i - 1]
    rho_i[i] = rho_i[i - 1]

    if Vboats * (i - 109) < V_boat_max:
        V_i[i] = V_i[i - 1] - Vboats
        Vboat[i] = Vboats * (i - 109)
    else:
```

```
        V_i[i] = V_i[i - 1]
        Vboat[i] = V_boat_max

    c_i[i] = (c_i[i - 1] * V_i[i] - (V_e_s_tot[i - 1] - V_e_s_tot[i - 2]) * rho_d) / V_i[i]
    c_c[i] = (c_c[i - 1] * V_c[i] - V_s_c[i - 1] * rho_d) / V_c[i]

    rho_i_s[i] = rho_i[i] * (1 - c_i[i] / rho_d) + c_i[i]
    rho_c_s[i] = rho_c[i] * (1 - c_c[i] / rho_d) + c_c[i]
    D_rho_o_s[i] = rho_o_s - rho_i_s[i]
    D_rho_oc_s[i] = rho_i_s[i] - rho_c_s[i]

    V_s_c[i] = Ac * (ws_eff_c / rho_d) * c_c[i] * timestep
    V_s_c_sum[i] = V_s_c_sum[i - 1] + V_s_c[i]
    G_s_c[i] = V_s_c[i] / Ac
    G_s_c_sum[i] = G_s_c_sum[i - 1] + G_s_c[i]
    V_s[i] = A * (ws_eff_i / rho_d) * c_i[i] * timestep
    V_s_sum[i] = V_s_sum[i - 1] + V_s[i]
    G_s[i] = V_s[i] / A
    G_s_sum[i] = G_s_sum[i - 1] + G_s[i]

    # Erosion
    u[i] = (Vboats / timestep) / (W * h_i[i] - b_d * d)
    Ch[i] = (1 / n) * h_i[i] ** (1/6)
    tau_b[i] = rho_i_s[i] * g * u[i]**2 / Ch[i]**2

    if tau_b[i] > tau_ce:
        E[i] = m_e * (tau_b[i] - tau_ce)
        V_e[i] = A_e_boat * (E[i] / rho_d) * timestep
    else:
        E[i] = 0
        V_e[i] = 0

    V_s_sum_s[i] = ((A - A_e_boat) / A) * V_s_sum[i]
    V_s_sum_e[i] = (A_e_boat / A) * V_s_sum[i]

    if V_e[i] < V_s_sum_e[i]:
        V_e_s[i] = V_s_sum_e[i] - V_e[i]
    else:
        V_e_s[i] = 0

    V_e_s_tot[i] = V_e_s[i] + V_s_sum_s[i]
    G_e_s_tot[i] = V_e_s_tot[i] / A

    V_chamb_susp[i] = (c_i[i] * V_i[i]) / rho_d
    V_chann_susp[i] = (c_c[i] * V_c[i]) / rho_d

# Phase 4 loop (t = 1440 to 2280 s) # 14 minutes
# Emptying to the right
for i in range(145, 229):
    h_o[i] = h_o[i - 1]
    rho_i[i] = rho_i[i - 1]

    D_V[i] = Q_FE[i - 1] * timestep
    D_hc[i] = max((D_hc[i - 1] - (D_V[i] / A)), 0)
    h_i[i] = h_i[i - 1] - (D_V[i] / A)
    D_ho[i] = h_o[i] - h_i[i]
    h_c[i] = h_c[i - 1] + (D_V[i] / Ac)
    v_FE[i] = np.sqrt(2 * g * np.abs(D_hc[i]))
    Q_FE[i] = a * C * v_FE[i]

    if D_hc[i] > 0:
        V_i[i] = V_i[i - 1] - D_V[i]
        V_c[i] = V_c[i - 1] + D_V[i]
    else:
        V_i[i] = V_i[i - 1]
        V_c[i] = V_c[i - 1]

    rho_c[i] = (D_V[i] / V_c[i]) * rho_i[i] + ((V_c[i] - D_V[i]) / V_c[i]) * rho_c[i - 1]
    c_c[i] = (((D_V[i] / V_c[i]) * c_i[i - 1] + ((V_c[i] - D_V[i]) / V_c[i]) * c_c[i - 1]) *
        V_c[i] - V_s_c[i - 1] * rho_d) / V_c[i]
    c_i[i] = (c_i[i - 1] * V_i[i] - (V_e_s_tot[i - 1] - V_e_s_tot[i - 2]) * rho_d) / V_i[i]
```

```
    rho_i_s[i] = rho_i[i] * (1 - c_i[i] / rho_d) + c_i[i]
    rho_c_s[i] = rho_c[i] * (1 - c_c[i] / rho_d) + c_c[i]
    D_rho_o_s[i] = rho_o_s - rho_i_s[i]
    D_rho_oc_s[i] = rho_i_s[i] - rho_c_s[i]

    V_s_c[i] = Ac * (ws_eff_c / rho_d) * c_c[i] * timestep
    V_s_c_sum[i] = V_s_c_sum[i - 1] + V_s_c[i]
    G_s_c[i] = V_s_c[i] / Ac
    G_s_c_sum[i] = G_s_c_sum[i - 1] + G_s_c[i]
    V_s[i] = A * (ws_eff_i / rho_d) * c_i[i] * timestep
    V_s_sum[i] = V_s_sum[i - 1] + V_s[i]
    G_s[i] = V_s[i] / A
    G_s_sum[i] = G_s_sum[i - 1] + G_s[i]

    # Erosion
    E[i] = 0
    V_e[i] = 0
    V_e_s[i] = V_s[i]

    V_e_s_tot[i] = V_s_sum[i]
    G_e_s_tot[i] = G_s_sum[i]

    V_chamb_susp[i] = (c_i[i] * V_i[i]) / rho_d
    V_chann_susp[i] = (c_c[i] * V_c[i]) / rho_d

# Phase 5 loop (t = 2280 to 2520 s) # 4 minutes
# Density currents right
for i in range(229, 253):
    h_i[i] = h_i[i - 1]
    h_o[i] = h_o[i - 1]
    h_c[i] = h_c[i - 1]
    D_ho[i] = h_o[i] - h_i[i]
    D_hc[i] = h_i[i] - h_c[i]
    V_i[i] = V_i[i - 1]
    V_c[i] = V_c[i - 1]

    Vvert[i] = 0.5 * f3 * W * h_i_0 * ((D_rho_oc_s[i - 1] / rho_c_0) * g * h_i_0) ** 0.5 *
        timestep

    if rho_i_s[i - 1] > rho_c_s[i - 1]:
        rho_i[i] = (Vvert[i] / V_i[i]) * rho_c[i - 1] + ((V_i[i] - Vvert[i]) / V_i[i]) *
            rho_i[i - 1]
        c_i[i] = (((Vvert[i] / V_i[i]) * c_c[i - 1] + ((V_i[i] - Vvert[i]) / V_i[i]) * c_i[i
            - 1]) * V_i[i] - (V_e_s_tot[i - 1] - V_e_s_tot[i - 2]) * rho_d) / V_i[i]
        rho_i_s[i] = rho_i[i] * (1 - c_i[i] / rho_d) + c_i[i]

        rho_c[i] = (Vvert[i] / V_c[i]) * rho_i[i - 1] + ((V_c[i] - Vvert[i]) / V_c[i]) *
            rho_c[i - 1]
        c_c[i] = (((Vvert[i] / V_c[i]) * c_i[i - 1] + ((V_c[i] - Vvert[i]) / V_c[i]) * c_c[i
            - 1]) * V_c[i] - V_s_c[i - 1] * rho_d) / V_c[i]
        rho_c_s[i] = rho_c[i] * (1 - c_c[i] / rho_d) + c_c[i]

        D_rho_o_s[i] = rho_o_s - rho_i_s[i]
        D_rho_oc_s[i] = rho_i_s[i - 1] - rho_c_s[i]

    else:
        rho_i[i] = rho_i[i - 1]
        c_i[i] = (c_i[i - 1] * V_i[i] - (V_e_s_tot[i - 1] - V_e_s_tot[i - 2]) * rho_d) / V_i[
            i]
        rho_i_s[i] = rho_i[i] * (1 - c_i[i] / rho_d) + c_i[i]

        rho_c[i] = rho_c[i - 1]
        c_c[i] = (c_c[i - 1] * V_c[i] - V_s_c[i - 1] * rho_d) / V_c[i]
        rho_c_s[i] = rho_c[i] * (1 - c_c[i] / rho_d) + c_c[i]

        D_rho_o_s[i] = rho_o_s - rho_i_s[i]
        D_rho_oc_s[i] = rho_i_s[i - 1] - rho_c_s[i]

    V_s_c[i] = Ac * (ws_eff_c / rho_d) * c_c[i] * timestep
    V_s_c_sum[i] = V_s_c_sum[i - 1] + V_s_c[i]
    G_s_c[i] = V_s_c[i] / Ac
```

```
    G_s_c_sum[i] = G_s_c_sum[i - 1] + G_s_c[i]
    V_s[i] = A * (ws_eff_i / rho_d) * c_i[i] * timestep
    V_s_sum[i] = V_s_sum[i - 1] + V_s[i]
    G_s[i] = V_s[i] / A
    G_s_sum[i] = G_s_sum[i - 1] + G_s[i]

    # Erosion
    u[i] = (Vvert[i] / timestep) / (W * 0.5 * h_i[i])
    Ch[i] = (1 / n) * h_i[i] ** (1/6)
    tau_b[i] = rho_i_s[i] * g * u[i]**2 / Ch[i]**2

    if tau_b[i] > tau_ce:
        E[i] = m_e * (tau_b[i] - tau_ce)
        V_e[i] = A_e_dens * (E[i] / rho_d) * timestep
    else:
        E[i] = 0
        V_e[i] = 0

    V_s_sum_s[i] = ((A - A_e_dens) / A) * V_s_sum[i]
    V_s_sum_e[i] = (A_e_dens / A) * V_s_sum[i]

    if V_e[i] < V_s_sum_e[i]:
        V_e_s[i] = V_s_sum_e[i] - V_e[i]
    else:
        V_e_s[i] = 0

    V_e_s_tot[i] = V_e_s[i] + V_s_sum_s[i]
    G_e_s_tot[i] = V_e_s_tot[i] / A

    V_chamb_susp[i] = (c_i[i] * V_i[i]) / rho_d
    V_chann_susp[i] = (c_c[i] * V_c[i]) / rho_d

# Phase 6 loop (t = 2520 to 2880 s) # 6 minutes
# Boat outside chamber to right
for i in range(253, 289):
    h_i[i] = h_i[i - 1]
    h_o[i] = h_o[i - 1]
    h_c[i] = h_c[i - 1]
    D_ho[i] = h_o[i] - h_i[i]
    D_hc[i] = h_i[i] - h_c[i]
    rho_c[i] = rho_c[i - 1]

    if Vboats * (i - 253) < V_boat_max:
        V_i[i] = V_i[i - 1] + Vboats
        V_c[i] = V_c[i - 1] - Vboats
        Vboat[i] = Vboats * (i - 253)
    else:
        V_i[i] = V_i[i - 1]
        V_c[i] = V_c[i - 1]
        Vboat[i] = V_boat_max

    rho_i[i] = (Vboat[i] / V_i[i]) * rho_c[i - 1] + ((V_i[i] - Vboat[i]) / V_i[i]) * rho_i[i
        - 1]
    c_i[i] = (((Vboat[i] / V_i[i]) * c_c[i - 1] + ((V_i[i] - Vboat[i]) / V_i[i]) * c_i[i -
        1]) * V_i[i] - (V_e_s_tot[i - 1] - V_e_s_tot[i - 2]) * rho_d) / V_i[i]
    c_c[i] = (c_c[i - 1] * V_c[i] - V_s_c[i - 1] * rho_d) / V_c[i]
    rho_i_s[i] = rho_i[i] * (1 - c_i[i] / rho_d) + c_i[i]
    rho_c_s[i] = rho_c[i] * (1 - c_c[i] / rho_d) + c_c[i]
    D_rho_o_s[i] = rho_o_s - rho_i_s[i]
    D_rho_oc_s[i] = rho_i_s[i] - rho_c_s[i]

    V_s_c[i] = Ac * (ws_eff_c / rho_d) * c_c[i] * timestep
    V_s_c_sum[i] = V_s_c_sum[i - 1] + V_s_c[i]
    G_s_c[i] = V_s_c[i] / Ac
    G_s_c_sum[i] = G_s_c_sum[i - 1] + G_s_c[i]
    V_s[i] = A * (ws_eff_i / rho_d) * c_i[i] * timestep
    V_s_sum[i] = V_s_sum[i - 1] + V_s[i]
    G_s[i] = V_s[i] / A
    G_s_sum[i] = G_s_sum[i - 1] + G_s[i]

    # Erosion
```

```
    u[i] = (Vboats / timestep) / (W * h_i[i] - b_d * d)
    Ch[i] = (1 / n) * h_i[i] ** (1/6)
    tau_b[i] = rho_i_s[i] * g * u[i]**2 / Ch[i]**2

    if tau_b[i] > tau_ce:
        E[i] = m_e * (tau_b[i] - tau_ce)
        V_e[i] = A_e_boat * (E[i] / rho_d) * timestep
    else:
        E[i] = 0
        V_e[i] = 0

    V_s_sum_s[i] = ((A - A_e_boat) / A) * V_s_sum[i]
    V_s_sum_e[i] = (A_e_boat / A) * V_s_sum[i]

    if V_e[i] < V_s_sum_e[i]:
        V_e_s[i] = V_s_sum_e[i] - V_e[i]
    else:
        V_e_s[i] = 0

    V_e_s_tot[i] = V_e_s[i] + V_s_sum_s[i]
    G_e_s_tot[i] = V_e_s_tot[i] / A

    V_chamb_susp[i] = (c_i[i] * V_i[i]) / rho_d
    V_chann_susp[i] = (c_c[i] * V_c[i]) / rho_d

# Phase 7 loop (t = 2880 to 3240 s) # 6 minutes
# Boat into chamber from right
for i in range(289, 325):
    h_i[i] = h_i[i - 1]
    h_o[i] = h_o[i - 1]
    h_c[i] = h_c[i - 1]
    D_ho[i] = h_o[i] - h_i[i]
    D_hc[i] = h_i[i] - h_c[i]
    rho_i[i] = rho_i[i - 1]

    if Vboats * (i - 289) < V_boat_max:
        V_i[i] = V_i[i - 1] - Vboats
        V_c[i] = V_c[i - 1] + Vboats
        Vboat[i] = Vboats * (i - 289)
    else:
        V_i[i] = V_i[i - 1]
        V_c[i] = V_c[i - 1]
        Vboat[i] = V_boat_max

    rho_c[i] = (Vboat[i] / V_c[i]) * rho_i[i - 1] + ((V_c[i] - Vboat[i]) / V_c[i]) * rho_c[i
        - 1]
    c_c[i] = (((Vboat[i] / V_c[i]) * c_i[i] + ((V_c[i] - Vboat[i]) / V_c[i]) * c_c[i - 1]) *
        V_c[i] - V_s_c[i - 1] * rho_d) / V_c[i]
    c_i[i] = (c_i[i - 1] * V_i[i] - (V_e_s_tot[i - 1] - V_e_s_tot[i - 2]) * rho_d) / V_i[i]

    rho_i_s[i] = rho_i[i] * (1 - c_i[i] / rho_d) + c_i[i]
    rho_c_s[i] = rho_c[i] * (1 - c_c[i] / rho_d) + c_c[i]
    D_rho_o_s[i] = rho_o_s - rho_i_s[i]
    D_rho_oc_s[i] = rho_i_s[i] - rho_c_s[i]

    V_s_c[i] = Ac * (ws_eff_c / rho_d) * c_c[i] * timestep
    V_s_c_sum[i] = V_s_c_sum[i - 1] + V_s_c[i]
    G_s_c[i] = V_s_c[i] / Ac
    G_s_c_sum[i] = G_s_c_sum[i - 1] + G_s_c[i]
    V_s[i] = A * (ws_eff_i / rho_d) * c_i[i] * timestep
    V_s_sum[i] = V_s_sum[i - 1] + V_s[i]
    G_s[i] = V_s[i] / A
    G_s_sum[i] = G_s_sum[i - 1] + G_s[i]

    # Erosion
    u[i] = (Vboats / timestep) / (W * h_i[i] - b_d * d)
    Ch[i] = (1 / n) * h_i[i] ** (1/6)
    tau_b[i] = rho_i_s[i] * g * u[i]**2 / Ch[i]**2

    if tau_b[i] > tau_ce:
        E[i] = m_e * (tau_b[i] - tau_ce)
```

```
        V_e[i] = A_e_boat * (E[i] / rho_d) * timestep
    else:
        E[i] = 0
        V_e[i] = 0

    V_s_sum_s[i] = ((A - A_e_boat) / A) * V_s_sum[i]
    V_s_sum_e[i] = (A_e_boat / A) * V_s_sum[i]

    if V_e[i] < V_s_sum_e[i]:
        V_e_s[i] = V_s_sum_e[i] - V_e[i]
    else:
        V_e_s[i] = 0

    V_e_s_tot[i] = V_e_s[i] + V_s_sum_s[i]
    G_e_s_tot[i] = V_e_s_tot[i] / A

    V_chamb_susp[i] = (c_i[i] * V_i[i]) / rho_d
    V_chann_susp[i] = (c_c[i] * V_c[i]) / rho_d

# Phase 8 loop (t = 3240 to 4080 s) # 14 minutes
# Filling from left to right
for i in range(325, 409):
    h_o[i] = h_o[i - 1]
    h_c[i] = h_c[i - 1]
    V_c[i] = V_c[i - 1]
    rho_c[i] = rho_c[i - 1]

    D_V[i] = Q_FE[i - 1] * timestep
    D_ho[i] = max((D_ho[i - 1] - D_V[i] / A), 0)
    h_i[i] = h_i[i - 1] + (D_V[i] / A)
    D_hc[i] = h_i[i] - h_c[i]
    v_FE[i] = np.sqrt(2 * g * np.abs(D_ho[i]))
    Q_FE[i] = a * C * v_FE[i]

    if D_ho[i] > 0:
        V_i[i] = V_i[i - 1] + D_V[i]
    else:
        V_i[i] = V_i[i - 1]

    rho_i[i] = (D_V[i] / V_i[i]) * rho_o + ((V_i[i] - D_V[i]) / V_i[i]) * rho_i[i - 1]
    c_i[i] = (((D_V[i] / V_i[i]) * c_o_0 + ((V_i[i] - D_V[i]) / V_i[i]) * c_i[i - 1]) * V_i[i
        ] - (V_e_s_tot[i - 1] - V_e_s_tot[i - 2]) * rho_d) / V_i[i]
    c_c[i] = (c_c[i - 1] * V_c[i] - V_s_c[i - 1] * rho_d) / V_c[i]
    rho_i_s[i] = rho_i[i] * (1 - c_i[i] / rho_d) + c_i[i]
    rho_c_s[i] = rho_c[i] * (1 - c_c[i] / rho_d) + c_c[i]
    D_rho_o_s[i] = rho_o_s - rho_i_s[i]
    D_rho_oc_s[i] = rho_i_s[i] - rho_c_s[i]

    V_s_c[i] = Ac * (ws_eff_c / rho_d) * c_c[i] * timestep
    V_s_c_sum[i] = V_s_c_sum[i - 1] + V_s_c[i]
    G_s_c[i] = V_s_c[i] / Ac
    G_s_c_sum[i] = G_s_c_sum[i - 1] + G_s_c[i]
    V_s[i] = A * (ws_eff_i / rho_d) * c_i[i] * timestep
    V_s_sum[i] = V_s_sum[i - 1] + V_s[i]
    G_s[i] = V_s[i] / A
    G_s_sum[i] = G_s_sum[i - 1] + G_s[i]

    # Erosion
    u[i] = Q_FE[i] / (W * h_i[i])
    Ch[i] = (1 / n) * h_i[i] ** (1/6)
    tau_b[i] = rho_i_s[i] * g * u[i]**2 / Ch[i]**2

    if tau_b[i] > tau_ce:
        E[i] = m_e * (tau_b[i] - tau_ce)
        V_e[i] = A_e_fe * (E[i] / rho_d) * timestep
    else:
        E[i] = 0
        V_e[i] = 0

    V_s_sum_s[i] = ((A - A_e_fe) / A) * V_s_sum[i]
    V_s_sum_e[i] = (A_e_fe / A) * V_s_sum[i]
```

```
650
651     if V_e[i] < V_s_sum_e[i]:
652         V_e_s[i] = V_s_sum_e[i] - V_e[i]
653     else:
654         V_e_s[i] = 0
655
656     V_e_s_tot[i] = V_e_s[i] + V_s_sum_s[i]
657     G_e_s_tot[i] = V_e_s_tot[i] / A
658
659     V_chamb_susp[i] = (c_i[i] * V_i[i]) / rho_d
660     V_chann_susp[i] = (c_c[i] * V_c[i]) / rho_d
661
662 # Phase 9 loop (t = 4080 to 4320 s) # 4 minutes
663 # Density currents left
664 for i in range(409, 433):
665     h_i[i] = h_i[i - 1]
666     h_o[i] = h_o[i - 1]
667     h_c[i] = h_c[i - 1]
668     D_ho[i] = D_ho[i - 1]
669     D_hc[i] = D_hc[i - 1]
670     V_i[i] = V_i[i - 1]
671     V_c[i] = V_c[i - 1]
672     rho_c[i] = rho_c[i - 1]
673
674     Vvert[i] = 0.5 * f3 * W * h_o_0 * ((D_rho_o_s[i - 1] / rho_o_s) * g * h_o_0) ** 0.5 *
            timestep
675
676     if rho_o_s > rho_i_s[i - 1]:
677         rho_i[i] = (Vvert[i] / V_i[i]) * rho_o + ((V_i[i] - Vvert[i]) / V_i[i]) * rho_i[i -
                1]
678         c_i[i] = (((Vvert[i] / V_i[i]) * c_o_0 + ((V_i[i] - Vvert[i]) / V_i[i]) * c_i[i - 1])
                 * V_i[i] - (V_e_s_tot[i - 1] - V_e_s_tot[i - 2]) * rho_d) / V_i[i]
679         c_c[i] = (c_c[i - 1] * V_c[i] - V_s_c[i - 1] * rho_d) / V_c[i]
680         rho_i_s[i] = rho_i[i] * (1 - c_i[i] / rho_d) + c_i[i]
681         rho_c_s[i] = rho_c[i] * (1 - c_c[i] / rho_d) + c_c[i]
682
683         D_rho_o_s[i] = rho_o_s - rho_i_s[i]
684         D_rho_oc_s[i] = rho_i_s[i] - rho_c_s[i]
685     else:
686         rho_i[i] = rho_i[i - 1]
687         c_i[i] = (c_i[i - 1] * V_i[i] - (V_e_s_tot[i - 1] - V_e_s_tot[i - 2]) * rho_d) / V_i[
                i]
688         c_c[i] = (c_c[i - 1] * V_c[i] - V_s_c[i - 1] * rho_d) / V_c[i]
689         rho_i_s[i] = rho_i[i] * (1 - c_i[i] / rho_d) + c_i[i]
690         rho_c_s[i] = rho_c[i] * (1 - c_c[i] / rho_d) + c_c[i]
691
692         D_rho_o_s[i] = rho_o_s - rho_i_s[i]
693         D_rho_oc_s[i] = rho_i_s[i] - rho_c_s[i]
694
695     V_s_c[i] = Ac * (ws_eff_c / rho_d) * c_c[i] * timestep
696     V_s_c_sum[i] = V_s_c_sum[i - 1] + V_s_c[i]
697     G_s_c[i] = V_s_c[i] / Ac
698     G_s_c_sum[i] = G_s_c_sum[i - 1] + G_s_c[i]
699     V_s[i] = A * (ws_eff_i / rho_d) * c_i[i] * timestep
700     V_s_sum[i] = V_s_sum[i - 1] + V_s[i]
701     G_s[i] = V_s[i] / A
702     G_s_sum[i] = G_s_sum[i - 1] + G_s[i]
703
704     # Erosion
705     u[i] = (Vvert[i] / timestep) / (W * 0.5 * h_i[i])
706     Ch[i] = (1 / n) * h_i[i] ** (1/6)
707     tau_b[i] = rho_i_s[i] * g * u[i]**2 / Ch[i]**2
708
709     if tau_b[i] > tau_ce:
710         E[i] = m_e * (tau_b[i] - tau_ce)
711         V_e[i] = A_e_dens * (E[i] / rho_d) * timestep
712     else:
713         E[i] = 0
714         V_e[i] = 0
715
716     V_s_sum_s[i] = ((A - A_e_dens) / A) * V_s_sum[i]
```

```
    V_s_sum_e[i] = (A_e_dens / A) * V_s_sum[i]

    if V_e[i] < V_s_sum_e[i]:
        V_e_s[i] = V_s_sum_e[i] - V_e[i]
    else:
        V_e_s[i] = 0

    V_e_s_tot[i] = V_e_s[i] + V_s_sum_s[i]
    G_e_s_tot[i] = V_e_s_tot[i] / A

    V_chamb_susp[i] = (c_i[i] * V_i[i]) / rho_d
    V_chann_susp[i] = (c_c[i] * V_c[i]) / rho_d

# Phase 10 loop (t = 4320 to 4680 s) # 6 minutes
# Boat outside chamber to left
for i in range(433, 469):
    h_i[i] = h_i[i - 1]
    h_o[i] = h_o[i - 1]
    h_c[i] = h_c[i - 1]
    D_ho[i] = D_ho[i - 1]
    D_hc[i] = D_hc[i - 1]
    V_c[i] = V_c[i - 1]
    rho_c[i] = rho_c[i - 1]

    if Vboats * (i - 433) < V_boat_max:
        V_i[i] = V_i[i - 1] + Vboats
        Vboat[i] = Vboats * (i - 433)
    else:
        V_i[i] = V_i[i - 1]
        Vboat[i] = V_boat_max

    rho_i[i] = (Vboat[i] / V_i[i]) * rho_o + ((V_i[i] - Vboat[i]) / V_i[i]) * rho_i[i - 1]
    c_i[i] = (((Vboat[i] / V_i[i]) * c_o_0 + ((V_i[i] - Vboat[i]) / V_i[i]) * c_i[i - 1]) *
        V_i[i] - (V_e_s_tot[i - 1] - V_e_s_tot[i - 2]) * rho_d) / V_i[i]
    c_c[i] = (c_c[i - 1] * V_c[i] - V_s_c[i - 1] * rho_d) / V_c[i]
    rho_i_s[i] = rho_i[i] * (1 - c_i[i] / rho_d) + c_i[i]
    rho_c_s[i] = rho_c[i] * (1 - c_c[i] / rho_d) + c_c[i]
    D_rho_o_s[i] = rho_o_s - rho_i_s[i]
    D_rho_oc_s[i] = rho_i_s[i] - rho_c_s[i]

    V_s_c[i] = Ac * (ws_eff_c / rho_d) * c_c[i] * timestep
    V_s_c_sum[i] = V_s_c_sum[i - 1] + V_s_c[i]
    G_s_c[i] = V_s_c[i] / Ac
    G_s_c_sum[i] = G_s_c_sum[i - 1] + G_s_c[i]
    V_s[i] = A * (ws_eff_i / rho_d) * c_i[i] * timestep
    V_s_sum[i] = V_s_sum[i - 1] + V_s[i]
    G_s[i] = V_s[i] / A
    G_s_sum[i] = G_s_sum[i - 1] + G_s[i]

    # Erosion
    u[i] = (Vboats / timestep) / (W * h_i[i] - b_d * d)
    Ch[i] = (1 / n) * h_i[i] ** (1/6)
    tau_b[i] = rho_i_s[i] * g * u[i]**2 / Ch[i]**2

    if tau_b[i] > tau_ce:
        E[i] = m_e * (tau_b[i] - tau_ce)
        V_e[i] = A_e_boat * (E[i] / rho_d) * timestep
    else:
        E[i] = 0
        V_e[i] = 0

    V_s_sum_s[i] = ((A - A_e_boat) / A) * V_s_sum[i]
    V_s_sum_e[i] = (A_e_boat / A) * V_s_sum[i]

    if V_e[i] < V_s_sum_e[i]:
        V_e_s[i] = V_s_sum_e[i] - V_e[i]
    else:
        V_e_s[i] = 0

    V_e_s_tot[i] = V_e_s[i] + V_s_sum_s[i]
    G_e_s_tot[i] = V_e_s_tot[i] / A
```

```
787
788     V_chamb_susp[i] = (c_i[i] * V_i[i]) / rho_d
789     V_chann_susp[i] = (c_c[i] * V_c[i]) / rho_d
790
791
792 print(f'After␣one␣operating␣cycle␣with␣an␣outside␣suspended␣sediment␣concentration␣of␣{c_o_0}
    ␣kg/m^3,␣outside␣WL␣{h_o_0}␣m␣and␣inside␣WL␣{h_i_0}␣m,␣the␣following␣is␣true:')
793 print(f'The␣suspended␣sediment␣concentration␣inside␣the␣chamber␣is␣{c_i[-1]}␣kg/m^3␣and␣the␣
    layer␣thickness␣{G_s_sum[-1]}␣m.')
794 print(f'The␣suspended␣sediment␣concentration␣inside␣the␣channel␣is␣{c_c[-1]}␣kg/m^3␣and␣the␣
    layer␣thickness␣{G_s_c_sum[-1]}␣m.')
795
796
797 plt.plot(time_steps, c_i)
798 plt.text(50, 3.1, 1)
799 plt.axvline(x=840, color='gray', linestyle='dashed')
800 plt.text(890, 3.1, 2)
801 plt.axvline(x=1080, color='gray', linestyle='dashed')
802 plt.text(1130, 3.1, 3)
803 plt.axvline(x=1440, color='gray', linestyle='dashed')
804 plt.text(1490, 3.1, 4)
805 plt.axvline(x=2280, color='gray', linestyle='dashed')
806 plt.text(2330, 3.1, 5)
807 plt.axvline(x=2520, color='gray', linestyle='dashed')
808 plt.text(2570, 3.1, 6)
809 plt.axvline(x=2880, color='gray', linestyle='dashed')
810 plt.text(2930, 3.1, 7)
811 plt.axvline(x=3240, color='gray', linestyle='dashed')
812 plt.text(3290, 3.1, 8)
813 plt.axvline(x=4080, color='gray', linestyle='dashed')
814 plt.text(4130, 3.1, 9)
815 plt.axvline(x=4320, color='gray', linestyle='dashed')
816 plt.text(4370, 3.1, 10)
817 plt.axvline(x=4680, color='gray', linestyle='dashed')
818 plt.xlim(0, 4680)
819 plt.ylim(0, 3.3)
820 #plt.title('SSC inside lock chamber')
821 plt.xlabel('Time␣[s]')
822 plt.ylabel('SSC␣[kg/m^3]');
823
824
825 plt.plot(time_steps, c_c)
826 plt.text(50, 0.00145, 1)
827 plt.axvline(x=840, color='gray', linestyle='dashed')
828 plt.text(890, 0.00145, 2)
829 plt.axvline(x=1080, color='gray', linestyle='dashed')
830 plt.text(1130, 0.00145, 3)
831 plt.axvline(x=1440, color='gray', linestyle='dashed')
832 plt.text(1490, 0.00145, 4)
833 plt.axvline(x=2280, color='gray', linestyle='dashed')
834 plt.text(2330, 0.00145, 5)
835 plt.axvline(x=2520, color='gray', linestyle='dashed')
836 plt.text(2570, 0.00145, 6)
837 plt.axvline(x=2880, color='gray', linestyle='dashed')
838 plt.text(2930, 0.00145, 7)
839 plt.axvline(x=3240, color='gray', linestyle='dashed')
840 plt.text(3290, 0.00145, 8)
841 plt.axvline(x=4080, color='gray', linestyle='dashed')
842 plt.text(4130, 0.00145, 9)
843 plt.axvline(x=4320, color='gray', linestyle='dashed')
844 plt.text(4370, 0.00145, 10)
845 plt.axvline(x=4680, color='gray', linestyle='dashed')
846 plt.xlim(0, 4680)
847 plt.ylim(0, 0.00155)
848 #plt.title('SSC inside channel')
849 plt.xlabel('Time␣[s]')
850 plt.ylabel('SSC␣[kg/m^3]');
851
852
853 plt.plot(time_steps, G_s_sum)
854 plt.axvline(x=2520, color='gray', linestyle='dashed')
```

```
plt.text(2570, 0.00068, 6)
plt.axvline(x=2880, color='gray', linestyle='dashed')
plt.text(2930, 0.00068, 7)
plt.axvline(x=3240, color='gray', linestyle='dashed')
#plt.plot(time_steps, G_e_s_tot, label='Sedimentation')
#plt.title('Sediment layer thickness inside lock chamber\n')
plt.xlabel('Time [s]')
plt.ylabel('Layer thickness [m]');
print(G_s_sum[-1])


plt.plot(time_steps, G_s_c_sum)
#plt.title('Sediment layer thickness inside channel\n')
plt.axvline(x=1440, color='gray', linestyle='dashed')
plt.text(1490, 0.00000036, 4)
plt.xlabel('Time [s]')
plt.ylabel('Layer thickness [m]');
print(G_s_c_sum[-1])


plt.plot(time_steps, tau_b)
#plt.title('Applied bottom shear stress\n')
plt.xlabel('Time [s]')
plt.ylabel('Tau_b [N/m^2]');
```

C

Model checks cyclic sedimentation

Tables C.1 - C.4 give the values of the model checks for the cyclic sedimentation simulation in Chapter 9. The checks are done for one operational cycle, one tidal cycle, one month and one year. In every table, the value from the model is shown on the left and the maximum determined value is shown on the right. When the model value stays under the maximum value, it suffices the check and a letter 'Y' is shown in the last column of the table. When the check is not sufficed, the letter 'N' will be shown.

Table C.1: Model checks sediment layer thicknesses, operational cycle.

Case		Model value $[m]$	Maximum value $[m]$	Check
Scenario 1				
	Chamber	$6.93 * 10^{-4}$	$1.49 * 10^{-3}$	Y
	Channel	$3.65 * 10^{-7}$	$1.44 * 10^{-6}$	Y
Scenario 2				
	Chamber	$7.30 * 10^{-4}$	$1.15 * 10^{-3}$	Y
	Channel	$2.14 * 10^{-7}$	$1.11 * 10^{-6}$	Y

Table C.2: Model checks sediment layer thicknesses, one tidal cycle.

Case		Model value $[m]$	Maximum value $[m]$	Check
Two way traffic				
Scenario 1				
	Chamber	$1.78 * 10^{-2}$	$2.75 * 10^{-2}$	Y
	Channel	$7.65 * 10^{-5}$	$3.19 * 10^{-4}$	Y
Scenario 2				
	Chamber	$8.81 * 10^{-3}$	$2.75 * 10^{-2}$	Y
	Channel	$6.56 * 10^{-5}$	$3.19 * 10^{-4}$	Y
Fully operat.				
Scenario 1				
	Chamber	$1.66 * 10^{-2}$	$2.75 * 10^{-2}$	Y
	Channel	$1.21 * 10^{-4}$	$6.40 * 10^{-4}$	Y
Scenario 2				
	Chamber	$1.76 * 10^{-2}$	$2.75 * 10^{-2}$	Y
	Channel	$9.88 * 10^{-5}$	$6.40 * 10^{-4}$	Y

Table C.3: Model checks sediment layer thicknesses, one month.

Case		Model value $[m]$	Maximum value $[m]$	Check
Two way traffic				
	Chamber	$5.32 * 10^{-1}$	$8.26 * 10^{-1}$	Y
	Channel	$2.54 * 10^{-3}$	$2.89 * 10^{-1}$	Y
Fully operat.				
	Chamber	$5.28 * 10^{-1}$	$8.26 * 10^{-1}$	Y
	Channel	$5.05 * 10^{-3}$	$5.76 * 10^{-1}$	Y

Table C.4: Model checks sediment layer thicknesses, one year.

Case		Model value $[m]$	Maximum value $[m]$	Check
Two way traffic				
	Chamber	6.50	10.1	Y
	Channel	$3.11 * 10^{-2}$	1.01	Y
Fully operat.				
	Chamber	6.45	10.1	Y
	Channel	$6.22 * 10^{-2}$	1.01	Y

D

Gate type figures

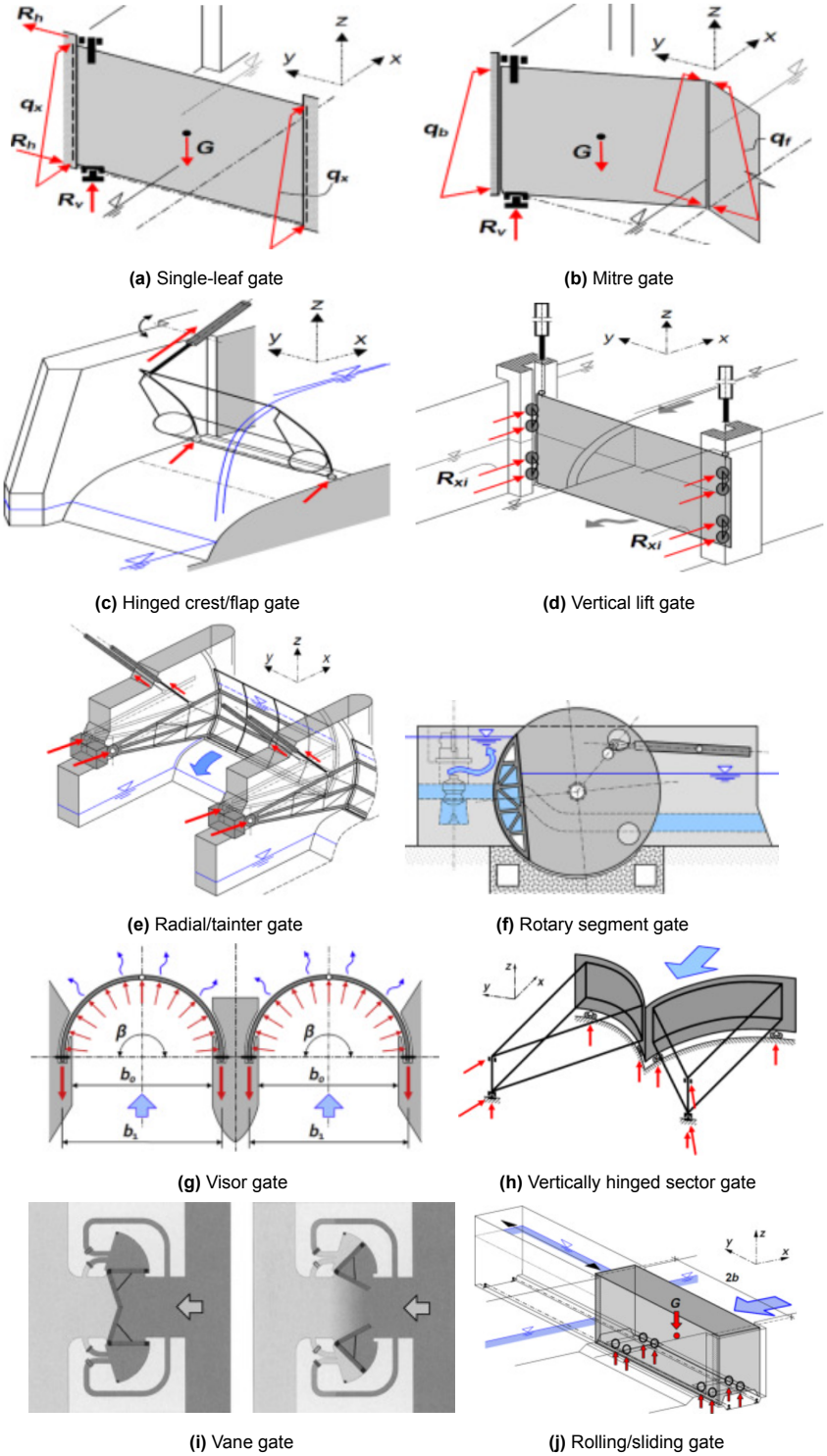

(a) Single-leaf gate

(b) Mitre gate

(c) Hinged crest/flap gate

(d) Vertical lift gate

(e) Radial/tainter gate

(f) Rotary segment gate

(g) Visor gate

(h) Vertically hinged sector gate

(i) Vane gate

(j) Rolling/sliding gate

Figure D.1: Gate type lay-out overview (Daniel & Paulus, 2019).